INSTITUTO POLITÉCNICO DE BRAGANÇA
Escola Superior de Tecnologia e Gestão

INSTITUTO FEDERAL
Rio Grande do Sul | Campus Erechim

Optimization of Parameters for Modifying Surface Wettability and Thermal Conductivity of PDMS

Lucas Boniatti Neves (a60548)

Bragança, Portugal

July 2024

Optimization of Parameters for Modifying Surface Wettability and Thermal Conductivity of PDMS

Lucas Boniatti Neves (a60548)

Dissertation presented to **Escola Superior de Tecnologia e Gestão de Bragança** in double degree program with **Instituto Federal de Educação,Ciência e Tecnologia do Rio Grande do Sul - Campus Erechim** to obtain the Master Degree in Mechanical Engineering.

Supervised by:

Professor Dr. João Eduardo P. C. Ribeiro
Professor Dr. Luiz Gustavo de Moura da Silva Barbosa

Bragança, Portugal

July 2024

Agradecimentos

Primeiramente, gostaria de agradecer à toda minha família, em especial à minha mãe Cleide, ao meu pai Marcos e ao meu irmão Vítor. Sou imensamente grato por todo o apoio e suporte que recebi ao longo dessa trajetória. Reconhecendo os sacrifícios que fizeram, sinto-me honrado em poder retribuir o investimento e orgulhoso por ter alcançado este feito. Agradeço por sempre confiarem em mim e acreditarem no meu potencial. Sem o apoio de vocês, eu não teria conseguido chegar tão longe.

À minha família, não de sangue, mas de coração, Carmem, Dallazen, Zico, Ilma, Jana, Camila e Giullia.

Aos meus amigos que tive a honra de conhecer e compartilhar esta experiência em Portugal, tornando única e memorável. Agradeço por tornarem mais leve esta jornada desafiadora. Em especial aos grupos “Aprovados IPB”, “Quarto do Levanta”, “Mestrado PT”, “Fam Bragança”, “Os guri e as guria” e ao pessoal da “casa das Brasileirinhas”, especialmente à Nathália.

Ao pessoal do laboratório LMFH, Gustavo, Felipe, Lucas Carrazedo e Lucas Panta. Obrigado por tornarem essa jornada mais bem-disposta desfrutando de muitas risadas e histórias.

Aos meus amigos do Brasil, particularmente ao Rafael, Nicolau, Daniel, Roger, Ricardo e em memória um grande amigo Jonatas Prado.

À toda a equipe docente e funcionários do IFRS, campus Erechim, agradeço pelos anos de aprendizado e pela oportunidade de participar de um programa de mobilidade e dupla- diplomação no Instituto Politécnico de Bragança (IPB). Em especial ao meu professor orientador do Brasil, Luiz Gustavo por toda orientação, dedicação e amizade ao longo desta trajetória.

Por fim, à toda a equipe docente e funcionários do IPB. Em especial ao meu professor orientador João Ribeiro (IPB), por toda dedicação, por toda ajuda, pelo apoio e reconhecimento depositado em meu desempenho e por acreditar e confiar no meu esforço. Também, a toda equipe da Universidade do Minho (UM), pela disponibilidade e ajuda, em especial ao Glauco e à Inês pela dedicação e amizade construída nessa caminhada.

Resumo

O polidimetilsiloxano (PDMS) tem atraído significativa atenção em diversas áreas devido às suas excelentes propriedades, mas sua hidrofobicidade inerente apresenta desafios em aplicações que exigem controle da molhabilidade. Este estudo fornece uma visão abrangente das principais estratégias para modificar a molhabilidade das superfícies de PDMS, focando nos métodos tradicionais e seu impacto no ângulo de contato e outras características relacionadas. Quatro técnicas principais foram estudadas, sendo elas o tratamento com plasma de oxigênio, a adição de surfactantes, o tratamento com UV-ozônio e a incorporação de nanomateriais, sendo a aplicada neste estudo a adição de surfactantes. Esses métodos são escolhidos entre os demais devido a sua ampla disponibilidade de literatura, menor complexidade e custo-benefício em comparação com técnicas mais novas. O tratamento com plasma de oxigênio melhora a hidrofilicidade do PDMS ao introduzir grupos funcionais polares através da oxidação. A adição de surfactantes possui uma abordagem versátil para alterar a molhabilidade, sendo a escolha e a concentração dos surfactantes fundamentais para obter as propriedades desejadas da superfície. O tratamento com UV-ozônio aumenta com eficácia a energia da superfície por meio da indução de oxidação e geração de grupos funcionais hidrofílicos. A incorporação de nanomateriais nas matrizes de PDMS possibilita modificações promissoras na molhabilidade, permitindo propriedades de superfície que são ajustáveis através da dispersão controlada e interações interfaciais. Os efeitos das nanopartículas e dos nanotubos melhoram significativamente o comportamento de molhamento e a energia da superfície. Adicionalmente, esse estudo aborda os desafios da recuperação hidrofóbica no PDMS, especialmente considerável para dispositivos microfluídicos comerciais que se tem a exigência do armazenamento e distribuição prolongados. Um estudo comparando três surfactantes não iônicos (Triton X-100, Brij L4 (BL4) e Polietileno Óxido (PEO)) apresenta que a seleção de surfactantes deve considerar a eficiência, estabilidade e durabilidade do comportamento hidrofílico. Diversos tipos e concentrações de surfactantes e a suas temperaturas de cura foram testados, revelando que 2,5% de PEO curado a 80°C atingiu um ângulo de contato de 12,8° imediatamente após a cura. Análises de condutividade térmica indicaram que 0,5% de TX-100 a 80°C era ideal inicialmente, enquanto 2,5% de BL4 a 25°C apresentou melhor desempenho após três semanas. Análises estatísticas, incluindo o método Taguchi e a Análise Relacional de Grey, validam ainda mais a influência de vários parâmetros na molhabilidade e condutividade térmica.

Palavras-chave: Modificação de superfícies; Hidrofilicidade; Microfluídica.

Abstract

Polydimethylsiloxane (PDMS) has attracted significant attention in several areas due to its excellent properties, but its inherent hydrophobicity presents challenges in applications that require control of wettability. This study provides a comprehensive overview of the main strategies for modifying the wettability of PDMS surfaces, focusing on traditional methods and their impact on the contact angle and other related characteristics. Four main techniques are discussed: oxygen plasma treatment, addition of surfactants, UV-ozone treatment and incorporation of nanomaterials. These methods are chosen over the others due to their wide availability in the literature, lower complexity and cost-effectiveness compared to newer techniques. Oxygen plasma treatment improves the hydrophilicity of PDMS by introducing polar functional groups through oxidation. The addition of surfactants has a versatile approach to change wettability, with the choice and concentration of surfactants being the key to obtain the desired surface properties. UV-ozone treatment effectively increases surface energy by inducing oxidation and generating hydrophilic functional groups. The incorporation of nanomaterials into PDMS matrices enables promising modifications in wettability, allowing for surface properties that are adjustable through controlled dispersion and interfacial interactions. The effects of nanoparticles and nanotubes significantly improve wetting behavior and surface energy. Additionally, this study addresses the challenges of hydrophobic recovery in PDMS, especially considerable for commercial microfluidic devices that require prolonged storage and distribution. A study comparing three non-ionic surfactants (Triton X-100, Brij L4 (BL4) and Polyethylene Oxide (PEO)) shows that the selection of surfactants must consider the efficiency, stability and durability of the hydrophilic behavior. Various types and concentrations of surfactants and their curing temperatures were tested, revealing that 2.5% PEO cured at 80°C reached a contact angle of 12.8° immediately after curing. Thermal conductivity analyses indicated that 0.5% TX-100 at 80°C was ideal right after the cure, while 2.5% BL4 at 25°C performed better after three weeks. Statistical analyses, including the Taguchi method and Grey's Relational Analysis, further validate the influence of various parameters on wettability and thermal conductivity.

Keywords: Surface modification; Hydrophilicity; Microfluidics.

Index

List of Figures

Listo f Tables

Abbreviations

Nomenclature		*Abbreviation*	
PDMS	Polydimethylsiloxane	θ	Contact angle
UV	Ultraviolet		
L	Liquid		
	Steam		
S	Solid		
O_2	Oxygen		
SiOH	Silanol group		
SEM	Scanning electron microscopy		
XPS–X-ray	Photoelectron spectroscopy		
DC	Direct current		
AFM	Atomic force microscopy		
SRMJ	Scanning radical microjet		
WCA	Water contact angle		
CA	Contact angle		
ccm	Cubic centimeters per minute		
PEG	Polyethylene glycol		
BSA	Bovine serum albumin		
RF	Radio frequency		
JKR	Johnson–Kendall–Roberts		

Chapter 1
Introduction

Polymeric materials have been used since ancient times, but only natural polymeric materials were known and employed back then. Polymers are macromolecules composed of smaller structural units called monomers. Monomers are low molecular mass molecules that, through polymerization reactions, form the polymeric macromolecules. It was only in the 20th century that artificial polymerization processes began to develop, and since then, these processes have been refined to produce plastics, rubbers, and resins, thanks to increasingly sophisticated molecular engineering, being widely applied in various industrial products [1]. Furthermore, the polymer industry has grown rapidly and currently surpasses the industries processing aluminum, copper, and other important traditional materials [2]. Within this category, elastomers constitute a significant subclass. They are weakly cross-linked polymers, generally with a low Young's modulus, capable of withstanding large deformations and returning to their original shape when the stress causing the deformation is removed. Examples of elastomers include natural and synthetic rubbers, silicone elastomers, and other copolymers [3]. One elastomer that has attracted significant interest is polydimethylsiloxane (PDMS), which consists of a mixture of fully methylated linear siloxane polymers, with structural units of the formula H(CH3)2SiO, stabilized by terminal units of the formula (CH3)2SiO. This material belongs to the group of polymeric organosilicones known as silicones. PDMS is the most widely used silicone based on organic polymers, presenting a clear, non-flammable, and non-toxic compound [4].

PDMS is widely used as a base for various micro and nano applications, including microcontact printing [5], microfluidics [6], [7], [8], [9], and microreactors [10]. Its attractive features, such as ease of fabrication, non-toxicity, optical transparency, low cost, and biocompatibility, make PDMS a highly promising material in many areas [11], [12], [13], [14]. However, to optimize its surface properties, such as wettability, it is very important to modify it to meet specific required conditions. This study focuses on modifying the wettability of PDMS, which is a critical aspect for applications that demand efficient interactions between materials and liquids.

Wettability, defined by the contact angle (θ), measures the adhesion between a liquid and a solid surface, being fundamental to understanding interactions in microfluidic systems [15], [16]. PDMS, which is naturally hydrophobic due to the presence of methyl groups in its structure, has limitations in applications that require hydrophilic surfaces, such as in certain medical devices, biotechnological devices, and others [17], [18], [19], [20], [21]. Given the need to improve the hydrophilicity of PDMS to expand its practical application, particularly in microfluidics, the choice of this topic is justified [22]. Improving the wettability of PDMS not only facilitates the handling of aqueous solutions in microchannels but can also optimize device fabrication processes and increase their efficiency.

The research problem mainly lies in the intrinsic hydrophobicity of PDMS and its incompatibility with applications requiring hydrophilic surfaces. The possibility is that incorporating surfactants into PDMS can significantly improve its wettability without compromising other fundamental properties of the material.

The utilization of polydimethylsiloxane (PDMS) is on the rise due to its attractive properties, such as flexibility, transparency, and biocompatibility, being widely employed in sectors like biomedical and microtechnology. However, the intrinsic hydrophobicity of PDMS limits its effectiveness in applications requiring hydrophilic surfaces, such as in microfluidic systems. Therefore, a detailed examination of surface modification techniques for PDMS, especially through the incorporation of surfactants, is essential to optimize these processes and enhance the material's functionality. With the significant growth in PDMS usage, it becomes imperative to study and evaluate methods to reduce its hydrophobicity, aiming for more effective and diverse applications. Considering these factors, this dissertation explores the modification of PDMS surface wettability to broaden its potential in various technological applications.

1.1. Goals

The general objective of this work is to investigate and optimize the modification of PDMS wettability through the addition of surfactants, while the specific objectives include

evaluating the influence of different surfactants on the wettability and thermal conductivity of PDMS, as well as analyzing their practical applications.

To achieve these objectives, methodological procedures were adopted, involving the preparation of PDMS samples with different concentrations and types of surfactants as well as curing temperatures. An orthogonal array by the Taguchi method was used for parameter combination selection, followed by detailed contact angle and thermal conductivity tests on the produced samples. Grey Relational Analysis was also applied to integrate the results of both tests and thus determine the optimal sample, considering the influence of each test.

This research enhances the knowledge of modifying polymeric materials by researching the selection and use of surfactants to enhance the hydrophilicity of PDMS in different applications.

1.2. Work structure

This work is structured into several chapters to facilitate understanding and organization of the obtained results. The first chapter is the introduction, presenting the context, objectives, and structure of the work. Then, in chapter 2, a literature review, which was transformed into a review article, provides an in-depth analysis of relevant studies in the literature on major traditional techniques for altering wettability on the PDMS surface. In the third chapter, also transformed into an article, the materials and methods used in the laboratory experiments are detailed, including the description of the materials used and the procedures for making the test samples. Furthermore, the results obtained, and their analysis are presented in the third chapter. Finally, in the last chapter, the conclusions drawn throughout the work and proposed future works in this area are presented.

With this structure, it is expected to contribute to a deeper understanding of the influence of each selected parameter and level on altering wettability as well as thermal conductivity on the PDMS surface. This study is relevant for the advancement of materials and process optimization, with potential significant impact on industrial sectors

Chapter 2

A Review of Methods to Modify the PDMS Surface Wettability and their Applications [1]

Abstract: Polydimethylsiloxane (PDMS) has attracted great attention in various fields due to its excellent properties, but its inherent hydrophobicity presents challenges in many applications that require controlled wettability. The purpose of this review is to provide a comprehensive overview of some key strategies for modifying the wettability of PDMS surfaces by providing the main traditional methods for this modification and the results of altering the contact angle and other characteristics associated with this property. Four main technologies are discussed, namely, oxygen plasma treatment, surfactant addition, UV-ozone treatment, and the incorporation of nanomaterials, as these traditional methods are commonly selected due to the greater availability of information, their lower complexity compared to the new techniques, and the lower cost associated with them. Oxygen plasma treatment is a widely used method for improving the hydrophilicity of PDMS surfaces by introducing polar functional groups through oxidation reactions. The addition of surfactants provides a versatile method for altering the wettability of PDMS, where the selection and concentration of the surfactant play an important role in achieving the desired surface properties. UV-ozone treatment is an effective method for increasing the surface energy of PDMS, inducing oxidation, and generating hydrophilic functional groups. Furthermore, the incorporation of nanomaterials into PDMS matrices represents a promising route for modifying wettability, providing adjustable surface properties through controlled dispersion and interfacial interactions. The synergistic effect of nanomaterials, such as nanoparticles and nanotubes, helps to improve wetting behaviour and surface energy. The present review discusses recent advances of each technique and highlights their underlying mechanisms, advantages, and limitations. Additionally, promising trends and future prospects for surface modification of PDMS are discussed, and the importance of tailoring wettability for applications ranging from microfluidics to biomedical devices is highlighted. Traditional methods are often chosen to modify the wettability of the PDMS surface because they have more information available in the literature, are less complex than new techniques, and are also less expensive.

[1] Neves, L. et al., 2024. A Review of Methods to Modify the PDMS Surface Wettability and their Applications. https://doi.org/10.3390/mi15060670

Keywords: polydimethylsiloxane; PDMS; wettability modification; surface treatment; nanomaterial incorporation; PDMS applications

2.1. Introduction

The silicone elastomer known as polydimethylsiloxane (PDMS) has been widely employed as the main substrate in various micro/nano applications. These include microcontact printing [5], microfluidics [6], [7], [8], [9], and microreactors [10], as well as in fabric coatings and water–oil separation [23], [24], [25], [26], [27], [28], among many other applications. This is due to its attractive characteristics, such as easiness of manufacturing, non-toxicity, optical transparency, low cost, favourable biocompatibility, elastic nature, ease to process and advantageous chemical and physical properties, the malleability for moulding on (sub)micrometric scales, and effective adhesion to itself and to the glass [29], [30], [31], [32], [33]. However, to improve the surface properties of PDMS, such as wettability, it is essential to modify the material to specific conditions.

Wettability, defined by the contact angle (θ), refers to the measure of adhesion between a liquid and a solid surface, which performs a fundamental role in understanding the interactions between materials and liquids. The hydrophobicity or hydrophilicity of a surface is defined by the surface energy of the material. For PDMS, hydrophobicity is given by the presence of methyl groups (-CH_3) in its structure, which gives it low polarity and weak interactions with water molecules, making it a hydrophobic surface. The presence of hydroxyl groups (-OH) or other polar groups increases hydrophilicity, providing a stronger interaction with water and making the surface more hydrophilic [15], [16]. The contact angle lesser than 10° characterises the surface as superhydrophilic; between $10° \leq \theta < 90°$ as hydrophilic, favouring the spread of the liquid; from $90° \leq \theta < 150°$ is considered hydrophobic; and greater than 150° defines the surface as superhydrophobic, where the droplet tends to take on a more spherical shape [17], [18], [19], [20], [21]. The basic model for the contact angle of an idealised solid surface is described by the Young equation, Equation (1) [34]:

$$\cos(\theta) = \frac{\gamma_{SV} - \gamma_{SL}}{\gamma_{LV}} \quad 1)$$

where θ is the contact angle, γ_{SV} is the interfacial tensions between solid and vapour, γ_{SL} is the interfacial tensions between solid and liquid, and γ_{LV} is the interfacial tensions between liquid and vapour. The relation can be better visualised in Figure 1.

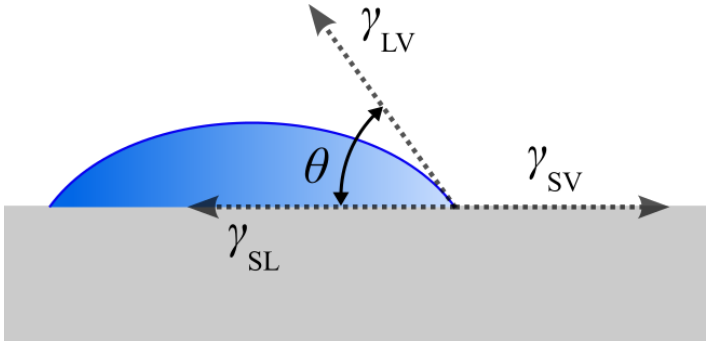

Figure 1 - Contact angle (θ) and interfacial tensions (γ) between the solid (S), liquid (L), and vapour (V).

As mentioned, the Young equation is nonetheless based on an ideal surface without roughness. However, when roughness is considered, the contact angle is corrected by a roughness factor. The Wezel Theory [35] for wettability on a rough surface is demonstrated in Equation (2):

$$\cos\,\theta^* = r\cos\,\theta \qquad 2)$$

where θ^* is the apparent contact angle and r is the roughness factor calculated as the ratio between the ideal and real surface. The equations show that an increase in roughness makes the hydrophilic surface more hydrophilic and the hydrophobic surface more hydrophobic.

The roughness, meanwhile, has only a fractional impact on the contact angle, as well as on parameters such as porosity and wettability of the material. Other models, such as the Cassie–Baxter model (Equation (3)), can be applied specifically to hydrophobic surfaces with sharp edges, for example [35], [36].

$$\cos\theta^* = f - 1 + rf\cos\,\theta \qquad 3)$$

where f is the projected wet area, and r represents the roughness factor.

Superhydrophobic or superhydrophilic characteristics can be applied in various areas. Examples of the use of superhydrophobic surfaces include self-cleaning paint and acrylics that prevent the adhesion of dirt, improving the surface's capacity to be cleaned by rain. These coatings can also be applied to avoid snow accumulation on tall structures such as antennas; in toilet urinals to repel urine, reducing the need for water; in paints for architectural heritage; in photovoltaic panels to remove dust and increase efficiency; in functional textiles with the use of nanoparticles; and in other diverse applications as anti-icing properties in the aerospace industry and wind blades beyond anti-fouling purpose [37], [38], [39], [40], [41]. Superhydrophilic applications include self-cleaning paint and coatings that expedite the cleaning process with a stream of water or rain. Antifogging mirrors, glasses, and shields are useful for preventing

fogging caused by humidity. Additionally, antifogging bags and packaging films are employed to increase the water capacity to extend [42]. Other applications in heat transfer may also be desirable: in a two-phase heat transfer device, a superhydrophilic surface improves the ability of water to wet the hot area where the evaporation occurs, while a superhydrophobic surface is effective in repelling droplets on the cold surface formed by the condensation of vapour [38].

Despite the great advantages as anti-corrosion, self-cleaning, and anti-icing [43] due to the inherently hydrophobic characteristics, PDMS imposes limitations for certain purposes. For example, for applications that require contact angles between 20 and 70°, such as liquid lenses, it is essential to reduce the hydrophobicity of PDMS [44]. In addition, there is a limitation in the use of PDMS as a biomaterial and cell adhesion on cell culture substrates [45] because of its hydrophobic nature. There is also a difficulty of specific equipment and time-consuming procedures, obstacles that can be manifested in surface hydrophilisation [37], [46], [47].

A wide range of papers were found on PDMS and its properties, specifically its wettability and how to modify it, mainly by traditional methods. These traditional methods are often chosen to change the wettability of the PDMS surface because they have more information available in the literature, are less complex than new techniques, and are less expensive. However, no research was found that objectively explained the main traditional methods of altering the wettability of the PDMS surface, the results of altering the contact angle, and other characteristics associated with this property.

Therefore, this article presents a brief review of the main treatments and their studies to change the wettability of the PDMS surface, detailing the phenomena involved in the interaction between the surface and the fluid, the advantages and disadvantages of using this type of method, and the main results achieved as well as their main applications. It also approaches the roughness, additives, changes in the molecular surface, and other parameters that have influence in the contact angle. The main observations on the methods and future prospects in the area are also addressed.

Table 1 presents a summary of some advantages and disadvantages of the main methods used for the fabrication of PDMS-based superhydrophilic/superhydrophobic coatings, as well as their major applications and water contact angle (WCA) changes over time. The methods considered most important are further discussed.

Table 1 - Some advantages and disadvantages of different methods to fabricate PDMS-based superhydrophilic/superhydrophobic coatings.

Methods	WCA (and Over Time) ≈	Advantages	Disadvantages	Applications	Ref.
Oxygen plasma treatment	17°–46° (50°–115°, after 6 h) *	Low cost, ease of implementation, and compatibility with sensitive materials	Fast hydrophobic recovery and limitations on penetration depth	Microfluidic devices	[48]
Oxygen plasma treatment	40°–101,17° *			Improvement of polydimethylsiloxane (PDMS) surface biocompatibility as the most used biomaterial in maxillofacial prostheses for intraoral defects	[42]
Oxygen plasma treatment (SRMJ)	70°	Biological cells adhered more easily to surfaces		Controlling biological cells' attachment on biocompatible polymer material	[49]
UV-ozone treatment	10°–40° (40°–95°, after 30 days) *	Quick process and room temperature operation	Temporary surface modification and potential for degradation	Microfluidic	[50]
UV-ozone treatment	7°, after 240 min UV/O treatment				[51]
Surfactant addition	18°–68° (Table 2)	Ease of application; immediate effect and versatility	Uniformity challenges and potential leaching	Microfluidic, microfluidic biomedical, and non-toxic antibiofouling coatings	[52]
Incorporation of nanomaterials	<150°	Long-lasting modification and improvement of mechanical properties	Dispersion challenges, ecological problems, and high costs	Antibacterial activity and oil–water separation	[53]
Incorporation of nanomaterials	<150°			Self-cleaning, oil–water separation, and flame-retardant properties	[54]
Incorporation of nanomaterials	158°			Oil–water separation	[55]

* Varies depending on the time of PDMS exposure to the treatment.

2.2. Oxygen Plasma Treatment

The PDMS surface modification through oxygen plasma treatment stands out as a fundamental approach, particularly in the fast prototyping of PDMS microfluidic devices [56]. This process involves the introduction of polar functional groups, notably the silanol group (SiOH), through oxidation processes and the subsequent removal of hydrocarbon groups by surface corrosion [44], [57], as demonstrated in Figure 2. These functional groups alter the surface characteristics of PDMS, converting it from hydrophobic to hydrophilic. However, it is important to note that, on one hand, plasma-treated surfaces exhibit a recovery of hydrophobicity within minutes of exposure [58], particularly when subjected to bonding and heat treatment [59]. On the other hand, prolonged plasma treatments can cause undesirable surface cracks that compromise the integrity of the device [57], [60], [61].

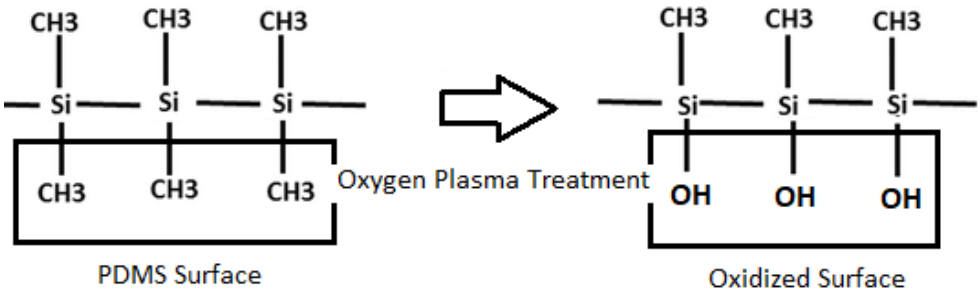

Figure 2 - Surface reaction of PDMS under O2 plasma treatment.

The hydrophobic recovery of PDMS has been extensively investigated using techniques such as measuring the WCA on the surface [62], scanning electron microscopy (SEM) [56], and X-ray photoelectron spectroscopy (XPS) [63]. Several factors play crucial roles in this process, including the reorientation of polar groups from the surface to the interior of the material, the diffusion of low molecular weight species from the bulk to the surface, and the condensation of hydroxyl groups [64]. In addition, the recovery rate is influenced by storage conditions such as temperature, humidity, and the presence of aqueous fluids and surfactants used to preserve PDMS devices [48], [65], [66], [67], [68], [69], [70]. Recently, several studies have been carried out an analysis of each of these parameters to alter the surface properties of PDMS, as is shown below.

However, such techniques may present some challenges, including sophisticated and time-consuming mechanisms, expensive demands for vacuum apparatus and DC power supply

for high voltage generation, safety issues, and well-trained technicians [47]. Also, this technique suffers from a short lifetime before hydrophobic recovery [57].

2.2.1. Principles of Oxygen Plasma Treatment and Applications of PDMS Treated with Oxygen Plasma

In oxygen plasma treatment, the oxygen is ionised by the application of high voltage to form ions and free electrons. These reactive species, such as oxygen ions, play a key role in their interactions with material surfaces, facilitating chemical and physical attacks. This process results in the breaking of chain bonds in the PDMS molecular structure, thus introducing oxygen-containing functional groups. In addition, oxygen plasma cleans surfaces, removes contaminants, and increases surface energy, facilitating the adhesion of coatings [71]. Precise control of the process parameters, such as exposure time, power, and gas composition, are essential to adapt the surface properties to the specific needs of the application [72].

The oxygen plasma chamber has a controlled environment which generally consists of a vacuum chamber equipped with electrodes. Oxygen gas is put into the chamber, and then an energy source, such as a high-frequency current, is applied to the electrodes, ionising the gas and thus generating a reactive plasma. This plasma interacts with the PDMS surface, causing chemical and physical changes. The structure of the chamber and the operating parameters, such as pressure, plasma power, and treatment time, are adjusted according to the application and to optimise the effectiveness of the modification [58]. In a study [67], this experiment was conducted on microchannels using an oxygen plasma reactor (Series 790, Plasma-Therm, Inc., St. Petersburg, FL, USA), and the results showed an improvement in the hydrophilicity of the PDMS surface, reducing the WCA from 120° to 17° with a 300 s treatment.

In oxygen plasma treatment for polydimethylsiloxane modification, power, time, speed, and oxygen concentration are the main factors. Increasing power can exacerbate surface attacks, but balance is key to avoiding damage in the PDMS. Exposure time affects the introduction of modification and needs to be optimised to achieve the desired properties without compromising the integrity of the material. Exposure speed affects the uniformity of the retouching and requires precise control. Oxygen concentration determines the introduction of

functional groups but needs to be balanced to avoid excessive degradation [73]. Careful adjustment of these parameters is crucial to obtaining the desired results when modifying the surface of PDMS. This technique is widely used to modify surfaces due to its ability to act on surface layers without deeply affecting the underlying structure. In addition, plasma is effective in sterilisation and in the chemical and morphological modification of surfaces [74], [75].

The oxygen plasma treatment technique plays a crucial role in several areas due to its ability to alter the surface properties of materials. This approach finds application in a wide range of sectors, including microfluidic devices [60], adhesives and sealants [76], microfabrication of electronic circuits [77], biomedical implants [78], packaging coatings [79], biomaterials [49], and chemical sensors [80], as well as in the manufacture of lenses and optics [78]. Oxygen plasma treatment is preferred in all these applications due to its ability to characterise surface properties, such as adhesion, wettability, and functionality, according to the specific needs of each sector.

2.2.2. Effects of Oxygen Plasma Treatment on PDMS

Typically, the changes resulting from plasma exposure depend on variables such as applied power, exposure time, and the type of precursor gas, directly affecting the properties of the treated surface [81]. Plasma technology offers flexibility and desirable cellular responses, making it a commercially viable option [82], [83], [84]. The hydrophilicity resulting from the formation of an oxide layer on the surface during exposure to plasma tends to decrease gradually over time, due to the migration of oligomers, molecules composed of a small number of monomers, which are the basic units of a macromolecule, from the interior to the surface and the reorientation of polar groups [58], [67], [85].

In a study conducted by Tan et al. [67], a simple protocol was developed to produce hydrophilic and usable PDMS microchannel devices. This protocol involves a second prolonged oxygen plasma treatment and proper storage of the devices. The results indicated that, under a plasma power of 70 W, prolonged treatment of more than 5 min resulted in a PDMS surface maintaining the hydrophilicity for more than 6 h. In addition, storing the treated devices in deionised water allowed them to maintain their hydrophilicity for weeks. Analysis using atomic force microscopy (AFM) revealed that a longer exposure time to the oxygen plasma resulted in

a smoother surface. The study used six different treatment times, ranging from 100 to 500 s, while the plasma power remained constant at 70 W. After plasma treatment, the devices were immersed in deionised water to remove air bubbles and stored in a vacuum chamber for seven days. AFM analyses were conducted within one hour of exposure to oxygen plasma. The roughness analysis revealed that the oxygen plasma treatment significantly reduced the roughness of the PDMS surface. For example, the root mean square (RMS) roughness dropped from 3.6 nm to 0.9 nm after a 500 s treatment, as shown in Figure 3. In addition, the formation of nano-cracks during oxygen plasma treatment proved potentially beneficial, as recent studies suggest that these nano-cracks can be furnished with adhesive proteins, which aids in the growth and modulation of biological cells [86].

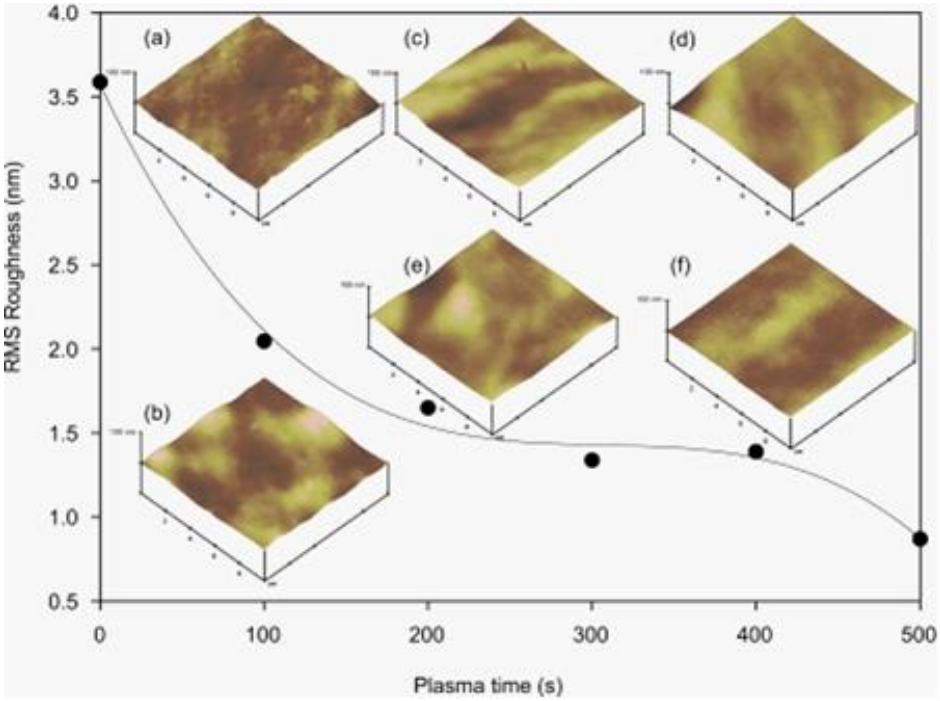

Figure 3 - Mean square roughness as a function of oxygen plasma treatment time. The respective AFM images are taken from the sample with oxygen plasma exposure of (a) 0 s, (b) 100 s, (c) 200 s, (d) 300 s, (e) 400 s, and (f) 500 s. Obtained from [67].

Figure 4 illustrates how the WCA varies over the air exposure time and, in general terms, how a longer plasma treatment reduces it. Untreated PDMS maintained a WCA of around 120°. After a 100 s treatment, the WCA dropped to 46° and then returned to around 115° after 6 h. With 200 s of treatment, the WCA dropped even further, reaching 21°, and then approached 115° again after 6 h. For treatments longer than 300 s, the initial WCA was 17°, and after 6 h, it remained between 50° and 60°. This highlights how the plasma treatment time has a notable impact on the wettability properties of the PDMS surface [67].

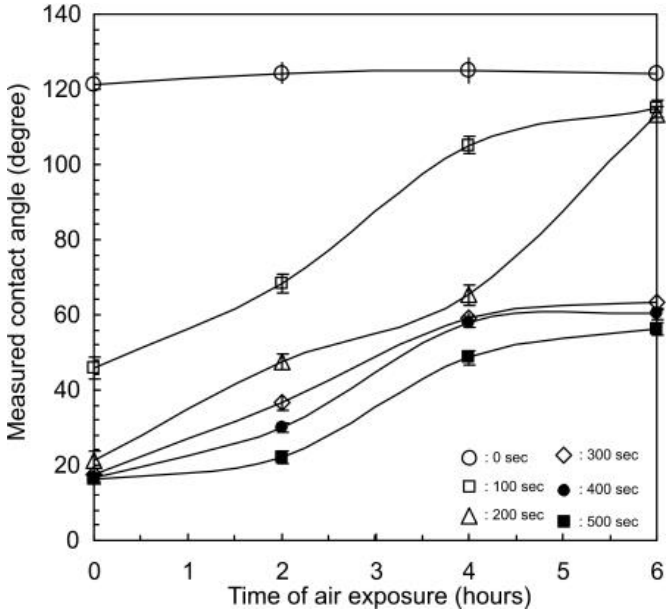

Figure 4 - Water contact angle (WCA) as a function of air exposure time. Obtained from [67].

The results indicate that storing PDMS samples in water and under a vacuum can extend the hydrophilicity for at least 7 days, due to the surface energy of the water, preventing the rearrangement of the silanol group (SiOH) on the channel walls. This suggests that the surface energy of the fluid can affect the storage time of hydrophilic PDMS devices. Furthermore, it should be considered that the analysis of the surface in channels cannot be directly compared to that of a flat surface due to the influence of channel confinement.

Duangkanya et al. [44] presented the dependence of the oxygen plasma treatment time on the hydrophilicity on the surface of different thicknesses of PDMS thin films. For a thickness of 43 ± 1.44 µm, the initial contact angle (CA) between glycerol and the untreated PDMS film was around 104°; as the film was treated with oxygen plasma, it decreased to 52° at a surface treatment time of 24 s. As can be seen in Figure 5a–e for a thickness of 15 ± 1.17 µm, the initial untreated angle was 77°, and, for the process, it decreased to 15° when the surface treatment time was 18 s. This shows the influence of the surface treatment on the CA, and it was also noted that the rate of hydrophilic transformation of the thin film was much faster than that of the thick PDMS film.

In the same work mentioned above, the PDMS films with a thickness of 43 ± 1.44 µm, without the oxygen plasma treatment time, had an average surface roughness of 38 nm and gradually increased to 519 nm at the oxygen plasma treatment time of 24 s (Figure 5f), contrary to Tan et al. [67] Similarly, PDMS films with a thickness of 15 ± 1.17 µm, without the oxygen plasma treatment time, had an average surface roughness of 59 nm and increased exponentially to 606 nm at the 24 s oxygen plasma treatment time.

The CA, in general, is inversely related to the roughness of the film, especially when it comes to hydrophilic surfaces, where the apparent CA is less than 90° [87]. Figure 5g illustrates how the CA decreased more slowly for thick PDMS films during a 24 s plasma treatment period. For thinner films, this decrease occurs more quickly.

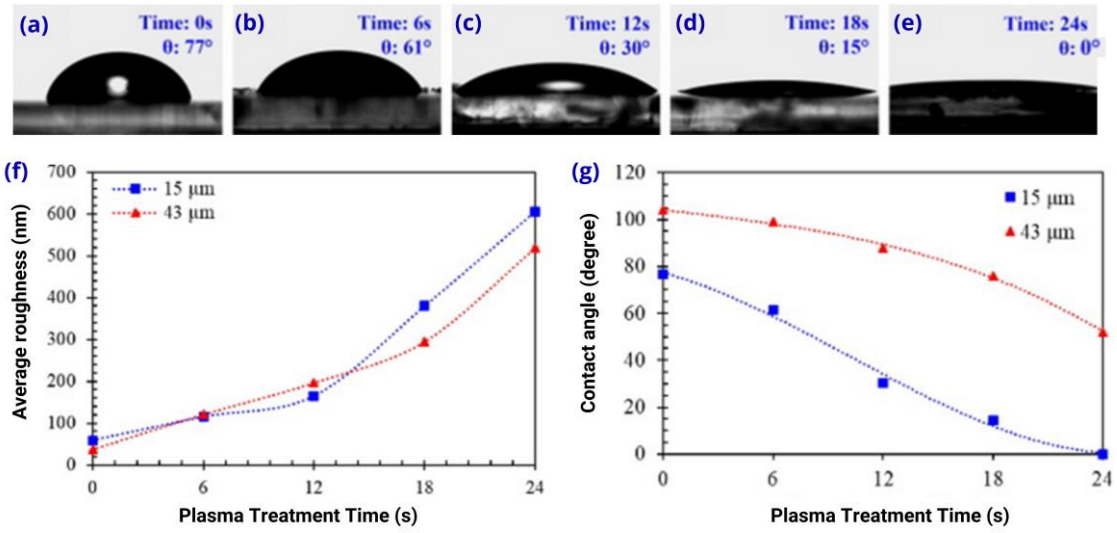

Figure 5 - The contact angle between the glycerol drop and the PDMS film with a thickness of 15 ± 1.17 µm without oxygen plasma treatment (**a**) and with oxygen plasma treatment times of 6 s (**b**), 12 s (**c**), 18 s (**d**), and 24 s (**e**). Average roughness of PDMS thin films at thicknesses of 43 ± 1.44 µm and 15 ± 1.17 µm (**f**). Glycerol contact angles on PDMS films with different plasma treatment times (**g**). Adapted from [44].

An innovative approach to surface modification with plasma [83], employed a scanning radical microjet (SRMJ) with a microplasma of O_2 to control the adhesion of biological cells. The used technique has several advantages, such as higher rates of surface modification while minimising damage compared to conventional plasma exposure. Furthermore, the additional scanning speeds contribute to improving the hydrophilicity of the surface and significantly reducing roughness. However, in agreement with Duangkanya et al. [44], the average roughness values (Ra) and root mean square (RMS) show a gradual increase in their values as oxygen flow rates increase [83].

Figure 6 displays the effects of oxygen flow rates on WCA on PDMS surfaces treated by SRMJ. As the oxygen flow rate increased from 20 to 40 ccm, there was a gradual reduction in the minimum angle (θ min) from 83° to around 69°. However, as the oxygen flow rate continued to increase, from 40 ccm to 110 ccm, the hydrophilicity of the PDMS surface stabilised, resulting in a practically constant WCA.

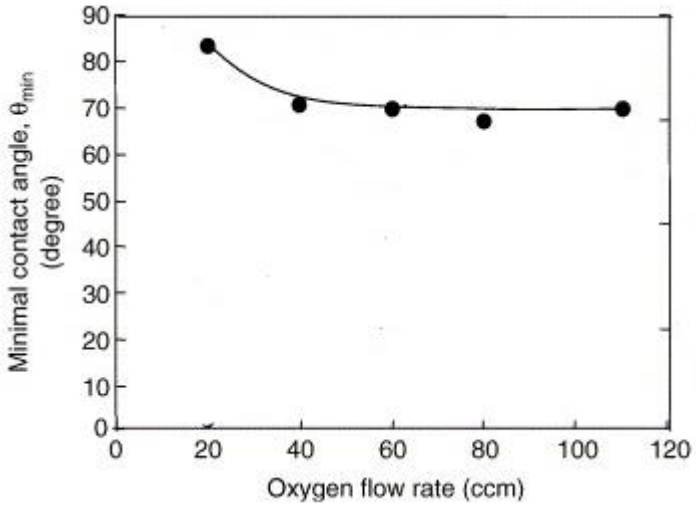

Figure 6 - Relationship between minimum contact angle, θ min, and width of treated line, W, for different oxygen flow rates. Adapted from [83].

The AFM observation results in this study demonstrated that biological cells attach more easily when the surface roughness values are higher. Tan et al. [83] also stated that although the result can be attributed to the presence of stronger cell–surface interactions on rough surfaces, it is essential to conduct further studies to clarify the cause-and-effect relationship between surface roughness and cell adhesion at the nanometric level.

Amerian et al. [47] exposed PDMS samples to plasma in a cylindrical reactor containing O_2 gas with variable plasma exposure times of 0.5 min, 2.5 min, and 5 min for analysis, keeping the other factors constant. The WCA of the PDMS strips for samples with only 30 s of plasma exposure decreased from 117.9° to around 101.17°, then changed to 87.18° after 2.5 min, and after 5 min, the WCA dropped to 40°.

The results of the study revealed that the roughness of the PDMS surface increases with the plasma exposure time interval, according to Figure 7. The authors also reported that the PDMS films used in this study tended to crack after long plasma exposure times.

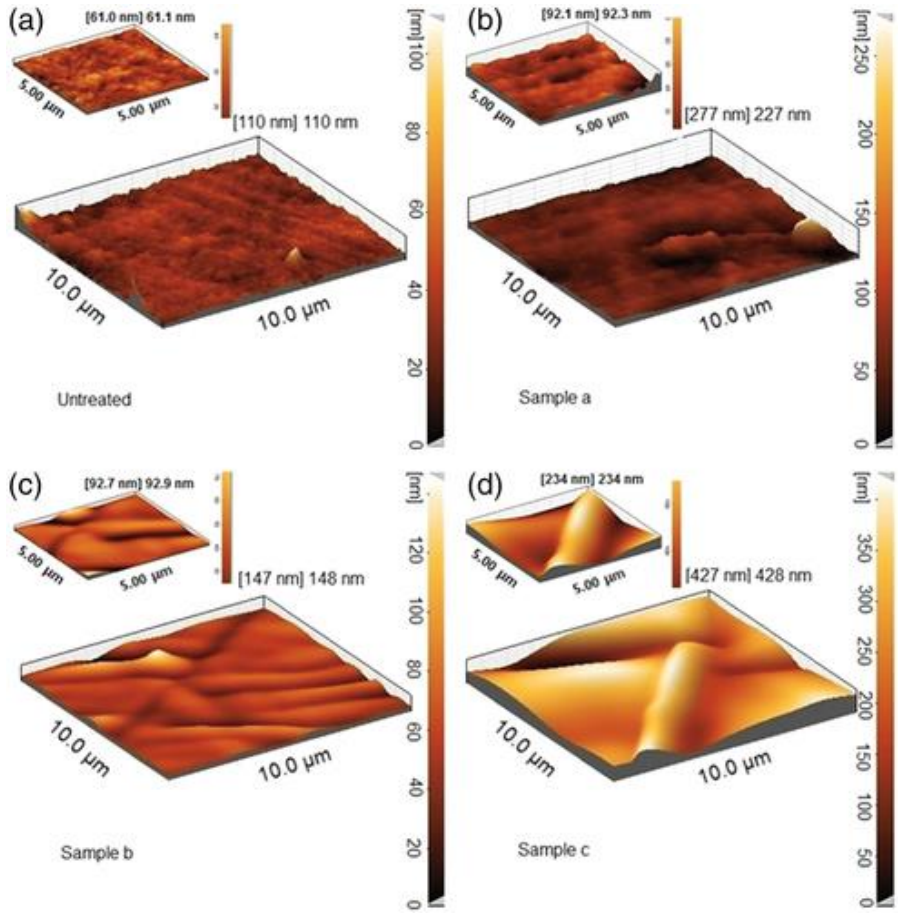

Figure 7 - AFM images: (a) untreated, (b) sample a (0.5 min), (c) sample b (2.5 min), and (d) sample c (5 min). AFM, atomic force microscopy. Adapted from [47].

2.3. UV-Ozone Treatment

In this section, UV-ozone treatment in order to modify the surface energy and incorporate polar groups is discussed, since UV irradiation in combination with ozone has been widely employed for these purposes [50], [88], [89], [90].

According to Berdichevsky et al., the combination of UV light and ozone proved to be effective in modifying the wettability of PDMS [51], with results comparable to oxygen plasma treatment, but at a slower rate [91], allowing for a precise control of wettability. For example, the oxygen plasma process of 400 W at 10 mTorr for 1 min resulted in a WCA of less than 10° [92], while UV ozone treatment required approximately 1 h to achieve a similar WCA, e.g., [91], [93].

Polydimethylsiloxane, when subjected to UV-ozone treatment, results in the oxidation of the chains on the surface in more internal layers in the PDMS, free of cracks, in contrast to the approach using oxygen plasma [94], [95]. One study described the use of UV/ozone treatment in the production of microfluidic devices [51]. In particular, they explored the mass conversion of PDMS by means of deep penetration, as well as the complete oxidation of thick membranes by means of UV-ozone treatment [52], [96].

The restoration of hydrophobicity in this study was noted on surfaces treated with RF oxygen plasma and bulk PDMS subjected to UV-ozone over 1 to 2 days. Similarly, the membrane treated for 60 min exhibited an analogous behaviour, while the membrane treated for 120 min, according to the authors, remained hydrophilic for more than 3 months, although Figure 8 only shows experimental points of approximately up to 21 days. The discrepancy in the results is attributed to the hydrophobic recovery mechanism, indicating the significant influence of the diffusion of low molecular weight PDMS chains. The rapid recovery after UV-ozone treatment is explained by the high diffusivity of the PDMS chains in the oxidised layer, while the slower recovery after UV-ozone treatment compared to RF oxygen plasma is associated with the greater thickness of the modified layer [97], [98].

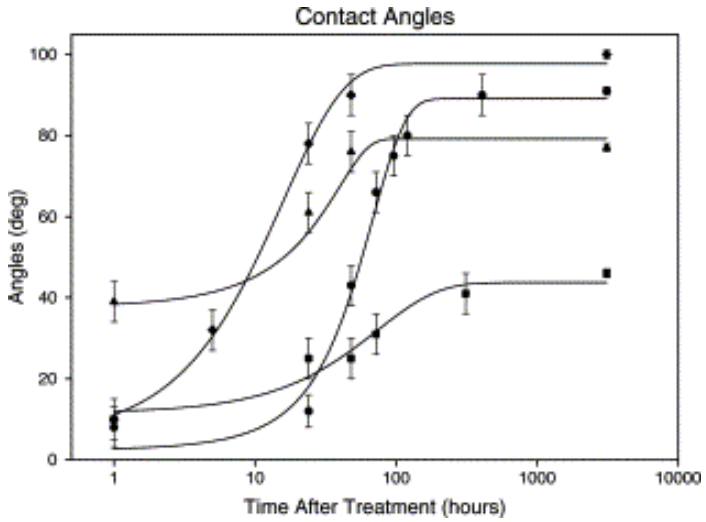

Figure 8 - Contact angles versus time (logarithmic scale). Symbols: (•) PDMS membrane treated with UV-ozone for 60 min of 14 μm; (♦) bulk PDMS treated with RF oxygen plasma for 1 min; (▲) treated with UV-ozone for 30 min the bulk PDMS; and (■) 120 min UV-ozone exposure of the 14 μm PDMS membrane. Obtained from [51].

Ma et al. [94] produced microfluidic devices with standard soft lithography techniques. The effects of curing time on surface modification by UV-ozone was presented where thermal curing eliminates low molecular weight species in PDMS, reducing hydrophobic recovery post plasma treatment. Additional curing time accelerates the surface hydrophilisation of PDMS.

According to Figure 9, for a fixed curing temperature of 80°C, in the first 60 min after UV-ozone treatment, there was a small discrepancy in the WCA for PDMS cured at different times, except for 60 min. However, notable differences emerged after 1 h of UV-ozone exposure, indicating that PDMS pieces with longer curing times show faster surface hydrophilisation. The maintenance of wettability by immersion in water was also analysed, where initially there was a reduction in the WCA with water for all PDMS parts, suggesting water absorption by the PDMS matrix.

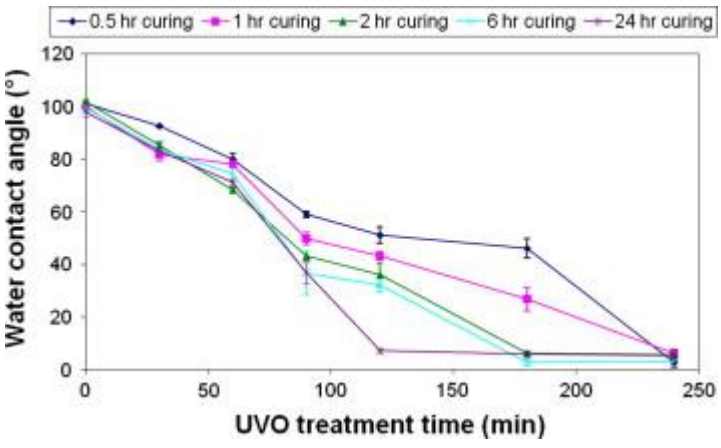

Figure 9 - The effect of curing time on the surface hydrophilisation process of PDMS at 80°C. Obtained from [94].

Oláh et al. [99] carried out a study focusing on the Johnson–Kendall–Roberts (JKR) contact mechanics methodology to investigate PDMS samples before and after surface treatment with UV-ozone. With increasing exposure to UV-ozone, the gradual formation of a hydrophilic surface layer similar to silica was observed below 20° WCA (Figure 10). Subsequently, there was a hydrophobic recovery evidenced by the increase in WCA (Figure 11). This phenomenon supports the hypothesis that hydrophobic recovery results, mainly from the progressive coverage of a permanent silica-like structure with free siloxanes and/or reorientation of polar groups.

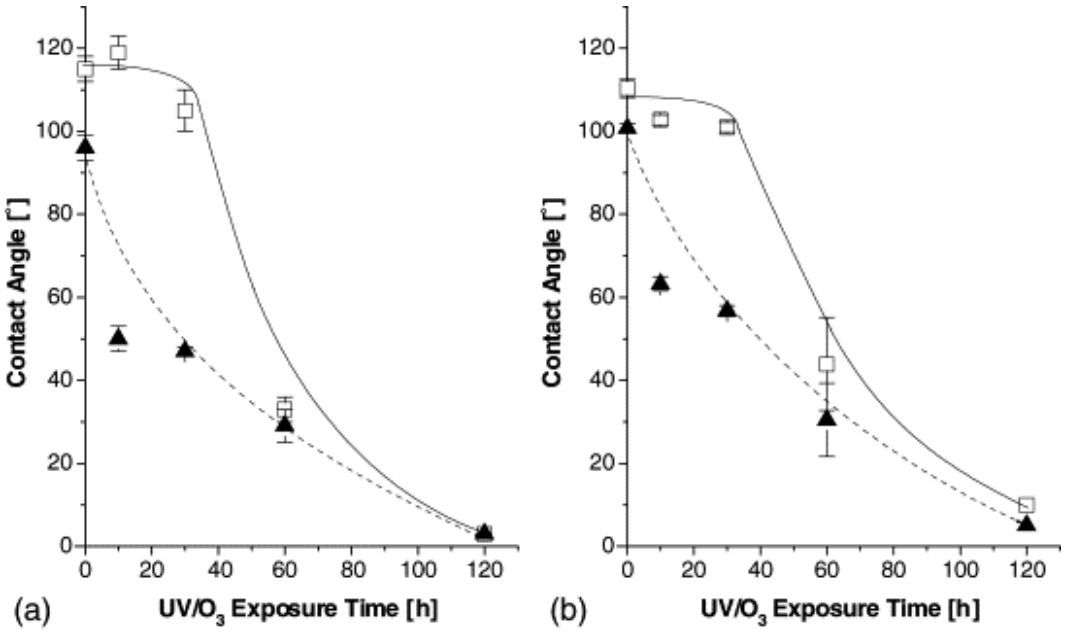

Figure 10- Water contact angles as a function of UV-ozone exposure time. (**a**) Sylgard 184, and (**b**) Sylgard 170. (□) Advancing and (▲) receding contact angles. The error bars indicate the standard deviation, and the dashed and solid lines serve to guide the eye only. Obtained from [99].

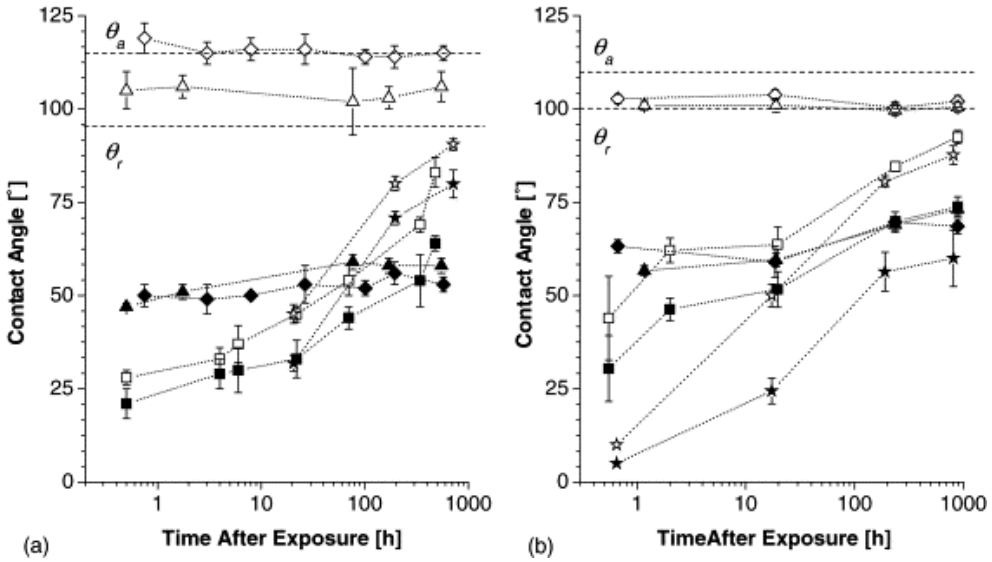

Figure 11 - Hydrophobic recovery of PDMS after 10–120 min exposure to UV-ozone: (**a**) Sylgard 184, (**b**) Sylgard 170. The dotted lines indicate the values of the initial advancing (θa) and receding contact angles (θr). Empty symbols: advancing contact angles, filled symbols: receding contact angles. Diamond: 10 min exposure; triangle: 30 min exposure; square: 60 min exposure. The horizontal, dashed lines indicate advancing and receding contact angles, respectively, of untreated PDMS. Obtained from [99].

The same study [99] showed that on PDMS with homogeneously dispersed filler (Sylgard 184), the surface roughness decreased as the oxidised region "collapsed" to form a smooth SiO x layer (final roughness < 2 nm). On the other hand, on PDMS with heterogeneously aggregated filler particles (Sylgard 170), the surface roughness increased with the treatment dose due to the "collapse" of the oxidised region, exposing the contours of the underlying filler aggregates (final roughness ≈140 nm). The effect of UV-ozone treatment on surface roughness varied between Sylgard 184 and 170, due to differences in filler content and type. Atomic force microscopy revealed that Sylgard 184 has smooth, homogeneous surfaces, with the root mean square of the roughness decreasing from 4.0 ± 0.4 to 1.9 ± 0.2 nm after exposure of 20 × 20 μm². This pattern is consistent with previous observations by Vasilets et al. [50] on PDMS exposed to UV-ozone. On the other hand, Sylgard 170 exhibited a rougher initial morphology, with a roughness of 24 ± 1.2 nm, and roughness values increasing with exposure time, probably due to the higher filler content [99].

2.4. Surfactant Addition

Several wettability modification methods have limitations, such as restricted chemical stability and complexity in microfluidic channels [100]. Problems such as surface cracking, increased roughness, and loss of elasticity occur in some modifications, limiting the usefulness of PDMS surfaces [101], [102]. To overcome these challenges, one of the possibilities is to use silicone-based molecules as direct functionalisation agents, preserving the natural characteristics of elastomers. Wetting agents, surfactants that usually consist of hydrophobic and hydrophilic portions, are widely recognised as useful substances for facilitating the dispersion of aqueous solutions on surfaces that are naturally hydrophobic [103], [104]. The main surface modification methods analysed in this section are modification by bulk mixing and immersion in a solution.

2.4.1. Effects of Surface Coating Treatment with Surfactants on PDMS

Fatona et al. [100] developed an innovative approach to functionalise PDMS in a single step, using standardised moulds to define the surface areas to be modified, with functionalisation taking place during the vulcanisation of the PDMS. This method allowed for the creation of matrices in which ionic and non-ionic surfactants were applied to the surface of the elastomer during the curing process. This resulted in the spatial organisation of charged and uncharged alkyl/polymer chains in the PDMS.

In their experiment, seven tested surfactants led to hydrophilic surfaces after one-step mould modification, with significantly lower WCA than unmodified PDMS (109°). The stability of the hydrophilicity of the modified surfaces and the intensity of the interactions between the PDMS and the surfactants were evaluated by immersing the treated PDMS surfaces in high-purity water (18.2 MΩ) for 20 h. It was observed that, in most cases, immersion of the treated surfaces resulted in a significant change in the WCA. As expected, the interactions between the

PDMS and the ionic surfactants proved to be weak, since these surfactants were solvated when the modified surfaces came in contact with water.

The influence of temperature on the hydrophilicity of the triblock copolymer and PDMS surfaces treated with Silsurf was also examined. After treatment, the modified surfaces were immersed in water for two hours, dried with nitrogen, and then incubated at different temperatures for one hour before the surface WCA was evaluated [100].

Table 2 represents a summary of the changes in WCA as a function of the addition of the seven surfactants, such as WCA measurements of surfactant functionalised PDMS surfaces; measurements performed on PDMS surfaces as prepared before soaking, after soaking, and after 11 days of storage in air; quantification of WCA measurements for all surfactant-modified PDMS surfaces; and quantification of WCA measurements for surfactant-modified PDMS surfaces at different temperatures, performed in the study mentioned above.

Table 2 - Representation of the wettability of PDMS surfaces functionalised with each surfactant molecule, based on the work of Fatona et al. [100].

Surfactant	WCA (Before Soaking)	WCA (After Soaking)	WCA (After 11 Days or More)	WCA (21°C)	WCA (60°C)	WCA (80°C)	WCA (100°C)	Chemical Structure	Morphology before Soaking
Unmodified PDMS	109°	-	-	-	-	-	-	$(-Si(CH_3)_2-O-)n$	-
Sodium dodecyl sulphate (SDS)	57°	114°	-	-	-	-	-	$CH_3(CH_2)_{11}OSO_3Na$	Opaque and roughened surfaces
Cetyl trimethylammonium bromide (CTAB)	38°	106°	-	-	-	-	-	$C_{16}H_{33}N(CH_3)_3Br$	Opaque and roughened surfaces
Tween 20	39°	91°	Complete reversal	-	-	-	-	$CH_3(CH_2)_{18}(OCH_2CH_2)nOH$	Optically clear and lowest surface roughness
Silsurf A008-UP	20°	63°	Complete reversal	≈40°	≈49°	≈67°	≈68°	-	Optically clear and surfaces presenting small dimples
* Alkyl (o-Wet)	43°	36°	-	≈40°	≈48°	≈53°	≈68°	(PEG) − (PDMS) − (PEG) − (Alkyl)	Smooth surfaces with depressions (microns wide)
* Siloxane (n-Wet)	47°	27°	-	≈38°	≈36°	≈38°	≈40°	(PEG) − (PDMS) − (PEG) − (Si-O)	Smooth surfaces with depressions (sub-micron wide)
* Siloxane (a-Wet) {has a more highly branched siloxane}	22°	25°	40°	≈21°	≈18°	≈19°	≈19°	(PEG)−(PDMS)−(PEG)−(Si-O) branched	-

* Poly(ethyleneglycol)-silicone-poly(ethyleneglycol) (PEG-PDMS-PEG) non-ionic triblock copolymers with terminal functionalities.

Based on the results provided in Table 2, it can be seen that the morphology of the treated surfaces varied, including opaque and roughened surfaces, smooth surfaces with depressions of various sizes, and surfaces with small dimples. Tween 20 exhibited complete WCA reversal post-soaking and had the smoothest and clearest surfaces with the lowest roughness. Silsurf A008-UP showed complete WCA reversal post-soaking and optically clear surfaces

with small dimples. Alkyl (o-Wet)-treated surfaces had micrometre-wide depressions, while siloxane (n-Wet)-treated surfaces had sub-micrometre-wide depressions. Siloxane (a-Wet) demonstrated a post-soaking WCA change and displayed a specific morphology with more highly branched siloxane.

Seo et al. [105] modified the surface of PDMS using the non-ionic surfactant Triton X- 100, varying its concentration, making it hydrophilic. As observed in Figure 12, in the PDMS groups modified with more than 1% TX-100 (group B), the WCA began to decrease in a matter of seconds. On the other hand, in the PDMS group with a concentration of less than 0.5% (group A), there was a delay before the change in WCA began. Compared to the gradual change in the WCA of the unmodified PDMS, the modified PDMS showed a sudden change, directly proportional to the concentration of TX-100 in the material. For example, within 150 s, the WCA decreased to 70° on PDMS with 3% TX-100.

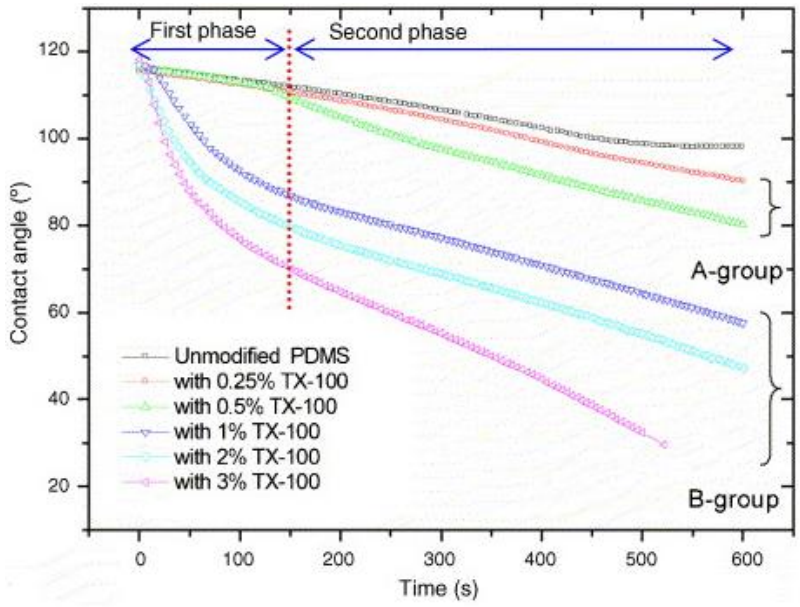

Figure 12 - Dynamic contact angle measurements on six different modified PDMS surfaces; the contact angle change shows two different phases consisting of a large initial change and a subsequent gradual change. Adapted from [105].

Immersed pairs of 3% PDMS TX-100 and unmodified PDMS substrates in deionised water for 45 min, 24 h, and 18 days shown are in Figure 13. WCA measurements were made after each surface was dried with dry nitrogen gas for 2 min after immersion.

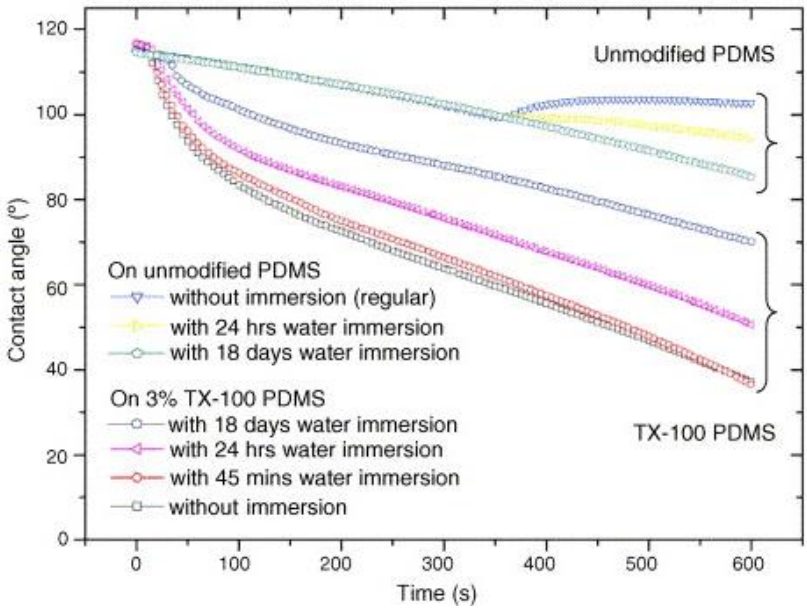

Figure 13 - Contact angle measurement before and after immersion. The contact angles were measured right after immersion. For 45 min to 18 days of immersion in water, the wettability of PDMS decreased. Surfactant depletion by solvent immersion is a useful technique to control the wettability of the modified PDMS. Adapted from [105].

The results indicated that the accumulation of surfactant at the interface between the modified PDMS and a drop of water caused a substantial change in the WCA in the initial phase. In addition, the reduction of surfactant through immersion in solvent represents a second strategy to control the wettability of the modified PDMS, complementing the initial control of the TX-100 concentration in the PDMS. In addition, it was shown that the WCA after 7 days did not show much difference, proving good durability [105].

Nam and Yoon [106] performed an experiment using surface/bulk treatment separately and also together, with the formation of a 3D interconnected pore network and the addition of a biocompatible surfactant (Silwet L-77). Porous PDMS (p-PDMS) was made into a 3D interconnected pore network with different pore sizes of 92.15, 176.78, 355.45, 634.40, and no pore (μm). The surfactant-added PDMS (s-PDMS) in which Silwet L-77 was added in different concentrations of 0.0, 0.1, 0.5, 1.0, 2.0, 4.0, and 8.0% by weight, and porous PDMS with added surfactant (ps-PDMS) with various pore sizes from 92.15 to no pores (μm), with various concentrations of Silwet L-77 from 0.0 to 8.0% by weight.

The results presented in this study reveal that the higher the percentage of Silwet L-77 surfactant, the lower the WCA. It was also noted that the smaller the pore sizes, the more hydrophobic the material became. There was a combined effect on the bonding of the two.

Another study with the surfactant Silwet L-77 by Montazeri et al. [107] where the concentration of 0, 0.2, 0.5, and 0.8% by weight of surfactant was altered, also by modification

by Bulk mixing, showed a decrease in the WCA as the concentration of Silwet L-77 increased, as shown in Figure 14.

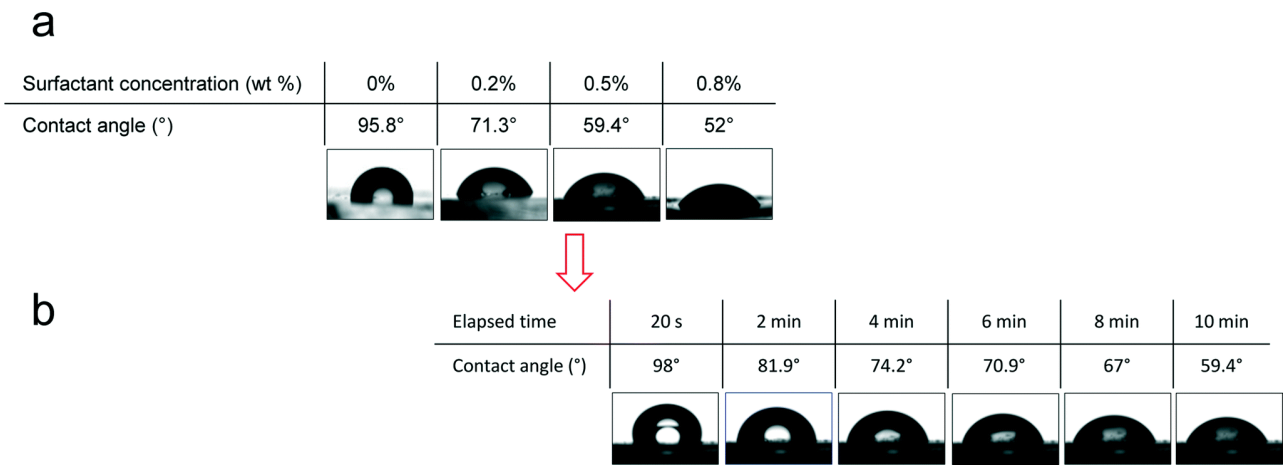

Figure 14 - Contact angles of the water droplets on the surface of surfactant-added PDMS. (**a**) Wettability profile of poly(dimethylsiloxane) (PDMS) with different concentrations of surfactant (Silwet L-77) after 10 min. (**b**) Kinetics of PDMS–Silwet L-77 (0.5%) wettability during 10 min. Obtained from [107].

Soriano-Jerez et al. [108] selected seven different commercial PDMS-PEG copolymer non-ionic surfactants, namely, CMS-626, DBE-224, DBE-311, DBE-814, DBE-821, DBE-C25, and DOWSIL™ OFX-0400. The coatings were prepared by mechanically mixing Sylgard 184™ (base: curing agent 10:1 *w*/*w*) with 4% surfactant by weight. The WCA was measured for 10 min, as shown in Figure 15. Their results confirmed other studies, previously presented, where the WCA decreased over time, making the surface hydrophilic.

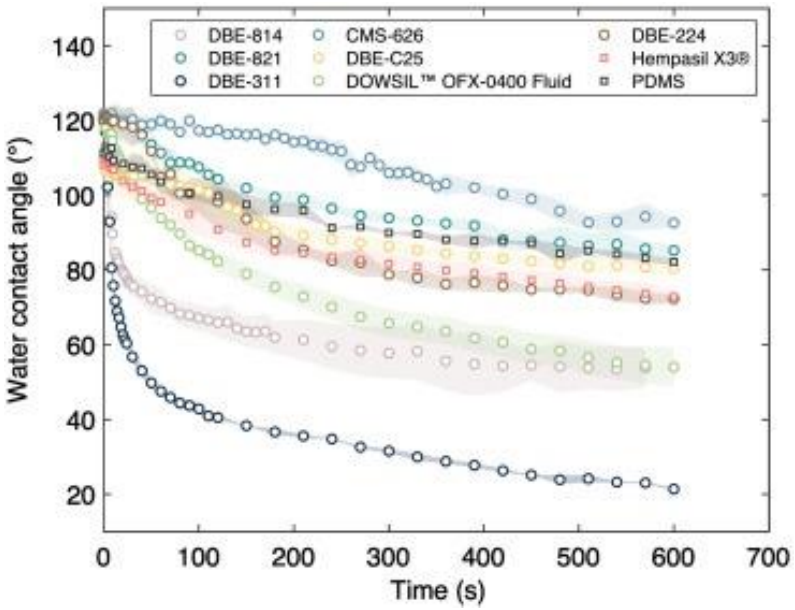

Figure 15 - Kinetics of water contact angle (θw) with time for each surfactant-based PDMS coating and for surfactant-free PDMS coating, using 120 μm thickness coatings. The shaded area represents the standard deviation of contact angle measurements. Obtained from [108].

The most effective coatings, such as those based on DBE-311 and DBE-814, showed a rapid change in the WCA over time, indicating a low adsorption of bovine serum albumin (BSA). This was also observed to a lesser degree in the DOWSIL™ OFX-0400 fluid and DBE-224-based PDMS coatings. High-performance surfactants tend to have shorter induction times, associated with a faster reduction in surface tension. Molecules with smaller surface areas and branched-chain surfactants showed a faster reduction in surface tension. Surfactants such as DBE-821 or CMS-626, with a high PEG content, should also have short induction times, but this was not evident in the WCA measurements.

Table 3 summarises the interactions between various surfactants and PDMS surfaces by categorising surfactants by their binding type (ionic or non-ionic), estimating bond strength and stability. The table highlights the prevalence of non-ionic surfactants interacting with PDMS through a combination of hydrogen bonding and hydrophobic interactions. While bond strength and stability are generally classified as moderate and medium-term for most entries, specific details regarding these properties require further investigation for several surfactants. Overall, the table provides a valuable overview of surfactant–PDMS interactions, but further studies are needed to explore the detailed binding mechanisms, the impact of surfactant structure, and the long-term stability of these modified surfaces. Additionally, application-specific optimisation remains an area for future research to tailor surfactant selection for specific functionalities.

Table 3 - Surfactant–PDMS interactions: binding type, strength, and stability.

Surfactant	Binding Type	Bond Strength	Bond Stability	Notes	References
Sodium dodecyl sulphate (SDS)	Ionic	Strong	Long-term	Bond strength and stability may vary depending on concentration and chain length.	[109]
Cetyl trimethylammonium bromide (CTAB)	Ionic (similar to SDS)	Strong	Long-term	Specific information on binding type, strength, and stability may require further research or data from the supplier.	[110]
Tween 20	Non-ionic (hydrogen bonding, hydrophobic interactions)	Moderate	Medium-term	Specific information on binding type, strength, and stability may vary depending on the specific alkyl surfactant.	[111]
Silsurf A008-UP	Non-ionic (likely hydrogen bonding, hydrophobic interactions)	Moderate	Medium-term	Specific information on binding type, strength, and stability may vary depending on the specific siloxane surfactant.	[112]
* Alkyl (o-Wet)	Non-ionic (hydrophobic interactions)	Moderate	Medium-term	Specific information on binding type, strength, and stability may vary depending on the specific siloxane surfactant.	[113]
* Siloxane (n-Wet)	Non-ionic (hydrophobic interactions, Van der Waals forces)	Moderate	Medium-term	Bond strength and stability may vary depending on concentration and temperature.	[114]
Siloxane (a-Wet)	Non-ionic (hydrophobic interactions, Van der Waals forces)	Moderate	Medium-term	Specific information on binding type, strength, and stability may require further research.	[115]
Triton X- 100	Non-ionic (hydrogen bonding, hydrophobic interactions)	Moderate	Medium-term	Specific information on binding type, strength, and stability may require further research.	[115]
Silwet L-77	Non-ionic (hydrophobic interactions, Van der Waals forces)	Moderate	Medium-term	Specific information on binding type, strength, and stability may require further research.	[107]
CMS-626	Non-ionic (likely hydrogen bonding, hydrophobic interactions)	Moderate	Medium-term	Specific information on binding type, strength, and stability may require further research.	[108]
DBE-224	Non-ionic (likely hydrogen bonding, hydrophobic interactions)	Moderate	Medium-term	Specific information on binding type, strength, and stability may require further research.	[108]
DBE-311	Non-ionic (likely hydrogen bonding, hydrophobic interactions)	Moderate	Medium-term	Specific information on binding type, strength, and stability may require further research.	[108]
DBE-814	Non-ionic (likely hydrogen bonding, hydrophobic interactions)	Moderate	Medium-term	Specific information on binding type, strength, and stability may require further research.	[108]
DBE-821	Non-ionic (likely hydrogen bonding, hydrophobic interactions)	Moderate	Medium-term	Specific information on binding type, strength, and stability may require further research or data from the supplier.	[108]
DBE-C25	Non-ionic (likely hydrogen bonding, hydrophobic interactions)	Moderate	Medium-term	Specific information on binding type, strength, and stability may require further research.	[108]

DOWSIL™ OFX-0400	Non-ionic (likely hydrogen bonding, hydrophobic interactions)	Moderate	Medium-term	Specific information on binding type, strength, and stability may require further research or data from the supplier.	[108]

2.4.2. Applications of Surfactant-Treated PDMS

The in-mould functionalisation strategy is used to produce self-driven microfluidic devices with stable flow rates, adjustable by the geometry of the device. The in-mould method has potential for various surface modifications in applications such as analytical separations, biosensing, cell isolation, and small molecule discovery [100]. Likewise, it is attractive in micro/nano biomedical applications [105], [116], [117].

It has been observed that wettability depends on the chemical structure of the surfactants and their concentration. A disadvantage of using a wetting agent to improve wettability is the potential to undesirably influence the composition of the solution. Therefore, very low concentrations of the wetting agent are often used, which can be complicated when limited quantities of the target solution are available. In this context, the controlled and gradual release of a wetting agent from the base material of a micro/nano device is preferable to the direct addition to the solution [118], [119].

2.5. Incorporation of Nanomaterials

There are several reasons for using nanomaterials to modify the wettability of PDMS. Firstly, the intrinsic hydrophobic characteristic of PDMS, stemming from its siloxane structure, can restrict its application in certain contexts that require hydrophilic surfaces. A versatile approach to overcoming these limitations is offered by the incorporation of nanomaterials, which allows the wettability properties to be tailored to the specific needs of the application [120], [121].

When added to PDMS, nanomaterials can considerably modify the interactions at the solid–liquid interface, which directly affects the wettability of the surface. Specific characteristics, such as controlled roughness, can be caused by the nanotopography resulting from the presence of these materials and affecting the interaction between PDMS and liquids. These adjustments to the surface morphology can cause alterations to the contact angle and therefore to the wettability in its entirety [78], [122], [123].

The underlying principles in this wettability modification include the interaction between the specific properties introduced by the nanocomponents and the PDMS surface. The presence of these factors in the stability and durability of wettability changes caused by nanomaterials is attested to in the scientific literature [39], [53], [54], [55].

This session aims to provide an understanding of the results obtained in research where nanomaterials have been used to alter the wettability of the PDMS surface by examining the most recent studies in this field.

The work of Wen et al. [124] addressed the production of fluorine-free superhydrophobic coatings applied to cotton fabrics. This process involved the use of silver nanoparticles (Ag), combined with the graft polymerisation technique and the application of PDMS to the fabric. During the manufacture of the coating, the surface of the cotton fabric was initially grafted with polyglycidyl methacrylate (PGMA) and functionalised with diethylenetriamine (DETA). Subsequently, silver nanoparticles were immobilised, followed by coating with PDMS (5% by mass of PDMS in ethyl acetate), resulting in a superhydrophobic coating on the cotton fabric.

The coated cotton fabric showed a good superhydrophobic capacity, with a WCA of 155° ± 1.5°. This characteristic was achieved by effectively combining PDMS with silver nanoparticles (Ag), which played the role of hydrophobic agents, decreasing the surface energy of the fabric and promoting robust adhesion of the nanoparticles to increase surface roughness. In addition, the durability of the coating was assessed at different pH levels and through a

weight abrasion method with more than 200 cycles. The results highlighted the remarkable strength and durability of the coating, maintaining superhydrophobicity with a WCA of over 150° in both acidic and alkaline environments [124].

Barthwal et al. [125] developed fluorine-free superhydrophobic coatings on copper mesh using PDMS in conjunction with a multi-walled carbon nanotube/zinc oxide (MWCNTs/ZnO) composite, using dip-coating techniques. In this study, the sol–gel technique was used to synthesise the MWCNTs/ZnO composite. It is noteworthy that the mesh coated with 2.5% by weight of the MWCNTs/ZnO composite exhibited greater superhydrophobicity, with a WCA of 156° and a sliding angle of 4°, compared to the coatings containing 1% by weight (151°) and 5% by weight (145°) of the composite, as illustrated in Figure 16.

The superhydrophobicity manifested by the copper mesh is the result of the presence of hierarchical micro/nanostructures, giving the coated surface greater roughness. Additionally, it was observed that the PDMS-based coating on the copper mesh preserves its superhydrophobic characteristic in the face of various unfavourable environmental conditions. This includes extreme temperature variations; exposure to corrosive environments, such as a 3.5% by weight NaCl solution; and resistance to strongly acidic/alkaline solutions. This ability to maintain superhydrophobicity highlights the robustness and adaptability of the coating proposed by the research in question [125].

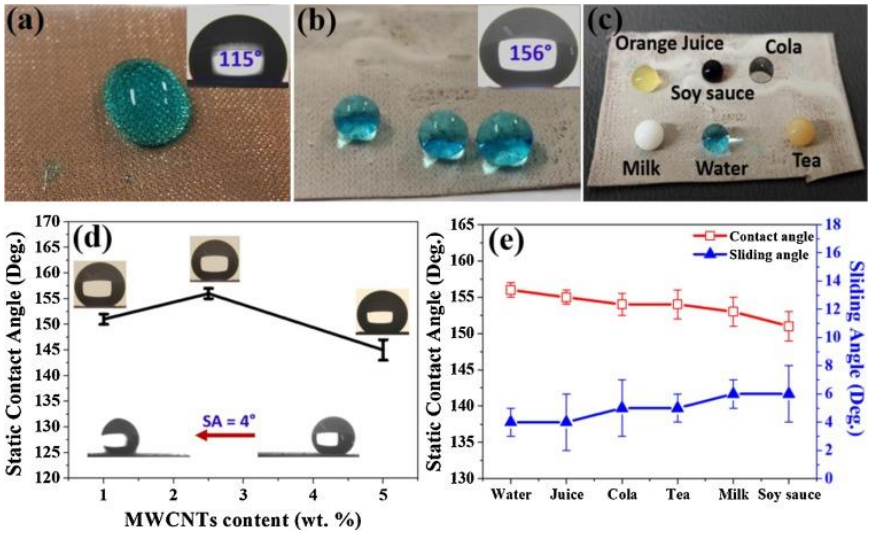

Figure 16 - Pictures of water droplets on the (**a**) untreated and (**b**) superhydrophobic Cu mesh (modified with 2.5 wt% composite coating), with corresponding WCAs. (**c**,**e**) The photo and WCAs of various liquid droplets on the coated mesh, respectively. (**d**) The change in the WCA of the prepared surfaces as a function of the content of MWCNTs in the composite coatings. Obtained from [125].

Sadler and Crick [126] developed an affordable and direct superhydrophobic filtration method by applying a PDMS coating to glass microfiber filters. This approach aimed to separate

oils from water both through suction pressure and under the influence of gravity. The average WCA of the PDMS-coated filter was determined to be 158 ± 3°, in contrast to the 95° observed on the flat PDMS surface. This significant difference can be attributed to the rough morphology induced by the filters, combined with the presence of PDMS as a low-surface-energy agent.

2.6. Modification of PDMS Surface Wettability for Microfluidic Applications

Given the growing use of treatments to modify the wettability of the PDMS surface for microfluidic applications, additional successful studies are described below, addressing the different methods mentioned in this review. PDMS's non-toxic, biocompatible, stable, and flexible properties make it a well-known material used in microfluidics. However, its inherent hydrophobicity presents challenges in fluid handling applications, as previously discussed. Various surface treatment methods have been studied to improve the wettability of PDMS, including gas-phase processing techniques such as oxygen plasma [127], [128], [129] and UV irradiation [40], as well as chemical methods such as LBL deposition [40] and others. Modification with surfactants has emerged as a promising approach to long-term hydrophilicity, offering simplicity and effectiveness without the need for complex procedures [130], [131].

Long et al. [129] performed a surface modification of PDMS material by oxygen plasma, followed by PEG coating, for hydrophilic enhancement on pure PDMS. By using rhodamine droplets, it was tested in a capillary-driven microfluidic device. From Figure 17, it is clear that at 8 s, the Rhodamine B fluid was halfway through the channel, and at 13 s, the channels were completely filled. With untreated PDMS, no flow was observed at least during the first 60. This method has shown long-term hydrophilic surface modification as the fluid could flow without external pumping for a period of 420 h.

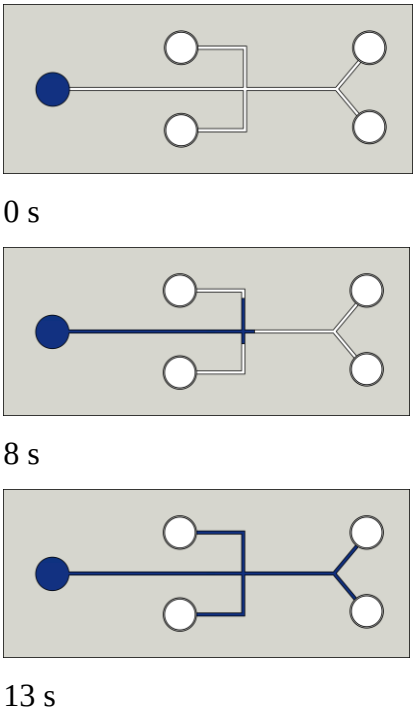

Figure 17 - Schematic diagram of a capillary test on PDMS after 420 h of treatment by O_2-plasma-PEG based on the work of Long et al. [129]. The images make it clear that at 8 s the Rhodamine B fluid was halfway through the channel and at 13 s the channels were completely filled. With untreated PDMS, no flow was observed at least during the first 60 s.

Peterson et al. [128] tested native and oxidised PDMS coatings (ox-PDMS) as biocompatible coatings for microfluidic devices. Glass-silicon microfluidic devices coated with hydrophilic ox-PDMS had an undisturbed flow rate over 14 min of operation, while the uncoated device suffered a loss in rate of 12%, and the native PDMS coating showed a loss of almost 40%.

By using surfactants to modify the surface of PDMS, Holczer et al. [132] carried out a controlled modification to develop an autonomous capillary-driven microfluidic system to be applied to bioanalytical devices. Vilčáková et al. [133] realised four types of CNT-based composites of various concentrations from 0 to 6% by volume of surfactants: anionic surfactant dodecylbenzene sulphonic acid (DBSA), cationic surfactant cetyltrimethylammonium bromide (CTAB), and a DBSA/CTAB surfactant mixture, which were prepared by simple mechanical mixing and sonication, leading to a homogeneous distribution of a filler in a silicone matrix.

Wu and Hjort [134] introduced a non-ionic surfactant, Pluronic F127, into the PDMS pre-polymer before curing. By filling the microchannel with water, the Pluronic F127 molecules incorporated into the PDMS migrated towards the water/PDMS interface to minimise surface energy. This phenomenon resulted in a hydrophobic interaction between the PPO and

PDMS segments, causing the hydrophilic PEO segments to extend outwards from the surface. The CA of the PDMS surface modified by Pluronic F127 changed from 99 to 63° after the sample was immersed in water for 24 h, compared to a CA of 104° for the native PDMS.

Recently Gonçalves et al. [135] modified the PDMS surface properties by using three different surfactants, i.e., Pluronic® F127, polyethylene glycol (PEG), and polyethylene oxide (PEO). In this study, they found that the bulk modification performed with the PEO surfactant at 2.5% was the most promising candidate to enhance blood plasma separation efficiency in microfluidic devices, as it facilitates the fluid flow, reduces cell aggregations and air bubble trapping, and achieves higher levels of sample purity.

2.7. Promising Trends and Future Prospects

After reviewing previous techniques, it can be seen that they had some limitations, such as the reduction in long-term efficacy for surfactant addition, the lack of precise control over plasma parameters for oxygen plasma treatment, non-uniformity, and lack of depth and degradation in the material to prolonged exposure to radiation in UV-ozone treatment. The challenges of guaranteeing uniform and stable dispersion of the nanomaterials in the PDMS matrix were also addressed, as well as concerns related to their toxicity and compatibility in biological applications. However, new techniques have emerged to overcome some of these shortcomings, as well as the combination of different methods to take advantage of the individual benefits of each one.

One of the emerging trends for modifying the surface of PDMS is surface nanotexturisation, which involves creating nanostructured patterns on the surface. These patterns can be achieved using techniques such as electron beam lithography, nanoimprint lithography, and nanoimprinting techniques [123], [136]. Nanotexturisation can increase the surface area available for interactions with water, resulting in greater hydrophilicity, and it also provides greater durability, precise control over surface characteristics, and biological compatibility. However, this process is more costly for small-scale production, despite being interesting on an industrial scale [137].

Another promising approach is the deposition of thin films of nanomaterials, such as metal oxides [138] or conductive polymers [139], on the PDMS surface. These films can be deposited using techniques such as sputtering [140], chemical vapour deposition (CVD), [139] or dipping techniques [141]. This technique has better uniformity and compatibility with manufacturing processes as it is versatile and compatible with a variety of manufacturing processes, and also it has a wide range of materials, providing greater flexibility in the choice of materials to meet the specific demands of each application.

As work progresses, it is likely, based on current studies, that there will be greater integration of multiple PDMS surface modification techniques. This may involve combinations of the traditional techniques that were discussed throughout the article, as well as new techniques such as nanotexturisation and thin film deposition, to achieve optimal combinations and enhance the desired properties of the material, seeking not only the optimisation of hydrophilicity but also to control other important properties such as biocompatibility, chemical resistance, and durability. However, a major disadvantage of this approach, when compared to traditional

methods of modifying wettability on the surface of PDMS, is the complexity and cost associated with the process.

2.8. Conclusions

This comprehensive review of the surface wettability of polydimethylsiloxane describes the importance and complexity of surface modification techniques for altering the inherent hydrophobicity of PDMS. The four main strategies, namely, oxygen plasma treatment, the addition of surfactants, UV-ozone treatment, and the incorporation of nanomaterials, are the traditional methods most used to modify the wettability of the PDMS surface due to the greater availability of information, having lower complexity compared to the new techniques and lower cost associated with them. This has highlighted the difference in methods that can be used to adapt PDMS surface properties to specific applications. Each of the techniques has its advantages and challenges. For example, oxygen plasma treatment has become an important method for increasing the hydrophilicity of the surface by introducing polar functional groups through oxidation reactions. The addition of surfactants, on the other hand, provides versatility for altering wettability, with the choice and concentration of the type and quantity of surfactant being decisive for achieving the desired surface properties. UV-ozone treatment stands out for its effectiveness in increasing surface energy, inducing oxidation and also generating hydrophilic functional groups. Finally, the incorporation of nanomaterials into PDMS matrices appears to be a promising technique for altering wettability, with the option of having adaptable surface properties through controlled distribution and interfacial interactions. In future works, the combination of these techniques has great potential to satisfy the future needs of various domains, as well as the use of new techniques that are emerging on the market, which will be increasingly explored and consequently have a lower cost and less complexity.

Chapter 3

Optimization of PDMS Hydrophobicity and Thermal Conductivity Analysis in Microfluidic Devices: Comparison of Non-Ionic Surfactants [2]

Abstract: The extensive use of polydimethylsiloxane (PDMS) in microfluidic devices is due to its remarkable characteristics. Although it possesses advantageous physical and chemical properties, its hydrophobic nature presents a challenge when pumping aqueous solutions through microchannels using only capillary forces. Several approaches have been proposed to make PDMS more hydrophilic; however, many face the problem of hydrophobic recovery after a relatively short period, while most commercial devices require long periods of storage and distribution. The addition of surfactant to PDMS has emerged as a new technique to overcome hydrophobicity and control hydrophobic recovery over time. However, the selection of an appropriate surfactant still demands a comprehensive methodology that considers the efficiency, stability, and durability of the hydrophilic behavior. In this study, three non-ionic surfactants with different critical micelle concentrations and chemical compositions were compared: Triton X-100, Brij L4 (BL4), and Polyethylene Oxide (PEO). For this purpose, different surfactant concentrations, curing temperatures, and types of surfactants were compared. Short- and long-term experiments were conducted, in which drops of deionized water were applied to the surface of PDMS prepared with the addition of surfactant for the wettability test. Additionally, an analysis of the influence of surfactants on thermal conductivity was performed, where samples were placed in a Hot Disk 5501 sensor to measure the thermal conductivity of the mixture. The results of the Taguchi method indicated that the optimal sample for both the initial wettability test (0 h) and after 3 weeks of curing is 2.5% PEO cured at 80°C, achieving a contact angle of 12.8° immediately after curing. For the initial thermal conductivity (0 h), it was 0.5% TX-100 at 80°C, and for after 3 weeks, BL4 2.5% at 25°C. For the analysis of the ideal sample using the combination of the two tests, the Grey Relational Analysis method was used. Additionally, to further delve into the methods, an ANOVA statistical analysis was presented to see the

[2] Neves, L. et al., 2024. Optimization of PDMS Hydrophobicity and Thermal Conductivity Analysis in Microfluidic Devices: Comparison of Non-Ionic Surfactants. Article in submission process in Journal Polymers, MDPI.

percentage of influence of each parameter, both in the Taguchi method, in individual tests, and the Grey Relational Analysis with the combination of both methods.

Keywords: PDMS (Polydimethylsiloxane); Microfluidic Devices; Non-Ionic Surfactants; Hydrophobicity Optimization.

3.1. Introduction

Poly(dimethylsiloxane) (PDMS) is a polymer widely used in various technological applications due to its unique properties, such as flexibility, transparency, biocompatibility, and ease of manufacture [11], [12], [13], [14]. However, the inherent hydrophobicity of PDMS represents a difficulty in microfluidic applications. This hydrophobic nature hinders the transfer of aqueous solutions, particularly evident in processes such as micro-contact printing, where the hydrophobic surface of PDMS impedes the flow of fluids. In addition, pressure-driven liquid processing equipment experiences a greater drop in internal pressure in the microchannels surrounding the hydrophobic PDMS surface, further exacerbating the problem. Various surface treatment methods have therefore been explored to reduce this challenge and improve the wettability of PDMS surfaces [22].

Among these methods, gas-phase processing techniques such as oxygen plasma [67], [142], [143], UV/ozone treatment [143], [144], [145], UV irradiation [146] and electrical discharge [147] have been widely investigated. Although these methods initially produce hydrophilic surfaces, their effectiveness is limited by the short lifetime of the hydrophilic modification due to the diffusion of low molecular weight chains [48], [57], [148]. Chemical processing methods, including chemical vapor deposition (CVD), layer-by-layer deposition (LBL), sol-gel coatings and salinization, have also been used to improve the hydrophilicity of PDMS [149], [150], [151], [152]. However, these methods often involve complex protocols, multi-step procedures and high-cost facilities, which present significant challenges, especially for those without experience. Another method widely used today is the incorporation of nanomaterials, but their varying stability, toxicity as well as the diffusion and migration of nanoparticles can be undesirable, especially if they are toxic particles [143].

Currently, the use of surfactants has come to the fore to address the hydrophobicity of PDMS surfaces effectively [100], [106], [153], [154], [155]. Surfactants, as wetting agents, offer a simple but promising approach to reducing fluidic resistance in microchannels by lowering surface tension and facilitating the spreading of liquids. This method avoids the need for specialized installations and complex procedures, making it accessible even to beginners. Surfactant-modified PDMS has demonstrated significant utility in various microfluidic applications, including the separation of biomolecules, blood cell sorting, immunological assays and drug delivery. The addition of surfactant to PDMS showed biocompatibility and stability, making it a viable option for various industrial and research applications [156].

This study investigated the addition of three different surfactants to PDMS: Polyethylene Oxide (PEO), Brij L4 (BL4) and Triton X-100 (TX-100). The main objective was to improve the wettability of the PDMS, facilitating the flow of fluid by capillarity in microchannels without the need for pumps or other forced movement devices. In conjunction with this, the thermal conductivity of the PDMS-surfactant composite was also analyzed, in order to see if it would make the mixture more hydrophobic or aid hydrophilization.

The methodology adopted involved preparing PDMS samples with different concentrations of each surfactant and different curing temperatures for the mixture. An orthogonal arrangement using the Taguchi method was used to select the combinations of parameters and sample levels. Once the arrangement had been defined, the samples were made and then the detailed wettability and thermal conductivity tests were carried out. Because the Taguchi method has a limitation in only presenting data for the ideal sample of the tests individually, Grey's Relational Analysis was used to unite both tests, overcoming this limitation. Thus, an ideal sample was presented, taking into account the percentage influence of each test on this sample.

The improvement in wettability was assessed through contact angle tests, where a reduction in the contact angle indicates an increase in the hydrophilicity of the surface, and thermal conductivity was measured using standardized techniques, allowing an assessment of the impact of surfactants on the heat dissipation capacity of PDMS.

The results of this study had important implications for the development of more efficient microfluidic devices. By increasing the hydrophilicity of PDMS, a significant improvement was achieved in capillary flow tests, allowing applications in areas such as medical diagnostics, small-scale chemical synthesis and cell manipulation, for example. The improvement in thermal conductivity, although low, opens greater possibilities for the use of PDMS in devices that require precise thermal control, such as cooling coils for microchips or other electronics, where there is a need for good wettability and thermal conductivity.

This work contributes to knowledge about the modification of polymeric materials, especially PDMS, thus offering insights into the choice and application of surfactants to improve the properties of various PDMS applications. By taking a diversified approach that considers both wettability and thermal conductivity, presents an important step in optimizing materials for more advanced applications in microtechnology and nanotechnology.

3.2. Materials and methods

3.2.1. Material

Non-ionic surfactants were selected, organic substances characterized by their amphiphilic behavior, which allows them to interact with both polar and apolar substances. These surfactants have different chemical names and HLB (Hydrophilic-Lipophilic Balance) values, a measure of a surfactant's relative affinity for water or oil, as shown in Table 4. The surfactants used were: Brij L4 (SIGMA-ALDRICH), Triton# X-100 (SIG-MA-ALDRICH) and Polyethylene Oxide (Polysciences Europe GmbH).

Table 4 - Chemical names and HLB of the analyzed surfactants.

Surfactant	Chemical name	HLB
Brij L4 (BL4)	Polyoxyethylene (4) lauryl ether	9
Polyethylene Oxide (PEO)	Poly(ethylene oxide)	-
Triton X-100 (TX-100)	t-Octylphenoxypolyethoxyethanol	13.5

3.2.2. Taguchi method

The Taguchi method [157] is a statistical approach to optimizing both processes and projects, which aims to reduce variation and increase performance through controlled experiments. This method is based on experiment planning procedures to identify the most influential factors in each system and thus be able to determine its optimal configurations, with the aim of improving the quality and robustness of the product or process.

In Taguchi's experiments, the signal-to-noise ratio is a measure of robustness. It helps to identify control factors that reduce variability in a product or process by minimizing the effects of uncontrollable factors (noise factors). Control factors are parameters that can be controlled, while noise factors cannot be controlled during the production or use of the product but can be controlled during experimentation.

- Nominal is the best:

$$S/N_t = 10 * \log\left(\frac{\bar{y}^2}{{s^2}_y}\right) \quad (1)$$

- Larger is the better (maximize):

$$S/N_L = -10 * \log\left(\frac{1}{n}\sum_{i=1}^{n}\frac{1}{{y_i}^2}\right) \quad (2)$$

- Smaller is the better (minimize):

$$S/N_S = -10 * \log\left(\frac{1}{n}\sum_{i=1}^{n}{y_i}^2\right) \quad (3)$$

where $\bar{y}$ is the average of observed data, ${s^2}_y$ is the variance of y, n is the number of observations, and y is the observed data. S/N_t is used if the aim is to reduce variability around a specific target, S/N_L if the system is optimized when the response is as large as possible and S/N_S if the system is optimized when the response is as small as possible.

The Taguchi method has the advantage of requiring a low number of tests. It is based on the use of orthogonal arrays to carry out small, highly fractional tests, up to larger, fully factorial tests. Although there are various approaches to designing experiments, the use of this type of array is considered very flexible and practical for a variety of situations, mainly due to its non-complexity as a statistical method. In addition, due to the smaller number of tests required, the Taguchi method is more economical compared to experimenting with all possible combinations of parameters. By adopting the Taguchi test design, it is possible to reduce both the time and cost associated with improving quality.

3.2.2.1. Application Taguchi method

One signal-to-noise ratio that was used in the experiment for wettability is the lower the better, because it is desired to achieve the lowest possible wettability, while the other signal-

to-noise ratio for thermal conductivity is the higher the better, because we want to achieve the highest conductivity.

Considering that the initial focus was mainly on improving the surface wettability of the PDMS, the parameters as well as the levels chosen to be changed were in accordance with the main relevant properties based on the literature and bibliographic review.

As presented in the literature, one of the methods for changing wettability, which was chosen for the present study, is the addition of surfactants both on the surface and in bulk to the PDMS. Therefore, the typical parameters to be changed and studied when adding surfactants are the type of surfactant used, the concentration percentage and the curing temperature of the PDMS/Surfactant mixture.

To choose the correct Taguchi's array, we have chosen 3 basis levels for each parameter, they are defined in Table 5, both the parameters and the levels were selected on the basis of effective studies carried out previously.

Table 5 - Parameters and levels Taguchi.

Parameter	Level 1	Level 2	Level 3
Surfactant concentration %	0.5%	1%	2.5%
Curing temperature (°C)	25°C	80°C	120°C
Type of surfactant	Brij L4	PEO	Triton X-100

Knowing the number of parameters and the number of levels, the proper orthogonal array can be selected. In this case, 3 parameters at 3 different levels, the proper Taguchi's orthogonal array is L_9. This means that nine combinations of parameters are needed, see Table 6. By replacing the levels and parameters in Table 6, we have Table 7.

Table 6 - Taguchi L_9 array.

Test number	Parameter 1	Parameter 2	Parameter 3
1	1	1	1
2	1	2	2
3	1	3	3
4	2	1	2
5	2	2	3
6	2	3	1
7	3	1	3
8	3	2	1
9	3	3	2

Table 7 - Taguchi L_9 array with parameters and levels.

	Surfactant concentration %	Curing temperature (°C)	Type of surfactant
1	0.5%	25°C	BL4
2	0.5%	80°C	PEO
3	0.5%	120°C	TX-100
4	1%	25°C	PEO
5	1%	80°C	TX-100
6	1%	120°C	BL4

7	2.5%	25°C	TX-100
8	2.5%	80°C	BL4
9	2.5%	120°C	PEO

The aim of this study is to analyze the decrease in the contact angle on the PDMS surface and the increase in thermal conductivity. Thus, once the wettability and conductivity study has been finalized, we will choose a combination of parameters that leads to the optimal combination of lower wettability and higher conductivity.

In addition to what has already been said about the Taguchi method, there are some other advantages and disadvantages. The Taguchi method offers significant advantages, prioritizing average performance close to the target value in order to improve product quality. Its experimental approach is straightforward and applies to a variety of engineering situations, making it easy to identify problems and analyze parameters with little experimentation. It also allows multiple parameters to be analyzed without the need for many experiments, thanks to the use of orthogonal arrays. However, the results are relative and may not indicate precisely which parameter most influences the performance characteristic. The inability to test all combinations of variables selected by the Taguchi method and difficulties in considering interactions between parameters are also limitations of this approach. In addition, the Taguchi method is best suited to the early stages of process development and may not be efficient in dynamic processes or when it is necessary to correct poor quality rather than just design quality [157].

3.2.3. ANOVA analysis

Analysis of variance (ANOVA) is a methodology used to compare different levels of one or more test variables, allowing for the determination of whether the means of three or more groups (levels) are significantly different. Variances, which measure dispersion, calculate the degree of deviation of the data relative to the sample mean. One of the main objectives of ANOVA is to identify whether there are significant differences between the distributions of results in a sample involving three or more groups [158].

To perform the analysis of variance, an ANOVA table is created, as demonstrated in, to calculate the effects of each factor included in the analysis. These factors are: Sequential sums of squares indicate the variation attributed to the different components of the model; Degrees of freedom (DF) represent the amount of information available in the model; Mean squares are obtained by dividing the sum of squares by the degrees of freedom and represent the

variation between sample means; The F-value is a test statistic used to determine whether a control factor in the model is related to the response and to measure the extent of its influence; The P-value is the probability of obtaining a value of the test statistic equal to or greater than the observed one. Generally, a P-value less than 0.05 is used as a criterion to reject the null hypothesis, indicating that an extreme value for the test statistic would occur less than 5% of the time if there were no significant difference [159], [160], [161].

3.2.4. Grey Relational Analysis

The Grey Relational Analysis technique is used to calculate the proximity between tests, using a specific relational grade. This method normalizes experimental results, such as wettability and thermal conductivity, on a scale from zero to one, based on their relevance. Grey's relational coefficient is then calculated from this normalized data, showing the relationship between the desired and actual results. The Grey relational grade is then achieved by averaging these coefficients, reflecting the overall assessment of the various responses in the process. The procedure, also known as "GRA" (Grey Relational Analysis), follows a sequence of defined steps [162], [163], [164].

Initially, the process begins with pre-processing the data to avoid inconsistencies regarding scales and units. Next, the experimental data is subjected to a normalization in the range of zero to one, to standardize the raw data, followed by a linear normalization of the S/N ratio. The normalization of the experimental data when the "less is better" property is chosen for the quality characteristic is given according to Eq.(4):

$$x_{ij} = \frac{max_{ij}n_{ij} - n_{ij}}{max_{ij}n_{ij} - min_{ij}n_{ij}} \quad (4)$$

When the "highest or best" attribute is chosen for the analyzed response, normalization is given according to the Eq.(5):

$$x_{ij} = \frac{n_{ij} - min_{ij}n_{ij}}{max_{ij}n_{ij} - min_{ij}n_{ij}} \quad (5)$$

where x_{ij} is normalized S/N ratio, n_{ij} represents the S/N value for each test with regard to wettability or thermal conductivity, $max_{ij}n_{ij}$ is represents the maximum value between tests 1 and 9 and $min_{ij}n_{ij}$ represents the minimum value between tests 1 and 9.

Next, Grey's relational coefficient ($\xi i(k)$) is calculated from the normalized experimental data to show the relationship between the normalized (ideal) S/N ratio and the real one, where the ζ (zeta) characteristic varies in the range $0 \leq \zeta \leq 1$. Grey's relational coefficient is calculated as follows Eq.(6):

$$\xi_{ij} = \frac{min_i min_j \left|x^0{}_i - x_{ij}\right| + \zeta max_i max_j \left|x^0{}_i - x_{ij}\right|}{\left|x^0{}_i - x_{ij}\right| + \zeta max_i max_j \left|x^0{}_i - x_{ij}\right|} \tag{6}$$

where ξ_{ij} is Grey's relational coefficient, $min_i min_j \left|x^0{}_i - x_{ij}\right|$ is minimum normalized value, $max_i max_j \left|x^0{}_i - x_{ij}\right|$ is maximum normalized value, $\left|x^0{}_i - x_{ij}\right|$ is the S/N value for each test in relation to Wettability or Thermal Conductivity and ζ (zeta) is the influence coefficient of the test.

The Grey relational grade is calculated using the average of the Grey relational coefficients corresponding to each performance characteristic. A higher Grey's ratio, closer to a value of one, indicates that the corresponding S/N ratio is closer to the ideally normalised S/N ratio. The Grey relational grade is calculated Eq.(7):

$$y_i = \frac{1}{n} \sum_{i=1}^{n} w_i \, \xi_{ij}(i) \tag{7}$$

where y_i is Grey's relational grade, n corresponds to the number of alternatives or elements compared and $w_i \xi_{ij}(i)$ is observed data.

If the experiments are carried out without repetitions, the data is normalised on the results obtained for each experiment and for each response analysed, applying the Eq.(4) and Eq.(5) equations, according to the characteristics of the responses. However, if the tests are repeated, normalisation is carried out on the S/N ratio calculated for each experiment and for each quality specificity, so that all the results achieved by the repetitions are grouped together [164], [165].

After calculating the Grey relational grade from the S/N ratio values derived from Taguchi and defining the optimal combination of control factors, it is essential to conduct a validation test to assess how much the Grey method aids in improving the process. This validation is necessary only when a sample of the combinations defined in the Taguchi orthogonal array has not been produced. The Grey relational grade, calculated using the optimal parameter levels identified by the Grey relational analysis, is determined by Eq.(8) [164], [165], [166], [167].

$$\hat{\eta} = \eta_m + \sum_{i=1}^{q} \bar{\eta}_i - \eta_m \tag{8}$$

where $\hat{\eta}$ is the estimated Grey relational grade for the optimal combination of parameters; η_m is the overall mean Grey relational grade of all experiments; $\bar{\eta}_i$ is the Grey relational grade for the optimal level of each parameter; and q is the number of significant parameters for the process.

3.2.5. Sample preparation

3.2.5.1. Bulk PDMS Modification Method

Firstly, the PDMS (Sylgard 184^{TM}, Silicone Elastomer Base, USA) was prepared by mixing a base and a curing agent in a 10:1 weight mixing ratio for 5 minutes in a slow spiral motion in the same direction. The mixture was then set to degas for 10 minutes. Following this process, the Brij L4, PEO and Triton X-100 surfactants were mixed in proportions of 0.5, 1 and 2.5 wt%, and the mixture was also degassed for 10 minutes [168]. The surfactant/PDMS mixture (s-PDMS) was then poured into a mold to standardize the diameter, thickness and surface roughness. It was then put back into the mold for degassing and, finally, cured at temperatures of 25°C, 80°C and 120°C, this whole process is shown, schematically, in Figure 18.

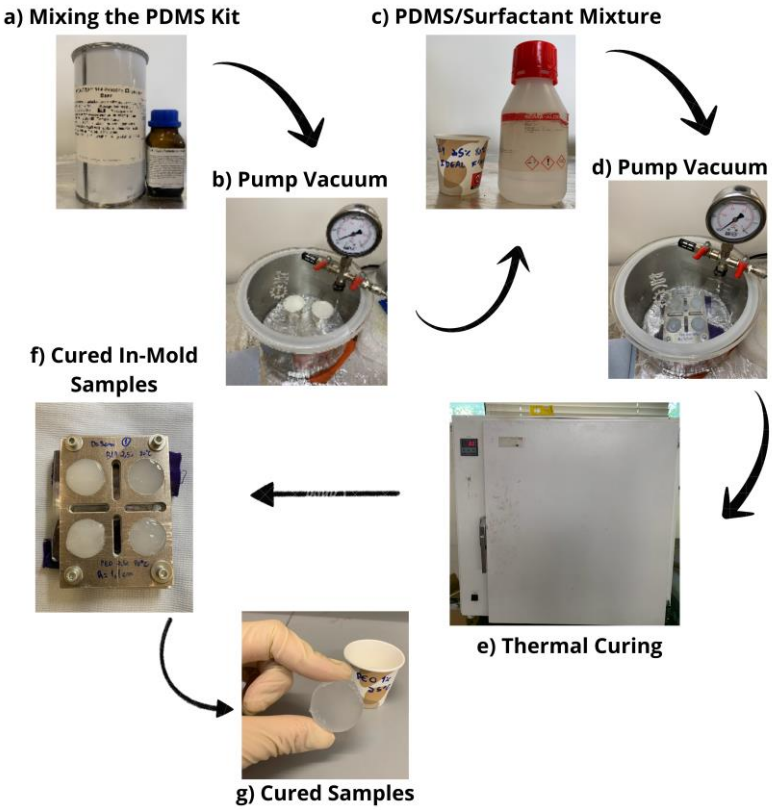

Figure 18 - Schematic of the manufacturing process for PDMS specimens with added surfactant, by bulk mixing. Where a) shows the PDMS kit (PDMS and curing agent), b) remove bubble from PDMS kit mix, c) mix PDMS kit with surfactants (Brij L4, PEO, Triton X-100) at 0.5, 1 and 2.5 wt%, d) removing bubble from the PDMS kit mixture with surfactants (already poured into the mold), e) curing the samples at 25°C, 80°C and 120°C, f) cured samples in the mold and g) final cured and demolded sample.

To meet the manufacturer's specifications for the Hot Disk 5501 F1 sensor, which was used for the thermal conductivity test, the samples were made in a mold with a thickness of 1.1 cm and a diameter of 3 cm. It consisted of a machined aluminium part with four holes and four gaps to contain excess material from each hole, preventing material placed in one hole from coming into contact with material in another hole, which usually happens when bubbles are removed, as the material on the surface expands and tends to go sideways. For the base of the mold, a rectangle of smooth glass is placed between the part with the holes and two small plates, where it is secured by screws, washers and nuts as shown in Figure 19.

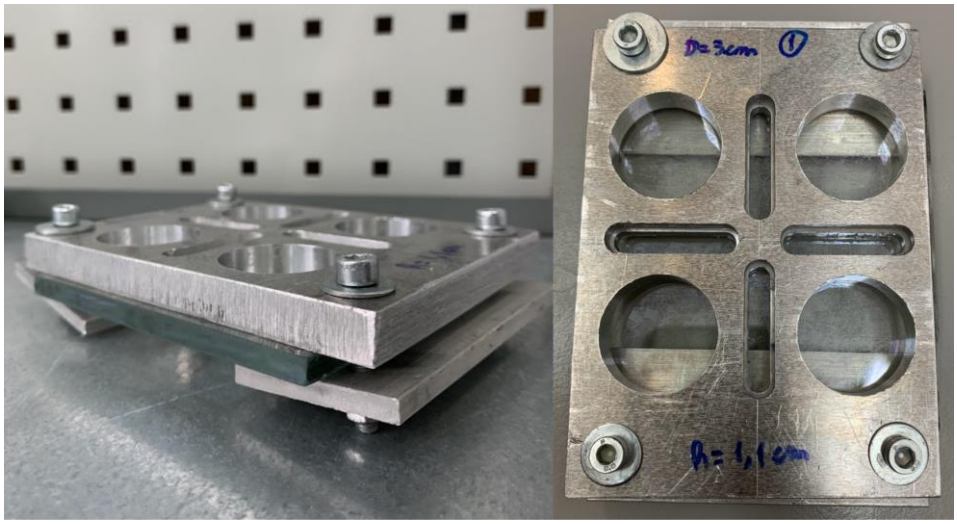

Figure 19 - Mold used to make the PDMS/Surfactant samples.

3.2.5.2. Microchannel Fabrication for Capillary Studies

3.2.5.2.1. Microchannel Design and 3D Printing of the Molds

The production of polymeric microfluidic devices for open capillary assays began with the creation of a standard design using the Inventor software (version 27.0, student license). Four types of channels were designed: (1) a straight rectangular channel with a length of 42 mm and a width of 1 mm (Figure 20A); (2) a spiral-shaped channel with a length of 42 mm and a width of 1 mm (Figure 20B); (3) a main channel with a width of 1 mm that splits into two equal branches (Figure 20C); and (4) a channel with bifurcation-confluence geometry (Figure 20D). All four channels had a depth of 0.4 mm [169].

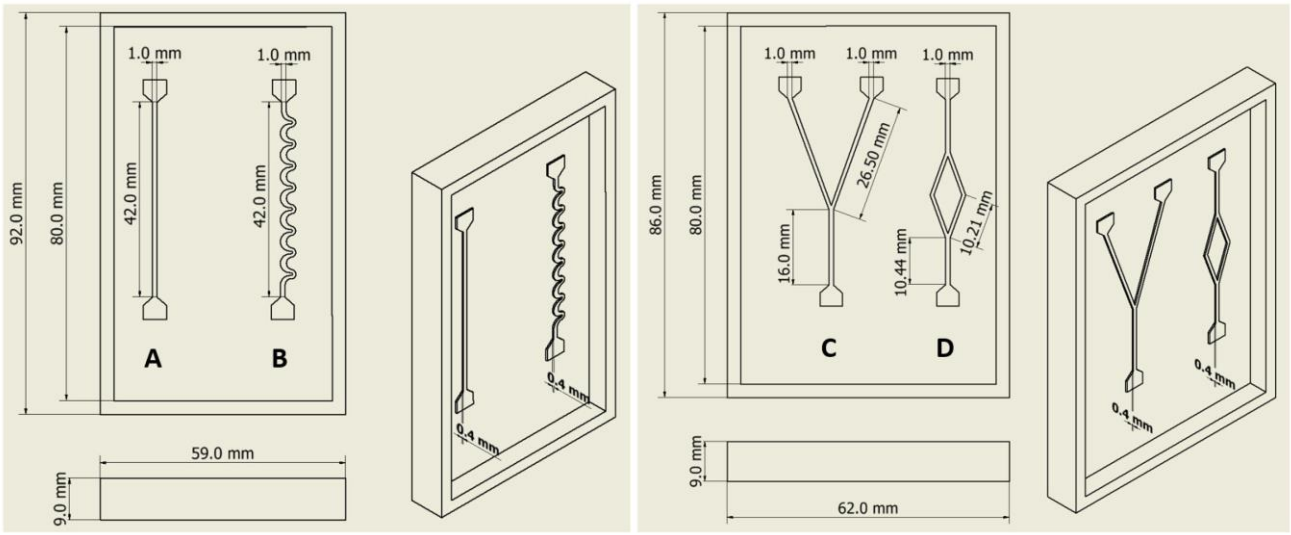

Figure 20 - Designs and dimensions of the different molds for the capillary microchannels. Four channels were drawn: (A) a straight rectangular channel; (B) a channel with spiral-shaped geometry; (C) a channel with a main channel that bifurcates into two equal branch channels; and (D) a channel with bifurcation-confluence geometry [169].

To obtain the microchannel molds, the drawings were transformed into .STL format to be sent to the 3D printer pre-processing software, CHITUBOX V1.9.5 (Shenzhen, China, CBD-Tech). The printer used was the Anycubic Photon D2 (Anycubic Company, China), a 3D printer based on Digital Light Processing. A specific translucent photosensitive resin (Standard Resin Clear, Anycubic Company, China) was used in the printing process and the high-resolution parameters were defined. Post to the printing process, the remaining uncured resin was washed with 99.9% isopropyl alcohol (EQM Soluciones Quimicas, Madrid, Spain), for 10 min, in the Anycubic Wash & Cure Plus Machine (Anycubic Company, China), to remove any excess of resin that remained on the microchannel surface mold. Afterwards, it was subjected to a UV curing session lasting 2 h in the Anycubic Wash & Cure Plus Machine (Anycubic Company, China). The UV light further cured the resin, making the molds more rigid, and improving their structural integrity. The curing time may vary based on the resin type and the UV source's intensity. Lastly, the mold was exposed to a 24 h thermal treatment at 80°C in an oven.

3.2.6. Contact angle measurements

3.2.6.1. Theory wetting of textured and chemically heterogeneous surface

When the droplet is small enough (low bond number), the surface tension exceeds gravity, and a spherical cap shape is formed on the droplet. According to Eq.(9), the three forces acting on the droplet define the contact angle of the droplet, so if the surface tension of the system and the volume of the droplet remain constant, the contact angle does not change. However, in practice, changes in surface tension or droplet volume can lead to changes in the contact angle. As the surface tension changes, a new balance of the three forces acting on the droplet establishes a different contact angle. When the volume of the droplet changes, this leads to a decrease in the contact angle in constant contact line mode, which is usually due to evaporation. Therefore, the factors that influence the dynamic contact angle over time are changes in surface tension and droplet volume on the impermeable surface [105], [170], [171].

The smoothness, rigidity, texture, and the presence, as well as the amount, of surfactant affects the contact angle of the water droplet on a surface [172]. When a liquid droplet is placed on an ideally flat, rigid, and chemically homogeneous surface, the equilibrium of solid, liquid and gas is described by Young's model [173].

$$\gamma_{SG} = \gamma_{SL} + \gamma_{LG} \cos\theta_Y \qquad (9)$$

where γ_{SG}, γ_{SL} and γ_{LG} are respectively interface tensions at solid/gas, solid/liquid, and liquid/gas, and θ_Y is a contact angle of the liquid at the equilibrium state. However, a real surface has its imperfections, contrary to ideal conditions. Therefore, considering the roughness present on the surface, Wenzel's model is used to develop the homogeneous wettability of a rough surface [174].

$$\cos\theta_m = r \cos\theta_Y \qquad (10)$$

where θ_m is an apparent contact angle, and r is a surface roughness ratio defined as the ratio of the actual surface area to the projected one. Heterogeneous wetting on a rough face, in which the fluid does not penetrate the textured cracks, is explained by the Cassie-Braxter model [175], [176].

$$\cos\theta_m = r_f f \cos\theta_Y + f - 1 \qquad (11)$$

where r_f and f are respectively the roughness ratio and area fraction of the surface wetted by the liquid. There are currently a few models for characterizing the equilibrium of

wetting on a textured face with homogeneous wetting (Eq.(10)) and heterogeneous wetting (Eq.(11)) [177], [178]. These characterize a shift between Wenzel and Cassie-Baxter, which are clarified by multiple Gibbs free energy minima.

When a liquid is applied to the polymer surface with the addition of surfactant, the surfactant molecules released from the polymer are continuously adsorbed onto the solid-liquid and liquid-gas interfaces. This results in a change in the wetting pattern of the polymer over time [104], [105]. The variation in the wetting pattern over time of a smooth surface in the presence of an amphiphilic surfactant is commonly explained by the theory developed by Starov [179], [180].

$$\cos\theta_m = \cos\theta_{m,0} - (\cos\theta_{m,0} - \cos\theta_{m,\infty})(1 - e^{-t/\tau}) \tag{12}$$

where $\theta_{m,0}$ e $\theta_{m,\infty}$ are respectively the initial ($t = 0$) and final ($t = \infty$) apparent contact angles of a liquid, and τ is a surfactant transfer time constant which is generally dependent on surfactant concentration and surface area fraction.

The continuous release of surfactant from the polymer into the liquid causes a temporal variation in $\cos\theta_{m,\infty}$ that is directly proportional to γ_{LG} according to the Zisman equation [181]. Using the Gibbs adsorption equation [182] and the Zisman equation, we have

$$\cos\theta_{m,\infty}(c) = \alpha + \beta \ln c \tag{13}$$

where α and β are the coefficients of surfactants. Putting Eq.(13) into Eq.(12) we can obtain the variation of wetting over time in a polymer that has an amphiphilic surfactant, so we have Eq.(14)

$$\cos\theta_m(c,t) = \cos\theta_{m,0} - \{\cos\theta_{m,0} - (\alpha + \beta \ln c)\}(1 - e^{-t/\tau}) \tag{14}$$

Given a textured and chemically heterogeneous surface, we arrive at the following equation

$$\begin{aligned}\cos\theta_m(d_p,c,t) &= f(d_p)\left[\cos\theta_{m,0} - \left\{\cos\theta_{m,0} - (\alpha + \beta \ln c)\right\}\left(1 - e^{-t/\tau(d_p,c)}\right)\right] \\ &\quad + f(d_p) - 1\end{aligned} \tag{15}$$

where f is area fraction of textures and d_p is pore size.

3.2.6.2. Contact angle measurements method

Static contact angle measurements were performed using the sessile drop technique to assess the wettability of the PDMS samples. Both modified and pure (control) PDMS samples were carefully cleaned with a damp paper. Using a 100 μL micropipette, a 10 μL volume of deionized water was carefully dispensed onto the sample surfaces. The water contact angle (WCA) was determined using a goniometer connected to an optical microscope and a computer with contact angle (CA) measurement software, including SCA202 software for OCA and PCA. To ensure accurate measurements, adjustments were made to lighting conditions, focus, baseline, and contour line. The image of the drop on the PDMS sample was captured immediately after sample preparation (0 h) and at subsequent intervals of 1 week, 2 weeks, and 3 weeks. During each test run, WCA was measured every minute for 10 minutes, obtaining 10 measurements over 10 minutes, at three different points in the sample, in order to have a detailed analysis of the changes in the hydrophobic properties of PDMS over time, as shown in Figure 21.

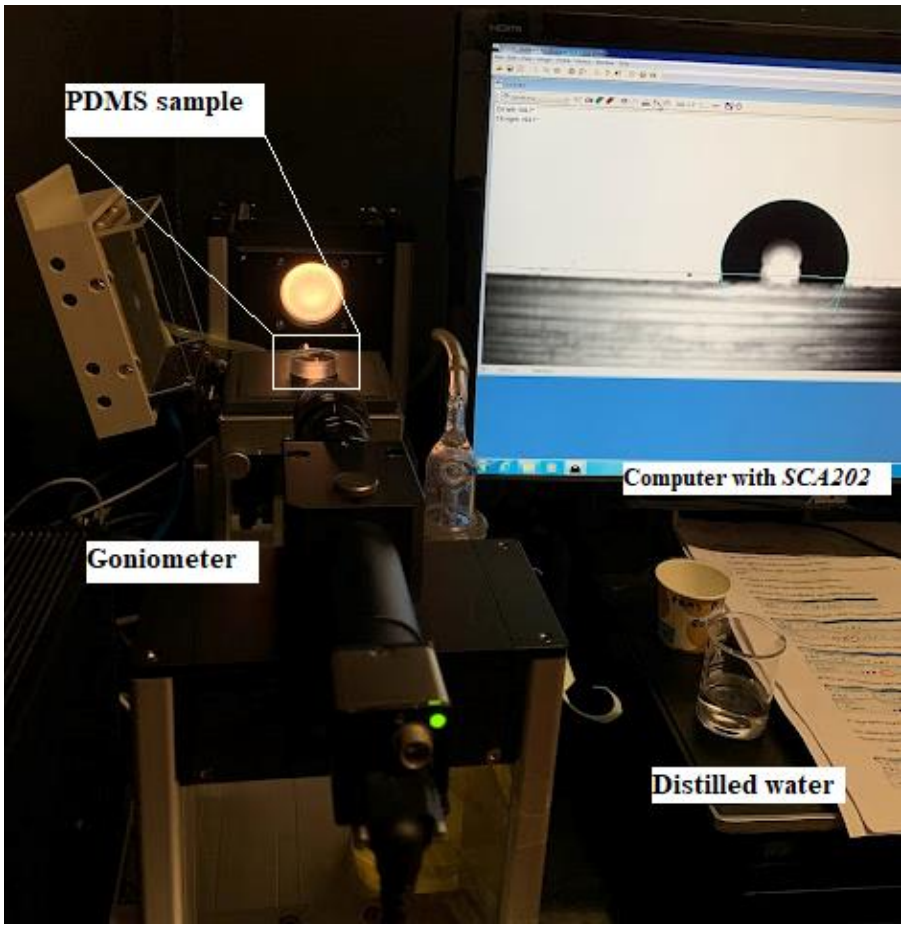

Figure 21 - Measurement of the contact angle using an optical microscope (goniometer), connected to a computer with the CA measurement software, SCA202. Images captured by goniometer of a 10 μL drop of distilled water on samples.

3.2.7. Thermal conductivity measurements

The thermal conductivity (κ) of a material is the property that defines its ability to conduct heat. It quantifies the amount of heat (Q) that passes through a material of thickness L and area A in each time interval (t), when there is a temperature difference (ΔT) between the opposite sides of the material. The relationship is given by the Fourier equation for heat conduction in one dimension [183].

$$Q = -\kappa \mathrm{A} \frac{\Delta T}{L} t \qquad (16)$$

The unit of measurement for thermal conductivity in the International System (SI) is the watt per meter-kelvin (W/mK).

Heat transfer in materials can occur in three main ways: conduction, convection, and radiation. In the context of the thermal conductivity in this work, the focus is on conduction, which can be divided into three different types. The first type is by phonons, which in solids, especially in non-metallic materials, heat is mainly conducted through the vibration of crystal lattices, or phonons. The second type involves free electrons, which in metals and some semiconductors, free electrons significantly contribute to thermal conduction. Finally, there is molecular diffusion, which in liquids and gases, thermal conduction occurs by the diffusion of high-energy molecules to regions of lower energy [184]. Various experimental methods are used to measure the thermal conductivity of polymeric materials such as PDMS, the method employed in this work was the Hot Disk method.

3.2.7.1. Hot Disk TPS 2500S

Transient plane source (TPS) equipment provides data on thermal properties, including thermal conductivity, thermal diffusivity and specific heat per unit volume of the material being analyzed, as specified by ISO 22007-2 standards and indicated by the manufacturer [185]. This method employs a flat heated sensor commonly referred to as a Hot Disk Thermal Constant Analyzer because of its shape. According to the TPS 2500S equipment manual, it can measure thermal conductivity values ranging from 0.005 to 1800 W/mK, with reproducibility commonly

exceeding 1% and accuracy exceeding 5%. It is compatible with both standard isotropic measuring modules and additional components [186].

3.2.7.2. Temperature and heat flux sensor

Hot Disk sensors, in this study we used the Hot Disk 5501 F1 sensor as shown in Figure 22, have thin polyimide films (Kapton®) with thicknesses between 12.7 µm and 25 µm for use at cryogenic temperatures of up to 300°C; the total thickness of the sensor varies from 60 to 80 µm. The sensor used has an external radius, r_{Kapton}, of 10 mm while its internal radius, r_{Hot}, of 6.4 mm in a spiral. Four electrical connections are provided for the sensor's double spiral, two for conducting the heating current and two for controlling the voltage drop. The TPS 2500S system has been adapted to monitor resistance variations during transient heating of the sample under investigation.

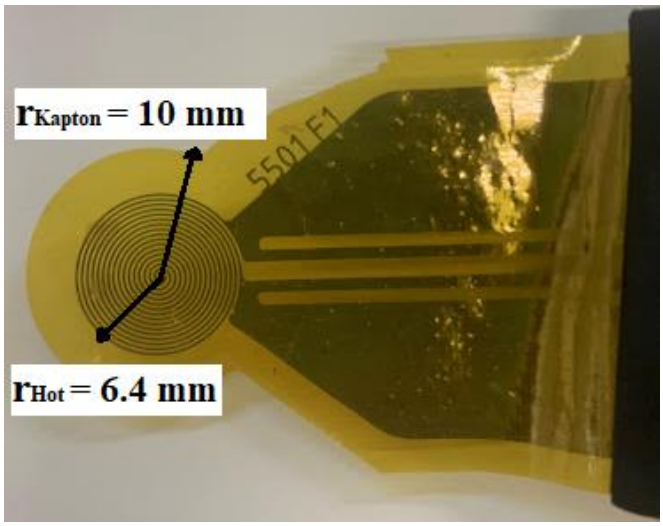

Figure 22 - Sensor Hot Disk 5501 F1 with Kapton® isolation.

For the Hot Disk 5501 F1 sensor, the manufacturer's specifications for sample thickness must be $r \leq h \leq 2r$ and for the sample diameter $4r \leq D \leq 6r$, where r is the r_{Kapton} of the sensor.

To take thermal property measurements, Figure 23, the Hot Disc sensor emits a controlled pulse of heat for a set period of time. The amplitude, penetration depth and duration of this pulse depend on the response of the material used as the test sample. To establish a reference, a pure PDMS sample was used and adjusted to the initial conditions, thus serving as a basis for other analyses. In addition, it is possible to guarantee the reliability of the measured

values by comparing them with studies in the literature on the thermal conductivity of pure PDMS or by consulting the manuals of the suppliers of this material.

Each series of tests consisted of five consecutive measurements, each lasting 40 seconds and applying 40 mW of power to the sample, with an interval of 2 minutes between each measurement, allowing the temperature to stabilize. The sample temperature was monitored using a PT100 sensor. For the analysis to be standardized, settings were used that included time correction, no offset compensation and standard heat capacity. Also considered were insulation conductivity values of 0.036 W/mK and diffusivity of 0.69 mm²/s.

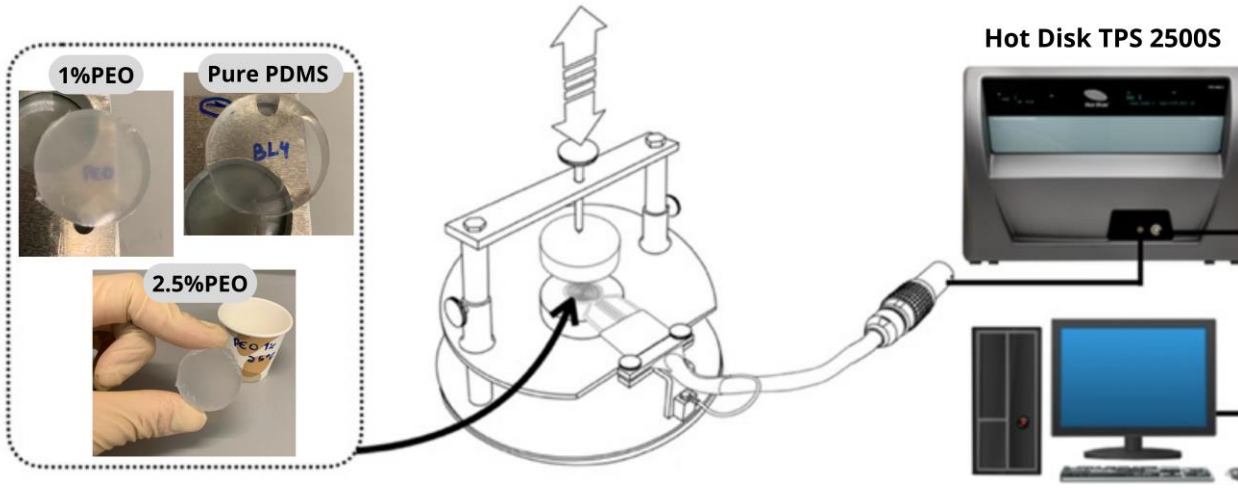

Figure 23 - PDMS sample attached to stainless steel support and Hot Disk TPS 2500S data acquisition system.

3.3. Results and discussion

This chapter presents and discusses the results obtained when measuring the contact angle and thermal conductivity of the s-PDMS and pure PDMS samples. Using the Taguchi method there are two main evaluations, the first being the evaluation of the signal-to-noise ratio, which makes it possible to define the level of variation for each parameter. The second is based on analysis of variance (ANOVA), which is used to determine the influence of each parameter.

Taguchi, ANOVA and Grey analysis were carried out on the results of the tests in the initial phase (0 h) and after 3 weeks, to analyze the immediate behavior of the surfactant addition and the medium/long-term behavior.

3.3.1. Wettability test

In order to obtain the wettability data from the contact angle, only the contact angle measurement method presented in 3.2.6.2 was considered, since in order to carry out the calculations in 3.2.6.1, other tests would have to be carried out, such as scanning electron microscopy, X-ray diffraction, X-ray photoelectron spectroscopy and Raman spectroscopy.

3.3.1.1. Taguchi method results

As the aim is to obtain the lowest possible surface wettability (lowest contact angle), the S/N ratio for this parameter is "lower is better", as it allows the value of the contact angle to be minimized. With the values obtained in the wettability tests (Figure 24) and Eq. (3), it was possible to determine the signal-to-noise ratios for the nine samples, thus obtaining Table 8 and Table 9, where the first is the test carried out immediately after curing and the second after 3 weeks. Figure *24* shows in pink a dotted line marking the transition from hydrophobic (greater than 90°) to hydrophilic (less than 90°).

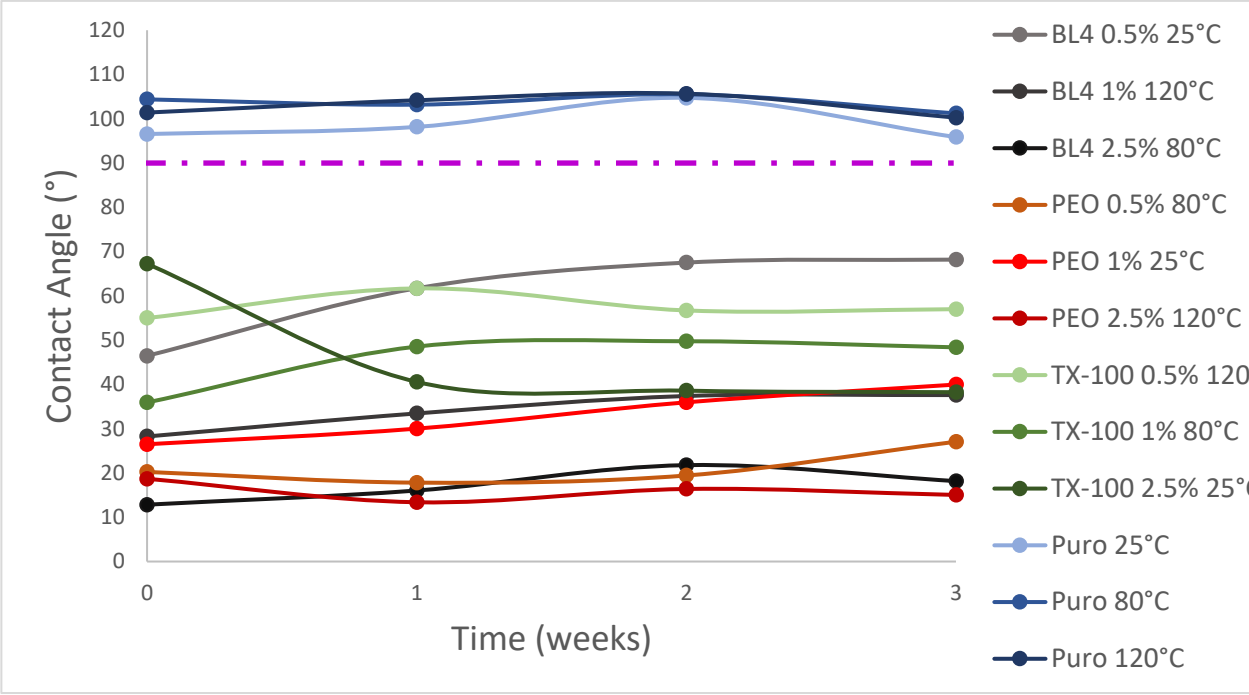

Figure 24 - Contact angle (°) x Time (weeks) for PDMS samples with different types of surfactants and curing temperatures.

Table 8 - S/N ratio value from the initial wettability test (0 h).

Test number	Surfactant concentration %	Curing temperature (°C)	Type of surfactant	Contact Angle (°)	S/N (dB)
1	0.5%	25°C	BL4	46,46	-33,3416
2	0.5%	80°C	PEO	20,4	-26,1926
3	0.5%	120°C	TX-100	55	-34,8073
4	1%	25°C	PEO	25,49	-28,1274
5	1%	80°C	TX-100	35,93	-31,1091
6	1%	120°C	BL4	28,25	-29,0204
7	2.5%	25°C	TX-100	67,24	-36,5526
8	2.5%	80°C	BL4	12,84	-22,1713
9	2.5%	120°C	PEO	13,39	-22,5356

Table 9 - S/N ratio value of the wettability test after 3 weeks.

Test number	Surfactant concentration %	Curing temperature (°C)	Type of surfactant	Contact Angle (°)	S/N (dB)
1	0.5%	25°C	BL4	68,19	-36,6744
2	0.5%	80°C	PEO	27,06	-28,6466
3	0.5%	120°C	TX-100	57	-35,1175
4	1%	25°C	PEO	39,97	-32,0347
5	1%	80°C	TX-100	48,38	-33,6933
6	1%	120°C	BL4	37,59	-31,5014
7	2.5%	25°C	TX-100	38,25	-31,6526
8	2.5%	80°C	BL4	18,17	-25,1871
9	2.5%	120°C	PEO	15,04	-23,5450

From Table 8 and Table 9, the test that shows the highest initial S/N ratio value is sample 8 (-22.1713 dB) and after 3 weeks sample 9 (-23.5450 dB), respectively, these results are confirmed by the lowest contact angle value, while sample 7 (-36.5526 dB), initial, and sample 1 (-36.6744 dB), after 3 weeks, gave rise to the lowest S/N ratio value which in turn are

the highest contact angle values. Figure 25 shows the average S/N ratio values for the different parameters in relation to initial wettability (0 h) and Figure 26 to wettability after 3 weeks.

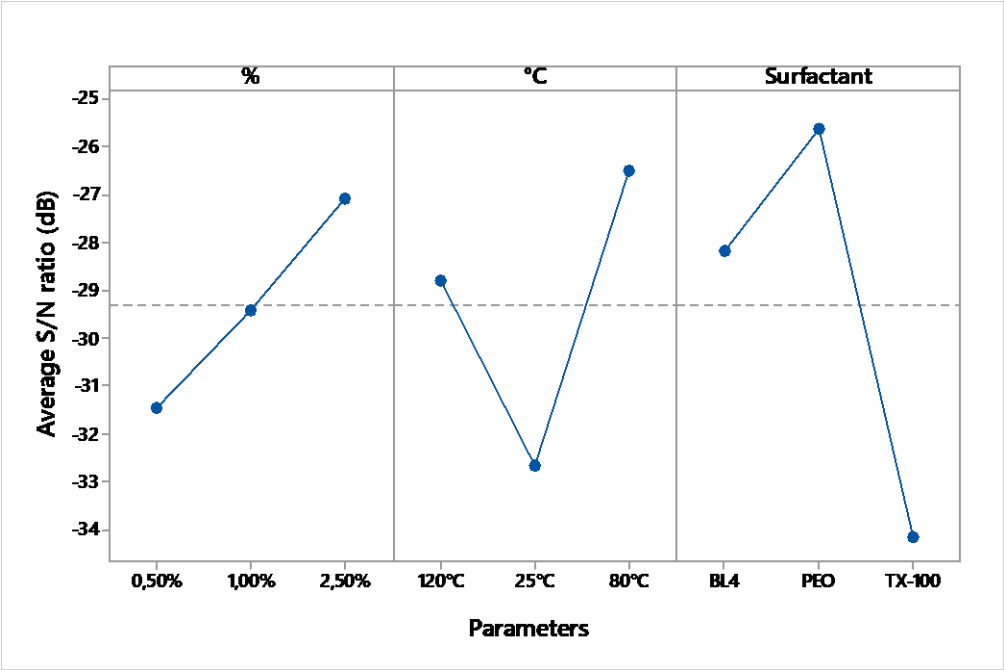

Figure 25 - Average S/N value for the different parameters in relation to initial wettability (0 h).

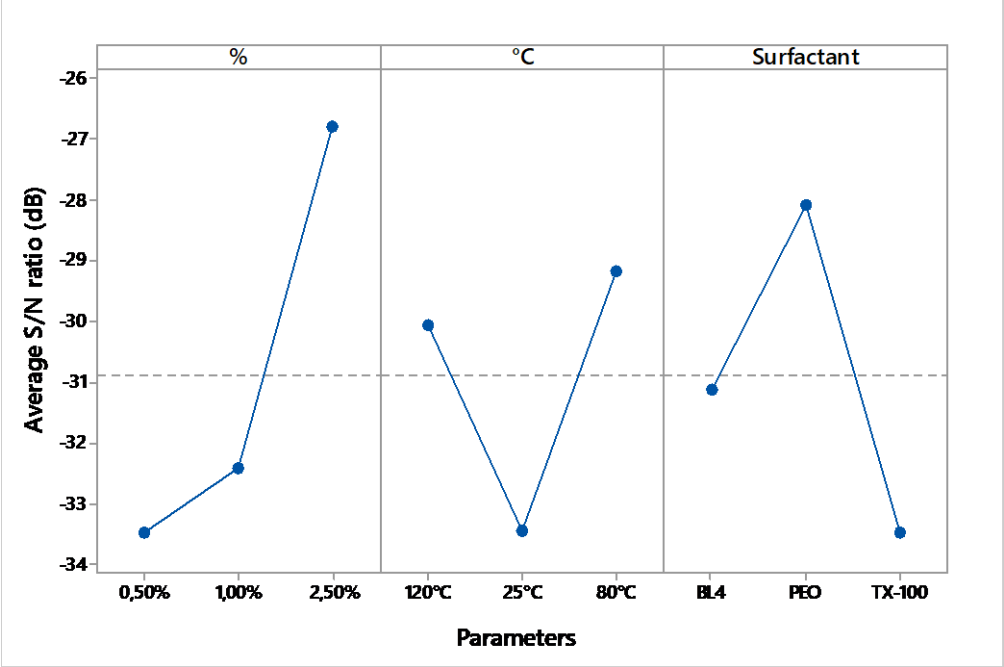

Figure 26 - Average S/N value for the different parameters in relation to wettability after 3 weeks.

Looking at Figure 25 and Figure 26, it is possible to conclude that the best combination for wettability is 2.5% PEO curing at 80°C, both for wettability measured initially and after 3 weeks. As expected, it can be analyzed that the higher the surfactant concentration, the greater the wettability. The curing temperature together with the comparison between the three

surfactants is new to the study, mainly due to the lack of studies. The Taguchi method was used to find the ideal temperature to be 80°C and the surfactant that most influenced wettability among the three analyzed was PEO.

Due to the ideal sample given by Taguchi not being included in the set of samples according to Taguchi's orthogonal array, Table *7*, and the analysis showing that the parameters and levels were excessively influential on the wettability characteristic, the ideal sample was then prepared, consisting of 2.5% PEO cured at 80°C. This ideal sample obtained an initial contact angle (0 h) of 12.87°, showing a reduction of 62.02% in the contact angle compared to the average initial contact angles (0 h) of the 9 samples produced according to the orthogonal array.

3.3.1.2. ANOVA results

For the ANOVA, the S/N values calculated using the Taguchi method were used for both wettability and conductivity tests. The analysis was conducted using the S/N values related to the contact angles from the wettability tests, with the aim of identifying the most influential parameters on the surface characteristics of the produced samples. The analysis of variance (ANOVA) was performed with the smallest contact angle recorded during the tests, using the statistical software Minitab 17. The data for this analysis, including the initial contact angle and the angle after 3 weeks, are presented in Table 8 and Table 9, respectively. The ANOVA results, both initial and after 3 weeks, are detailed in Table 10 and Table 11, respectively.

In the following tables, "DF" stands for degrees of freedom, "SS" denotes the sum of squares, "MS" represents the mean square, and "F Value" and "P Value" are statistical tools used to determine which parameters have the greatest influence on the quality characteristic studied. The mean square (MS) is calculated by dividing the sum of squares (SS) by the number of degrees of freedom (DF).

Table 10 - ANOVA values for initial wettability test (0 h).

Initial wettability test						
Source	DF	Adj SS	Adj MS	F-Value	P-Value	% influence
%	2	28,569	14,285	3,64	0,216	13,5902
°C	2	58,604	29,302	7,46	0,118	27,8777
Surfactant	2	115,187	57,593	14,66	0,064	54,7941
Error	2	7,858	3,929			3,7380
Total	8	210,218				100,0

Table 11 - ANOVA values for wettability test after 3 weeks.

Wettability test after 3 weeks						
Source	DF	Adj SS	Adj MS	F-Value	P-Value	% influence
%	2	77,355	38,6777	96,34	0,01	50,5717
°C	2	30,631	15,3156	38,15	0,026	20,0254
Surfactant	2	44,172	22,0859	55,01	0,018	28,8779
Error	2	0,803	0,4015			0,5250
Total	8	152,961				100,0

From Table 10, the most influential parameter on the contact angle of the samples with surfactant is the type of surfactant, with an influence of almost 55%. The curing temperature accounts for approximately 28%, and the surfactant concentration has a 13.6% influence on the reduction of the contact angle. For Table 11, after 3 weeks of curing the samples, the most influential factor is the surfactant concentration at 50.57%, followed by the type of surfactant at 28.88%, and finally the curing temperature at 20%, which aligns with expectations.

3.3.2. Thermal conduction test

3.3.2.1. Taguchi method results

Unlike wettability, the aim is to obtain the highest possible thermal conductivity. The S/N ratio for this parameter is "higher is better", as it allows the thermal conductivity value to be maximized. With the values obtained in the conductivity tests and Eq.(2), it was possible to determine the signal/noise ratios for the nine samples, thus obtaining Table 12 and Table 13, the first being the test carried out immediately after curing and the second after 3 weeks.

Table 12 - S/N ratio value from the initial thermal conductivity test (0 h).

Test number	**Surfactant concentration %**	**Curing temperature** (°C)	**Type of surfactant**	**Thermal conductivity (W/mK)**	**S/N (dB)**
1	0.5%	25°C	BL4	0,2106	-13,5308
2	0.5%	80°C	PEO	0,2264	-12,9025
3	0.5%	120°C	TX-100	0,1975	-14,0887
4	1%	25°C	PEO	0,199	-14,0229
5	1%	80°C	TX-100	0,2116	-13,4897
6	1%	120°C	BL4	0,2031	-13,8458
7	2.5%	25°C	TX-100	0,225	-12,9563
8	2.5%	80°C	BL4	0,2	-13,9794
9	2.5%	120°C	PEO	0,197	-14,1107

Table 13 - S/N ratio value of the thermal conductivity test after 3 weeks.

Test number	**Surfactant concentration %**	**Curing temperature** (°C)	**Type of surfactant**	**Thermal conductivity (W/mK)**	**S/N (dB)**
1	0.5%	25°C	BL4	0,2006	-13,9534
2	0.5%	80°C	PEO	0,1966	-14,1283
3	0.5%	120°C	TX-100	0,1972	-14,1019
4	1%	25°C	PEO	0,1952	-14,1904
5	1%	80°C	TX-100	0,198	-14,0667
6	1%	120°C	BL4	0,1981	-14,0623
7	2.5%	25°C	TX-100	0,1993	-14,0099
8	2.5%	80°C	BL4	0,1993	-14,0099
9	2.5%	120°C	PEO	0,1962	-14,1460

From Table 12 and Table 13, the test that shows the highest initial S/N ratio value is sample 2 (-12,9025 dB) and after 3 weeks sample 1 (-13,9534 dB), respectively, these results are confirmed by the higher thermal conductivity value. The values of both the thermal conductivity and consequently the S/N are very close between the samples, due to PDMS being an insulating material and surfactants in general being poor thermal conductors, so it shows a low increase in conductivity regardless of the percentage, type of surfactant and curing temperature. Figure 27 shows the average values of the S/N ratio for the different parameters in relation to the initial thermal conductivity (0 hours) and Figure 28 the thermal conductivity after 3 weeks.

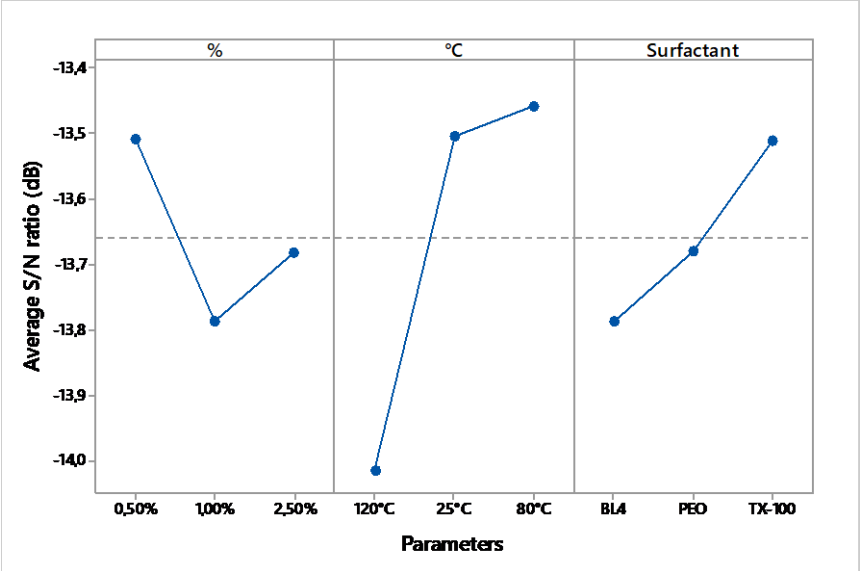

Figure 27 - Average S/N value for the different parameters in relation to the initial thermal conductivity (0 hours).

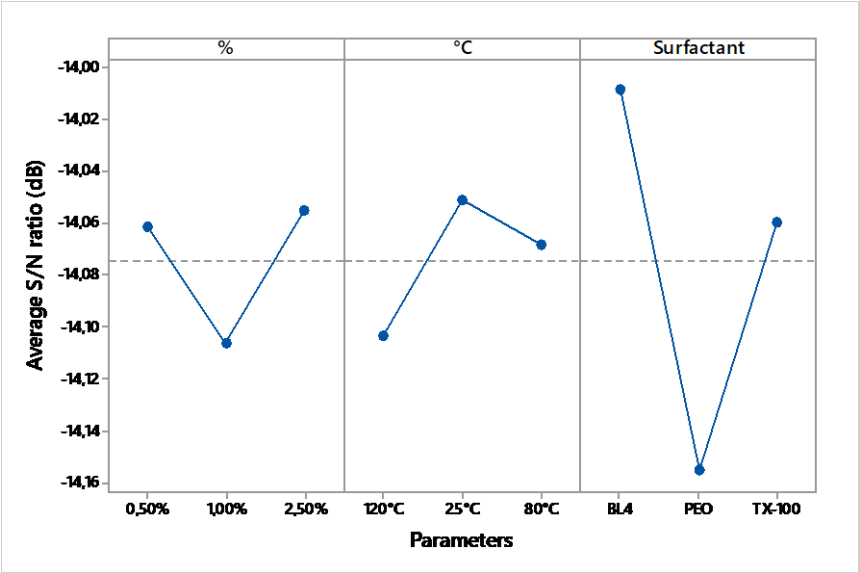

Figure 28 - Average S/N value for the different parameters in relation to thermal conductivity after 3 weeks.

As shown in Figure 27, it can be seen that the optimal sample, based on the immediate results after curing the samples, is 0.5% TX-100 cured at 80°C. Based on the results after 3 weeks of curing the samples, Figure 28, the ideal sample is 2.5% BL4 cured at 25°C. There was a big difference between the optimal samples immediately after curing and after 3 weeks, but, as mentioned above, these are not the optimal parameters for increasing thermal conductivity. It was noted that the variation in the thermal conductivity and S/N values is very low between one sample and another, and this change between the optimal samples for the two tests is not as relevant as when compared to the wettability S/N values, where the parameters that were chosen to be analyzed have a major influence on this characteristic.

3.3.2.2. ANOVA results

Similarly to the wettability test, this analysis was conducted using the S/N values, but this time related to the thermal conductivity test values. The ANOVA was performed with the average thermal conductivity values recorded during the tests, using the same software. The data for this analysis, both initial and after 3 weeks, are presented in Table 12 and Table 13, respectively. The ANOVA results, both initial and after 3 weeks, are detailed in Table 14 and Table 15, respectively.

Table 14 - ANOVA values for the initial thermal conductivity test (0 hours).

Initial thermal conductivity test						
Source	DF	Adj SS	Adj MS	F-Value	P-Value	% influence
%	2	0,1191	0,0596	0,12	0,89	6,7296
°C	2	0,5751	0,2876	0,6	0,626	32,4952
Surfactant	2	0,1143	0,0571	0,12	0,894	6,4584
Error	2	0,9612	0,4806			54,3112
Total	8	1,7698				100,0

Table 15 - ANOVA values for the thermal conductivity test after 3 weeks.

Final thermal conductivity test						
Source	DF	Adj SS	Adj MS	F-Value	P-Value	% influence
%	2	0,00471	0,0024	1,41	0,415	10,3671
°C	2	0,00425	0,0021	1,27	0,44	9,3480
Surfactant	2	0,03314	0,0166	9,94	0,091	72,9442
Error	2	0,00334	0,0017			7,3406
Total	8	0,04543				100

From Table 14, the most influential parameter on the thermal conductivity of the samples with surfactant is the residual error, with an influence of approximately 54%. This error represents the variability that remains in the model after identifying all the main effects [164]. In other words, roughly half of the variations in the results are not explained by the selected model. This may be associated with the selection of parameters and levels that were not able to adequately explain the model. Thus, it indicates that the selected parameters are not suitable for altering the thermal conductivity. Despite the high value of the residual error, the model applied in the experimental part achieved an improvement compared to the initially defined conditions, demonstrating the effectiveness of using the Taguchi method. For Table 15, after 3 weeks of curing the samples, the most influential factor is the type of surfactant, at approximately 73%,

followed by the surfactant concentration percentage at 10.37%, and finally, the curing temperature at 9.34%.

3.3.3. Grey relational analysis of the tests

According to the Grey Relational Analysis method, the S/N ratio values from the wettability and thermal conductivity tests, calculated for the PDMS samples with surfactant using the Taguchi method, were used as presented previously.

3.3.3.1. Grey relational analysis of initial tests (0 h)

The first step in the Grey relational analysis involves reprocessing the data, as shown in Table 16, to normalize them. This process aims to eliminate variations in the responses and make them dimensionless by standardizing the results on a scale from 0 to 1. The normalization of the S/N ratio is done using Eq.(5) (for the "larger is better" characteristic), since the values used to calculate the Grey relational analysis were the S/N ratio, this equation must be used. The "larger is better" and "smaller is better" conditions were already established for each test in the Taguchi method, so the best S/N result will always be the largest. If the means of the values obtained in the tests were used, it would be necessary to use Eq.(4) when the test objective is "smaller is better" and Eq.(5) for "larger is better" [164]. The normalized values of the results are presented in Table 17.

Table 16 - S/N ratio values for initial wettability and thermal conductivity tests (0h).

Sample	S/N Wettability (dB)	S/N Conductivity (dB)
1	-33,3416	-13,5308
2	-26,1926	-12,9025
3	-34,8073	-14,0887
4	-28,1274	-14,0229
5	-31,1091	-13,4897
6	-29,0204	-13,8458
7	-36,5526	-12,9563
8	-22,1713	-13,9794
9	-22,5356	-14,1107

Table 17 - Normalized S/N ratio values for the initial wettability and thermal conductivity tests (0 h).

Sample	S/N Wettability	S/N Conductivity
1	0,2233	0,4799
2	0,7204	1,0000
3	0,1214	0,0182
4	0,5858	0,0726
5	0,3785	0,5140
6	0,5238	0,2192
7	0,0000	0,9554
8	1,0000	0,1087
9	0,9747	0,0000

Subsequently, the Grey relational coefficient was calculated using the values from Table 17 and Eq.(5). First, $\left|x^0{}_i - x_{ij}\right|$ is determined, as shown in Table 18, which is the difference between the ideal sequence value (indicating the optimal value for the normalization of the signal-to-noise ratio, i.e., the ideal result for the S/N ratio) and the normalized value obtained for each experiment, and each analyzed response. Based on these values, the Grey relational coefficients were determined and presented in Table 19. For our analysis, the distinctive coefficient (ζ) used was 0.5 for the wettability test results and 0.5 for the thermal conductivity test results, aiming to analyze an ideal sample that equally combines the best conditions for wettability and thermal conductivity.

Table 18 - $x^0{}_i - x_{ij}$ values for the initial wettability and thermal conductivity tests (0 h).

Sample	$x^0{}_i - x_{ij}$ Wettability	$x^0{}_i - x_{ij}$ Conductivity
1	0,7767	0,5201
2	0,2796	0,0000
3	0,8786	0,9818
4	0,4142	0,9274
5	0,6215	0,4860
6	0,4762	0,7808
7	1,0000	0,0446
8	0,0000	0,8913
9	0,0253	1,0000

Table 19 - Grey relational coefficient values for the initial wettability and thermal conductivity test (0 h).

Sample	Grey's relational coefficient for wettability testing	Grey's relaional for conductivity testing
1	0,3916	0,4902
2	0,6413	1,0000
3	0,3627	0,3374
4	0,5470	0,3503
5	0,4458	0,5071
6	0,5122	0,3904
7	0,3333	0,9181

8	1,0000	0,3594
9	0,9518	0,3333

Finally, based on Table *19* and using Eq.(7), Grey's relational grade is calculated, Table 20. In this table it is also possible to observe the order of the results, where the number 1 represents the highest value of Grey's relational grade and 9 the lowest value.

Table 20 - Values for the relational grade of Grey and their respective order for the initial tests (0 h).

Sample	Grey's relational grade	Order
1	0,4409	8
2	0,8207	1
3	0,3501	9
4	0,4486	7
5	0,4765	5
6	0,4513	6
7	0,6257	4
8	0,6797	2
9	0,6426	3

This brings us to Table 21, which shows the average Grey's relational grade for each level, as well as the total average. With this information it is possible to identify the best combination, and the higher the value of the Grey's relational grade, the better the combination.

Table 21 - Response table for the initial Grey's ratio (0 h).

Grey's relational grade					
Parameters	Level 1	Level 2	Level 3	Max-Mín	Total average
Percentage (%)	0,5372	0,4588	0,6493	0,1905	0,5484
Temperature (°C)	0,5051	0,6589	0,4813	0,1776	
Surfactant	0,5240	0,6373	0,4841	0,1532	

Table 21 shows that the best combination (ideal sample) of parameters obtained from the Grey analysis is a percentage of 2.5% (level 3), a curing temperature of 80°C (level 2) and the type of surfactant PEO (level 2). This is confirmed graphically in Figure 29. This is the same ideal sample as that used by the Taguchi method, both for initial wetting and after 3 weeks. This proves that, because the parameters and levels are more appropriate for altering wettability, with a much more significant improvement in this property than in thermal conductivity, the values of the wettability S/N ratio had a greater influence, even when placing the two properties equally, when the weight of each test was chosen in the Grey analysis to have 50% wettability and 50% thermal conductivity.

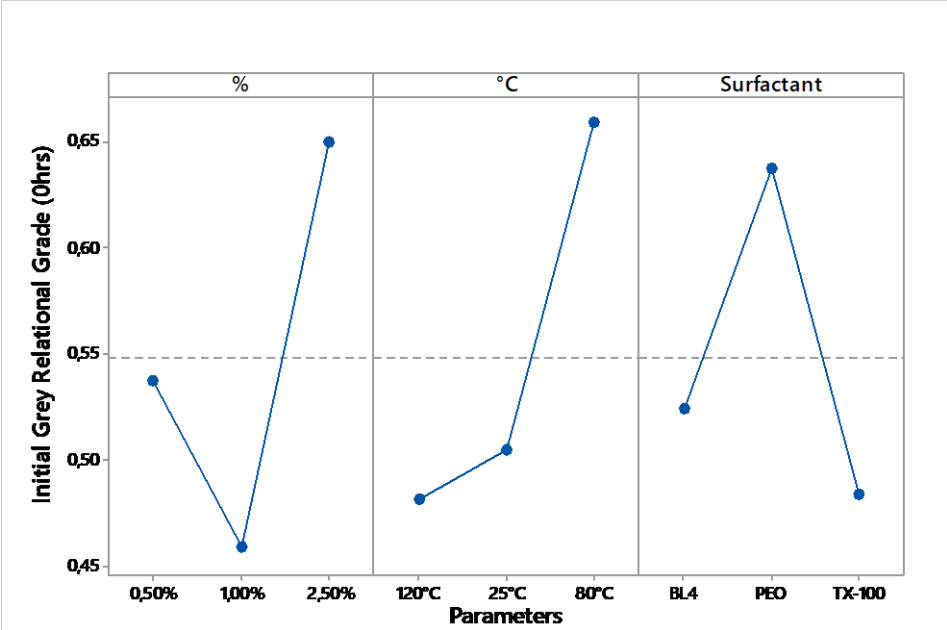

Figure 29 - Response from the initial Grey's relational analysis (0 h).

3.3.3.2. Confirmation of initial Grey's results (0 h)

After determining the optimal level of the parameters and confirming that this configuration had not been executed in all the tests planned by the Taguchi orthogonal array, additional experiments were conducted to validate the results. First, using Eq.(8), the estimated Grey relational grade for the optimal combination, which was 2.5% - 80°C - PEO, was calculated.

Subsequently, three tests were conducted using this optimal combination, called Ideal Sample Counterproof. From the results of the wettability and thermal conductivity tests, the S/N ratio of each test was calculated, as shown in Table 22.

Table 22 - S/N initial wettability and thermal conductivity test (0 h) - Counterproof Ideal Sample.

Sample	S/N Wettability (dB)	S/N Conductivity (dB)
Counterproof - 1	-22,1916	-14,0667
Counterproof - 2	-22,5551	-14,1904
Counterproof - 3	-22,0692	-14,2325

Applying the same methodology used previously, the Grey relational analysis was performed using the data obtained from the counterproof tests, determining the Grey Relational Grade of the experiment. Table 23 presents the average of the initial Grey Relational Grades (0 h), the estimated Grey Relational Grade by calculation, and the Grey Relational Grade from the

counterproof tests. Additionally, the table compares the percentage improvement between the calculated prognosis and the counterproof results of the optimal combination, with the average of the Grey relational grades.

Table 23 - Comparison and improvement between relational degrees of Grey.

Comparison and improvement between relational grades of Grey		
	Grey's Relational Grade	Improvement in relation to the average of Grey's relational grades
Average Initial Grey Relational Grades (0 h)	0,5484	-
Grey's Relational Grade Counter-proof	0,8325	52%
Ideal Grey's Relational Grade calculated	0,8487	55%

Based on Table 23, it can be seen that the Taguchi method and Grey's relational analysis achieved a 52% improvement in the process, compared to the calculated ideal of 55%, with the results being very close, showing that the theoretical value was consistent with the practical value.

3.3.3.3. ANOVA analysis results

ANOVA is now carried out on the Grey's ratio values obtained in the initial wettability and thermal conductivity tests (0 h). These values are shown in Table 20 and the ANOVA values are shown in Table 24.

Table 24 - ANOVA values of the Grey's ratio analysis initial tests (0 h).

Source	**DF**	**Adj SS**	**Adj MS**	**F-Value**	**P-Value**	**% influence**
%	2	0,00573	0,00286	1,6	0,385	3,1513
°C	2	0,03162	0,01581	8,81	0,102	17,3972
Surfactant	2	0,14082	0,07041	39,23	0,025	77,4759
Error	2	0,00359	0,0018			1,9751
Total	8	0,18177				100

These figures show that the type of surfactant has the greatest influence on the combination of wettability and thermal conductivity in an immediate analysis of the samples after curing, with approximately 77.5%. The curing temperature was the second parameter with 17.39% and the surfactant concentration percentage came last with 3.15%.

3.3.3.4. Grey's relational analysis for trials after 3 weeks

The Grey's ratio analysis of the final tests, after 3 weeks, was carried out in the same way as above, using the S/N ratio values obtained in the tests, Table 25.

Table 25 - S/N ratio values for the final wettability and thermal conductivity tests after 3 weeks.

Sample	S/N Wettability (dB)	S/N Conductivity (dB)
1	-36,6744	-13,9534
2	-28,6466	-14,1283
3	-35,1175	-14,1019
4	-32,0347	-14,1904
5	-33,6933	-14,0667
6	-31,5014	-14,0623
7	-31,6526	-14,0099
8	-25,1871	-14,0099
9	-23,5450	-14,1460

As previously mentioned, the step-by-step process for this method is the same. First, the data is reprocessed to normalize the results, Table 26.

Table 26 - Normalized S/N values for final wettability and thermal conductivity tests, after 3 weeks.

Sample	S/N Wettability	S/N Conductivity
1	0	1
2	0,6114	0,2619
3	0,1186	0,3736
4	0,3534	0,0000
5	0,2271	0,5219
6	0,3940	0,5404
7	0,3825	0,7617
8	0,8749	0,7617
9	1	0,1873

Next, the normalized S/N ratio values, Table 24, and Eq.(5) were used to calculate Grey's relational coefficient. Table *27* shows the $\left|x^0{}_i - x_{ij}\right|$ values and, based on these values, the Grey's ratio coefficient is shown in Table 28. In the same way as for the initial tests, the value of the distinctive coefficient (ζ) of 0.5 was used for each test.

Table 27 - $\left|x^0{}_i - x_{ij}\right|$ values for final wettability and thermal conductivity tests after 3 weeks.

Sample	$\left\|x^0{}_i - x_{ij}\right\|$ Wettability	$\left\|x^0{}_i - x_{ij}\right\|$ Conductivity
1	1	0
2	0,3886	0,7381
3	0,8814	0,6264
4	0,6466	1

5	0,7729	0,4781
6	0,6060	0,4596
7	0,6175	0,2383
8	0,1251	0,2383
9	0	0,8127

Table 28 - Grey's relational coefficient values for final wettability and thermal conductivity tests after 3 weeks.

Sample	Grey's relational coefficient for wettability testing	Grey's relational for conductivity testing
1	0,3333	1
2	0,5627	0,4038
3	0,3619	0,4439
4	0,4361	0,3333
5	0,3928	0,5112
6	0,4521	0,5211
7	0,4474	0,6773
8	0,7999	0,6773
9	1	0,3809

Finally, Table 28 and Eq.(7) are used to calculate the relational degree of Grey, shown in Table 29 along with the order of the results.

Table 29 - Values for Grey's relational grade for the final wettability and conductivity tests, after 3 weeks.

Sample	Grey's relational degree	Order
1	0,6667	3
2	0,4833	6
3	0,4029	8
4	0,3847	9
5	0,4520	7
6	0,4866	5
7	0,5623	4
8	0,7386	1
9	0,6904	2

Table 30 shows the average Grey's relational grade for each of the levels and the total average. In this way, it is possible to identify the best combination, and the higher the value of the Grey's relational grade, the better the combination. The best combination for the two tests presented, 50% for each test, is the sample with a 2.5% percentage surfactant concentration (level 3), at a curing temperature of 80°C (level 2) and BL4 surfactant (level 1). This can be seen graphically in Figure 30. This optimal combination was 37% better than the average of Grey's relational grades.

Table 30 - Response table for the Relational Grey grade for final wettability and thermal conductivity tests after 3 weeks.

Grey's relational degree					
Parameters	Level 1	Level 2	Level 3	Max-Mín	Total average
Percentage %	0,5176	0,4411	0,6638	0,2227	0,5408
Temperature °C	0,5379	0,5580	0,5266	0,0313	
Surfactant	0,6306	0,5195	0,4724	0,1582	

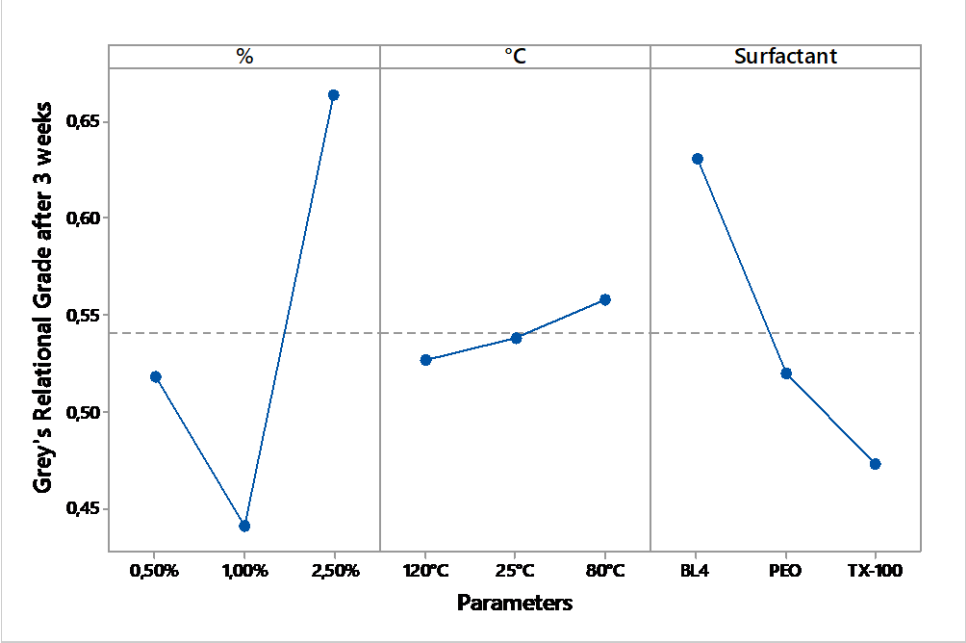

Figure 30 - Response table for the Relational Grey grade for final wettability and thermal conductivity tests after 3 weeks.

3.3.3.5. ANOVA analysis results

In the same way as for the initial wettability and thermal conductivity tests, the Grey's relational grade values, Table 29, were used for the tests carried out after 3 weeks of curing. Table 31 shows that the factor that most influenced the combined wettability and thermal conductivity after 3 weeks of curing was the percentage of surfactant concentration in the PDMS surfactant mixture, with approximately 57%. This was followed by the type of surfactant, with 29.2%, and the curing temperature with only 1.1% influence. There was a difference in the percentages of influence of the parameters compared to the initial tests, which could again be explained by the choice of parameters that were not suitable for thermal conductivity, thus giving rise to an unexpected variation.

Table 31 - ANOVA values from Grey's relational analysis for the final wettability and thermal conductivity tests after 3 weeks.

Source	DF	Adj SS	Adj MS	F-Value	P-Value	% influence
%	2	0,07682	0,0384	4,41	0,185	56,7621
°C	2	0,00151	0,0008	0,09	0,92	1,1150
Surfactant	2	0,03959	0,0198	2,27	0,306	29,2533
Error	2	0,01742	0,0087			12,8695
Total	8	0,13534				100

3.4. Validation of the optimal wetting sample using the Taguchi method

Based on the optimal sample presented in the Taguchi method, it was decided to carry out an application to validate this result. The best sample from the wettability test was chosen, as there was a very significant improvement in this aspect, while the improvement in thermal conductivity was practically insignificant. For this reason, it was decided to carry out the application focused on wettability, and not on thermal conductivity or Grey's relational analysis, which considered 50% wettability and 50% thermal conductivity, thus having a great influence on the thermal conductivity part.

It was therefore decided to carry out an application of microchannels, on pure PDMS and another with the ideal sample for wettability presented in the Taguchi method, a sample with 2.5% PEO cured at 80°C, to analyze the improvement. It is necessary to increase the hydrophilicity in PDMS for microchannel applications because greater hydrophilicity improves the flow of fluids by capillarity, allowing the liquid to move through the microchannels without the need for pumps or other forced movement devices. As well as, for other applications, reducing the adsorption of proteins and cells on the channel walls and increasing compatibility with various aqueous reagents, this optimizes the performance of microfluidic devices, making them more efficient and simplifying their design and operation [100], [154], [155].

The fabrication of the microchannels was carried out in the same way as for the samples, the difference being that instead of pouring the mixture and the pure PDMS into the circular mold, Figure 19, it was poured into the microchannel mold, Figure 20.

3.4.1. Capillary Flow Studies

Capillary flow tests were conducted to evaluate surface wettability by observing the self-movement of a fluid through the devices. A small volume of water ($v = 100\ \mu L$) was pipetted at the inlet, and its flow was monitored by measuring the time, in seconds, required to reach the outlet of the device, Figure 31. The PDMS microchannels were fabricated using both control and bulk-modified PDMS. The results from the control samples showed that the hydrophobic nature of PDMS hinders the flow of a liquid, in this case, distilled water, through the channels (Figure 31A). Subsequently, tests were conducted on the devices with added surfactant (Figure 31B), where the rapid and immediate movement of the liquid was clearly observed, the results are shown in Table 32, where two tests were carried out and the average of the tests was taken, with the control PDMS and 2.5% PEO cured at 80°C, the ideal sample for wettability, immediately after curing (0 h) and after 24 h of curing. The fluid detachment time is given in seconds.

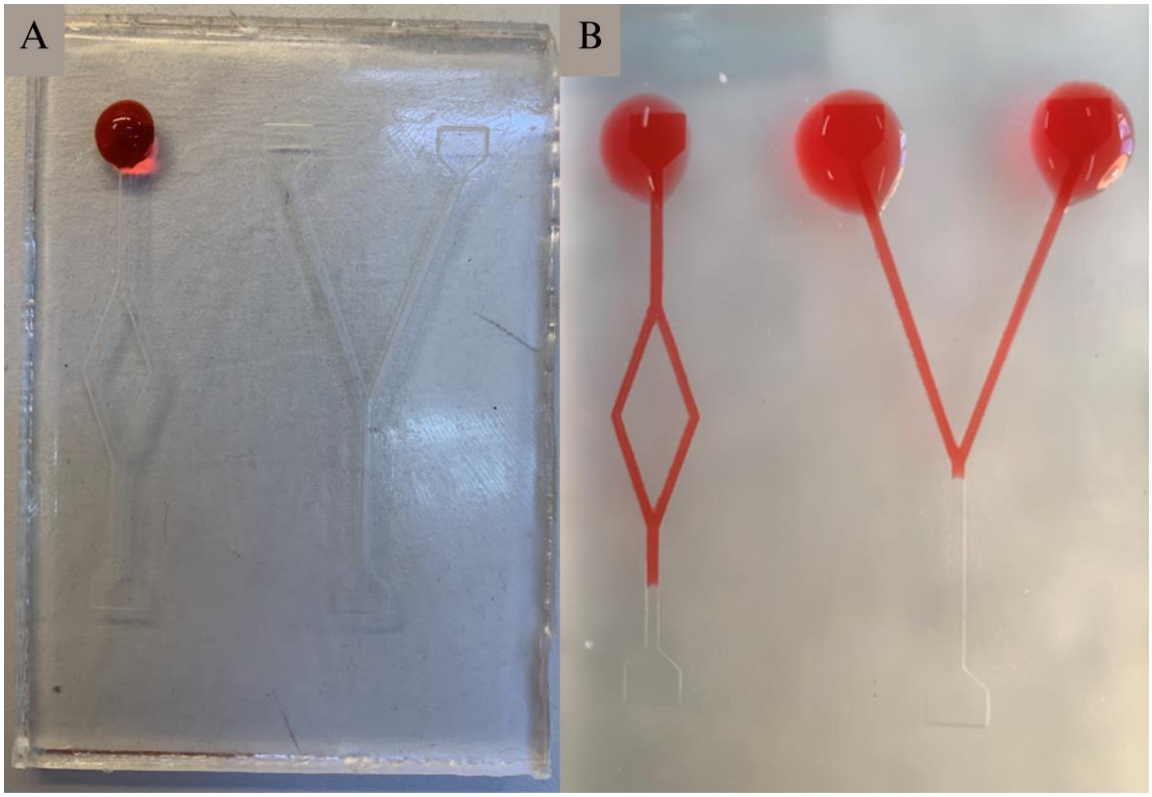

Figure 31 - Samples of microchannels in a 10:1 ratio in (A) pure PDMS, control, and (B) PDMS mixed with 2.5% PEO surfactant cured at 80°C.

Table 32 - Capillary tests were carried out on the devices in Figure 20 at 0 hours and 24 hours after curing. The measurements were obtained by measuring the fluid flow time(s).

	Microchannels	**Time (seconds)**			
		Control PDMS		PEO 2.5% 80°C	
		0 h	24 h	0 h	24 h
A		– *	– *	63.04	86.67
B		– *	– *	84.21	83.46
C	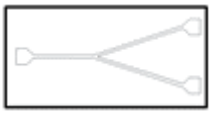	– *	– *	50.12	52.65
D		– *	– *	54.09	56.54

* Due to the hydrophobic nature of PDMS, there was no fluid movement.

The results showed that the samples modified with 2.5% PEO cured at 80°C exhibited a very considerable improvement compared to pure PDMS (control) as well as to some analyses with other methods in the literature. According to the data in Table *32*, hydrophobic recovery was very low for microchannels C and D, with a low increase in capillary flow times, while it remained constant for microchannel B. Microchannel A had a significant increase in capillary flow times, from 63.04 seconds just after curing (0 h) to 86.67 seconds after 24 hours, indicating considerable hydrophobic recovery. Overall, hydrophobic recovery was low according to the capillary flow data presented, suggesting that the modification carried out with these parameters could be a good candidate for modifying the PDMS surface for in vitro studies.

3.5. Conclusions

The aim of this study was to optimize the wettability and thermal conductivity parameters of samples containing three types of surfactants: Polyethylene Oxide (PEO), Brij L4 (BL4) and Triton X-100 (TX-100). Three different concentration percentages of these surfactants were analyzed, with variations in curing temperature, using the contact angle as a criterion for wettability and standardized criteria for thermal conductivity. To find the optimum combination, the Taguchi method and Grey's relational analysis were used, as well as analysis of variance (ANOVA) to assess the influence of each parameter on the results.

The results showed that the best combination for wettability is a concentration of 2.5% PEO with curing at 80°C, both initially and after three weeks. Analysis of the graph of the

average S/N values showed that higher surfactant concentrations increase wettability, and among the parameters chosen, the type of surfactant was the most influential parameter, followed by the curing temperature and, finally, the surfactant concentration. The type of surfactant influenced the initial contact angle by almost 55%, while the curing temperature and surfactant concentration influenced it by 28% and 13.6%, respectively. After three weeks, surfactant concentration became the most influential factor with 50.57%, followed by surfactant type with 28.88% and curing temperature with 20%.

With regard to thermal conductivity, the best initial combination was 0.5% TX-100 cured at 80°C, and after three weeks it was 2.5% BL4 cured at 25°C. However, the variation in thermal conductivity was not as significant compared to wettability, since the parameters chosen are not suitable for this purpose. Grey's analysis for the initial tests (0 h) confirmed that the optimum combination, taking into account both tests, is 2.5% PEO cured at 80°C, a 52% improvement on the other samples made using the orthogonal Taguchi arrangement. Grey's relational analysis after three weeks showed 2.5% BL4 cured at 80°C and his analysis of variance showed that the surfactant concentration had the greatest influence, with approximately 57%, followed by the type of surfactant with 29.2% and the curing temperature with only 1.1%.

Based on the results of the tests and methods, validation was focused on wettability due to the significant improvement observed in the reduction of the contact angle, while thermal conductivity showed little improvement. As a result, the sample with 2.5% PEO cured at 80°C was used to manufacture microchannels. Increased hydrophilicity in PDMS is essential for microchannel applications, as it improves the flow of fluids by capillarity, among other applications, optimizing the performance of microfluidic devices. According to the data obtained from the capillarity tests, hydrophobic recovery was low for microchannels C and D, while microchannel B remained constant. Microchannel A, however, showed a significant increase in capillary flow times, suggesting considerable hydrophobic recovery. Overall, the low hydrophobic recovery observed suggests that the modification performed may be promising for altering the surface of PDMS in in vitro studies. The effectiveness of the Taguchi method in optimizing wettability parameters was validated, showing the importance of considering both wettability and thermal conductivity in future studies and practical applications.

Chapter 4

4.1. Global conclusions

The comprehensive review of polydimethylsiloxane surface wettability and the optimization study of wettability and thermal conductivity parameters highlight the importance and complexity of surface modification techniques to alter the inherent hydrophobicity of PDMS. Usually, four main strategies are addressed: oxygen plasma treatment, addition of surfactants, UV-ozone treatment and incorporation of nanomaterials. These techniques are widely used due to their greater availability of information, lower production complexity and reduced cost compared to new emerging techniques.

Each method has its specific advantages and challenges. Oxygen plasma treatment is effective in increasing the hydrophilicity of the surface by introducing polar functional groups through oxidation reactions. The addition of surfactants offers versatility for altering wettability, with the choice and concentration of surfactant being essential for achieving the desired properties. UV-ozone treatment is considerable for its effectiveness in increasing surface energy, inducing oxidation and generating hydrophilic functional groups. The incorporation of nanomaterials into PDMS is a promising technique for modifying wettability, allowing adaptable surface properties through controlled distribution and interfacial interactions.

The optimization study focused on the analysis of three surfactants (Polyethylene Oxide - PEO, Brij L4 - BL4, and Triton X-100 - TX-100), varying their concentrations and curing temperatures. Using methods such as Taguchi, Grey's relational analysis and ANOVA, it was determined that the best combination for wettability was a concentration of 2.5% PEO cured at 80°C, both initially and after three weeks. The analysis revealed that higher surfactant concentrations increase wettability, with surfactant type being the most influential parameter initially, while surfactant concentration became the most significant factor after three weeks.

As far as thermal conductivity is concerned, the best initial combination was 0.5% TX-100 cured at 80°C, and after three weeks it was 2.5% BL4 cured at 25°C. However, the variation in thermal conductivity was not as significant as in wettability, indicating that the parameters selected were not the most suitable for this specific purpose. Grey's relational analysis

confirmed that the optimum initial combination was 2.5% PEO cured at 80°C, providing a 52% improvement over the other samples based on Taguchi's orthogonal arrangement.

Based on the results, the sample with 2.5% PEO cured at 80°C was used to manufacture microchannels, due to the significant increase in hydrophilicity, which is essential for microchannel applications, improving the flow of fluids by capillarity and optimizing the performance of microfluidic devices. The effectiveness of the Taguchi method in optimizing wettability parameters was validated, highlighting the importance of considering both wettability and thermal conductivity in future studies and practical applications.

4.2. Future Directions

In future work, the combination of the surface modification techniques analyzed in the literature review, together with the exploration of new emerging techniques, has great potential to meet the needs of various areas with lower costs and complexity. In addition, the use of wettability improvement techniques presented in this work together with thermal conductivity improvement techniques will enable a wider range of applications using PDMS. In addition, three new tests were carried out, namely PDMS adhesion to glass laminate, optical transparency and mechanical tests, to broaden the scope of knowledge about the properties of PDMS with surfactant.

References

[1] D. Feldman, “Polymer History,” *Des Monomers Polym*, vol. 11, no. 1, pp. 1–15, Feb. 2008, doi: 10.1163/156855508X292383.

[2] M. Z. S. S. R. A. U. Muhammad Arshad, *Polymers for advanced applications*, Elsevier. 2020.

[3] L. McKeen, *The Effect of Sterilization on Plastics and Elastomers*. Elsevier, 2012.

[4] X. Li *et al.*, “Amino-functionalized ZIFs-based porous liquids with low viscosity for efficient low-pressure CO2 capture and CO2/N2 separation,” *Chemical Engineering Journal*, vol. 429, p. 132296, Feb. 2022, doi: 10.1016/J.CEJ.2021.132296.

[5] Y. Xia and G. M. Whitesides, “Extending Microcontact Printing as a Microlithographic Technique,” *Langmuir*, vol. 13, no. 7, pp. 2059–2067, 1997, doi: 10.1021/la960936e.

[6] J. M. K. Ng, I. Gitlin, A. D. Stroock, and G. M. Whitesides, “Components for integrated poly(dimethylsiloxane) microfluidic systems,” *Electrophoresis*, vol. 23, no. 20, pp. 3461–3473, 2002, doi: 10.1002/1522-2683(200210)23:20<3461::AID-ELPS3461>3.0.CO;2-8.

[7] J. Friend and L. Yeo, “Fabrication of microfluidic devices using polydimethylsiloxane,” *Biomicrofluidics*, vol. 4, no. 2, p. 026502, 2010, doi: 10.1063/1.3259624.

[8] J. C. McDonald *et al.*, “Fabrication of microfluidic systems in poly(dimethylsiloxane),” *Electrophoresis*, vol. 21, no. 1, pp. 27–40, 2000, doi: 10.1002/(SICI)1522-2683(20000101)21:1<27::AID-ELPS27>3.0.CO;2-C.

[9] A. Dhall *et al.*, “Characterization and Neutral Atom Beam Surface Modification of a Clear Castable Polyurethane for Biomicrofluidic Applications,” *Surfaces*, vol. 2, no. 1, pp. 100–116, 2019, doi: 10.3390/surfaces2010009.

[10] T. Yamamoto, T. Fujii, and T. Nojima, “PDMS–glass hybrid microreactor array with embedded temperature control device. Application to cell-free protein synthesis,” *Lab Chip*, vol. 2, no. 4, pp. 197–202, 2002, doi: 10.1039/B205010B.

[11] J. P. Rolland, E. C. Hagberg, G. M. Denison, K. R. Carter, and J. M. De Simone, “High-Resolution Soft Lithography: Enabling Materials for Nanotechnologies,” *Angewandte Chemie International Edition*, vol. 43, no. 43, pp. 5796–5799, Nov. 2004, doi: 10.1002/ANIE.200461122.

[12] C. Hansen and S. R. Quake, “Microfluidics in structural biology: smaller, faster… better,” *Curr Opin Struct Biol*, vol. 13, no. 5, pp. 538–544, Oct. 2003, doi: 10.1016/J.SBI.2003.09.010.

[13] J. M. K. Ng, I. Gitlin, A. D. Stroock, and G. M. Whitesides, “Components for integrated poly(dimethylsiloxane) microfluidic systems”, doi: 10.1002/1522-2683(200210)23:20.

[14] J. C. McDonald and G. M. Whitesides, “Poly(dimethylsiloxane) as a Material for Fabricating Microfluidic Devices,” *Acc Chem Res*, vol. 35, no. 7, pp. 491–499, Jul. 2002, doi: 10.1021/ar010110q.

[15] I. Y. Sulym *et al.*, “Structural and hydrophobic–hydrophilic properties of nanosilica/zirconia alone and with adsorbed PDMS,” *Appl Surf Sci*, vol. 258, no. 1, pp. 270–277, 2011, doi: 10.1016/j.apsusc.2011.08.045.

[16] P. G. Gezer, S. Brodsky, A. Hsiao, G. L. Liu, and J. L. Kokini, “Modification of the hydrophilic/hydrophobic characteristic of zein film surfaces by contact with oxygen plasma treated PDMS and oleic acid content,” *Colloids Surf B Biointerfaces*, vol. 135, pp. 433–440, Nov. 2015, doi: 10.1016/J.COLSURFB.2015.07.006.

[17] Z. He *et al.*, “Antifouling induced by surface wettability of poly(dimethyl siloxane) and its nanocomposites,” *Nanotechnol Rev*, vol. 12, no. 1, 2023, doi: 10.1515/ntrev-2022-0552.

[18] J. Kim, U. P. Kumar, S.-J. Lee, C.-L. Kim, and J.-W. Lee, “Implementation of endurable superhydrophobic surfaces through dilution rate control of the PDMS coating on micro-nano surface structures,” *Polymer (Guildf)*, vol. 275, p. 125929, 2023, doi: 10.1016/j.polymer.2023.125929.

[19] Y. Si, Z. Dong, and L. Jiang, “Bioinspired Designs of Superhydrophobic and Superhydrophilic Materials,” *ACS Cent Sci*, vol. 4, no. 9, pp. 1102–1112, 2018, doi: 10.1021/acscentsci.8b00504.

[20] K. Liu, X. Yao, and L. Jiang, “Recent developments in bio-inspired special wettability,” *Chem Soc Rev*, vol. 39, no. 8, pp. 3240–3255, 2010, doi: 10.1039/B917112F.

[21] J. Drelich, E. Chibowski, D. Desheng Meng, and K. Terpilowski, “Hydrophilic and superhydrophilic surfaces and materials,” *Soft Matter*, vol. 7, no. 21, pp. 9804–9828, 2011, doi: 10.1039/C1SM05849E.

[22] R. Ariati, F. Sales, A. Souza, R. A. Lima, and J. Ribeiro, “Polydimethylsiloxane Composites Characterization and Its Applications: A Review,” *Polymers 2021, Vol. 13, Page 4258*, vol. 13, no. 23, p. 4258, Dec. 2021, doi: 10.3390/POLYM13234258.

[23] S. Bayraktaroglu, S. Kizil, and H. Bulbul Sonmez, “A highly reusable polydimethylsiloxane sorbents for oil/organic solvent clean-up from water,” *J Environ Chem Eng*, vol. 9, no. 5, p. 106002, 2021, doi: 10.1016/j.jece.2021.106002.

[24] S.-J. Choi *et al.*, “A Polydimethylsiloxane (PDMS) Sponge for the Selective Absorption of Oil from Water,” *ACS Appl Mater Interfaces*, vol. 3, no. 12, pp. 4552–4556, 2011, doi: 10.1021/am201352w.

[25] A. Turco, C. Malitesta, G. Barillaro, A. Greco, A. Maffezzoli, and E. Mazzotta, “A magnetic and highly reusable macroporous superhydrophobic/superoleophilic PDMS/MWNT nanocomposite for oil sorption from water,” *J Mater Chem A Mater*, vol. 3, no. 34, pp. 17685–17696, 2015, doi: 10.1039/C5TA04353K.

[26] H. Guo *et al.*, “A Robust Cotton Textile-Based Material for High-Flux Oil–Water Separation,” *ACS Appl Mater Interfaces*, vol. 11, no. 14, pp. 13704–13713, 2019, doi: 10.1021/acsami.9b01108.

[27] C. Cao *et al.*, “Robust fluorine-free superhydrophobic PDMS–ormosil@fabrics for highly effective self-cleaning and efficient oil–water separation,” *J Mater Chem A Mater*, vol. 4, no. 31, pp. 12179–12187, 2016, doi: 10.1039/C6TA04420D.

[28] G. Pan, X. Xiao, and Z. Ye, “Fabrication of stable superhydrophobic coating on fabric with mechanical durability, UV resistance and high oil-water separation efficiency,” *Surf Coat Technol*, vol. 360, pp. 318–328, 2019, doi: 10.1016/j.surfcoat.2018.12.094.

[29] J. Zhou, D. A. Khodakov, A. V Ellis, and N. H. Voelcker, “Surface modification for PDMS-based microfluidic devices,” *Electrophoresis*, vol. 33, no. 1, pp. 89–104, 2012, doi: 10.1002/elps.201100482.

[30] M. L. van Poll, F. Zhou, M. Ramstedt, L. Hu, and W. T. S. Huck, “A Self-Assembly Approach to Chemical Micropatterning of Poly(dimethylsiloxane),” *Angewandte Chemie*, vol. 119, no. 35, pp. 6754–6757, 2007, doi: 10.1002/ange.200702286.

[31] A. Mata, A. J. Fleischman, and S. Roy, “Characterization of Polydimethylsiloxane (PDMS) Properties for Biomedical Micro/Nanosystems,” *Biomed Microdevices*, vol. 7, no. 4, pp. 281–293, 2005, doi: 10.1007/s10544-005-6070-2.

[32] T. C. Merkel, V. I. Bondar, K. Nagai, B. D. Freeman, and I. Pinnau, “Gas sorption, diffusion, and permeation in poly(dimethylsiloxane),” *J Polym Sci B Polym Phys*, vol. 38, no. 3, pp. 415–434, 2000, doi: 10.1002/(SICI)1099-0488(20000201)38:3<415::AID-POLB8>3.0.CO;2-Z.

[33] J. C. McDonald and G. M. Whitesides, “Poly(dimethylsiloxane) as a Material for Fabricating Microfluidic Devices,” *Acc Chem Res*, vol. 35, no. 7, pp. 491–499, 2002, doi: 10.1021/ar010110q.

[34] T. Young, “III. An essay on the cohesion of fluids,” *Philos Trans R Soc Lond*, vol. 95, pp. 65–87, 1997, doi: 10.1098/rstl.1805.0005.

[35] C. G. Jothi Prakash and R. Prasanth, “Approaches to design a surface with tunable wettability: a review on surface properties,” *Journal of Materials Science 2020 56:1*, vol. 56, no. 1, pp. 108–135, Sep. 2020, doi: 10.1007/S10853-020-05116-1.

[36] J. Jeevahan, M. Chandrasekaran, G. Britto Joseph, R. B. Durairaj, and G. Mageshwaran, “Superhydrophobic surfaces: a review on fundamentals, applications, and challenges,” *J Coat Technol Res*, vol. 15, no. 2, pp. 231–250, 2018, doi: 10.1007/s11998-017-0011-x.

[37] T. Darmanin and F. Guittard, “Wettability of conducting polymers: From superhydrophilicity to superoleophobicity,” *Prog Polym Sci*, vol. 39, no. 4, pp. 656–682, 2014, doi: 10.1016/j.progpolymsci.2013.10.003.

[38] J. B. Boreyko, Y. Zhao, and C.-H. Chen, “Planar jumping-drop thermal diodes,” *Appl Phys Lett*, vol. 99, no. 23, p. 234105, 2011, doi: 10.1063/1.3666818.

[39] M. Jozanović *et al.*, “Nanomaterials in microchip electrophoresis – A review,” *TrAC Trends in Analytical Chemistry*, vol. 165, p. 117111, 2023, doi: 10.1016/j.trac.2023.117111.

[40] J. Zhou, A. V. Ellis, and N. H. Voelcker, “Recent developments in PDMS surface modification for microfluidic devices,” *Electrophoresis*, vol. 31, no. 1, pp. 2–16, 2010, doi: 10.1002/elps.200900475.

[41] S. P. Dalawai *et al.*, “Recent Advances in durability of superhydrophobic self-cleaning technology: A critical review,” *Prog Org Coat*, vol. 138, p. 105381, Jan. 2020, doi: 10.1016/J.PORGCOAT.2019.105381.

[42] J. Drelich and A. Marmur, “Physics and applications of superhydrophobic and superhydrophilic surfaces and coatings,” *Surf Innov*, vol. 2, no. 4, pp. 211–227, 2014, doi: 10.1680/si.13.00017.

[43] D. V Antonov, A. G. Islamova, and P. A. Strizhak, “Hydrophilic and Hydrophobic Surfaces: Features of Interaction with Liquid Drops,” *Materials*, vol. 16, no. 17, p. 5932, 2023, doi: 10.3390/ma16175932.

[44] K. Duangkanya, A. Kopwitthaya, S. Chanhorm, and Y. Infahsaeng, “Oxygen plasma treatment time induced hydrophilicity of polydimethylsiloxane (PDMS) thin films for liquid lenses application,” *Mater Today Proc*, vol. 65, pp. 2442–2445, 2022, doi: 10.1016/j.matpr.2022.06.121.

[45] A. B. Shrirao, F. H. Kung, D. Yip, C. H. Cho, and E. Townes-Anderson, “Vacuum-assisted fluid flow in microchannels to pattern substrates and cells,” *Biofabrication*, vol. 6, no. 3, p. 035016, 2014, doi: 10.1088/1758-5082/6/3/035016.

[46] M. Kakuta, F. G. Bessoth, and A. Manz, “Microfabricated devices for fluid mixing and their application for chemical synthesis,” *The Chemical Record*, vol. 1, no. 5, pp. 395–405, 2001, doi: 10.1002/tcr.1023.

[47] M. Amerian, M. Amerian, M. Sameti, and E. Seyedjafari, “Improvement of PDMS surface biocompatibility is limited by the duration of oxygen plasma treatment,” *J Biomed Mater Res A*, vol. 107, no. 12, pp. 2806–2813, 2019, doi: 10.1002/jbm.a.36783.

[48] D. T. Eddington, J. P. Puccinelli, and D. J. Beebe, “Thermal aging and reduced hydrophobic recovery of polydimethylsiloxane,” *Sens Actuators B Chem*, vol. 114, no. 1, pp. 170–172, Mar. 2006, doi: 10.1016/J.SNB.2005.04.037.

[49] C. Karthik, S. Rajalakshmi, S. Thomas, and V. Thomas, “Intelligent polymeric biomaterials surface driven by plasma processing,” *Curr Opin Biomed Eng*, vol. 26, p. 100440, 2023, doi: 10.1016/j.cobme.2022.100440.

[50] V. N. Vasilets, K. Nakamura, Y. Uyama, S. Ogata, and Y. Ikada, “Improvement of the micro-wear resistance of silicone by vacuum ultraviolet irradiation,” *Polymer (Guildf)*, vol. 39, no. 13, pp. 2875–2881, 1998, doi: 10.1016/S0032-3861(97)00594-6.

[51] Y. Berdichevsky, J. Khandurina, A. Guttman, and Y.-H. Lo, “UV/ozone modification of poly(dimethylsiloxane) microfluidic channels,” *Sens Actuators B Chem*, vol. 97, no. 2, pp. 402–408, 2004, doi: 10.1016/j.snb.2003.09.022.

[52] J. Pan *et al.*, “Cell membrane damage and cargo delivery in nano-electroporation,” *Nanoscale*, vol. 15, no. 8, pp. 4080–4089, 2023, doi: 10.1039/D2NR05575A.

[53] A.-J. Wang, J.-J. Xu, Q. Zhang, and H.-Y. Chen, “The use of poly(dimethylsiloxane) surface modification with gold nanoparticles for the microchip electrophoresis,” *Talanta*, vol. 69, no. 1, pp. 210–215, 2006, doi: 10.1016/j.talanta.2005.09.029.

[54] A.-J. Wang, J.-J. Xu, and H.-Y. Chen, “Proteins modification of poly(dimethylsiloxane) microfluidic channels for the enhanced microchip electrophoresis,” *J Chromatogr A*, vol. 1107, no. 1, pp. 257–264, 2006, doi: 10.1016/j.chroma.2005.12.040.

[55] W. Wang, L. Zhao, F. Zhou, J.-J. Zhu, and J.-R. Zhang, “Electroosmotic flow-switchable poly(dimethylsiloxane) microfluidic channel modified with cysteine based on gold nanoparticles,” *Talanta*, vol. 73, no. 3, pp. 534–539, 2007, doi: 10.1016/j.talanta.2007.04.024.

[56] D. Bodas and C. Khan-Malek, “Hydrophilization and hydrophobic recovery of PDMS by oxygen plasma and chemical treatment—An SEM investigation,” *Sens Actuators B Chem*, vol. 123, no. 1, pp. 368–373, 2007, doi: 10.1016/j.snb.2006.08.037.

[57] H. Hillborg, J. F. Ankner, U. W. Gedde, G. D. Smith, H. K. Yasuda, and K. Wikström, "Crosslinked polydimethylsiloxane exposed to oxygen plasma studied by neutron reflectometry and other surface specific techniques," *Polymer (Guildf)*, vol. 41, no. 18, pp. 6851–6863, Aug. 2000, doi: 10.1016/S0032-3861(00)00039-2.

[58] S. Bhattacharya, A. Datta, J. M. Berg, and S. Gangopadhyay, "Studies on surface wettability of poly(dimethyl) siloxane (PDMS) and glass under oxygen-plasma treatment and correlation with bond strength," *Journal of Microelectromechanical Systems*, vol. 14, no. 3, pp. 590–597, 2005, doi: 10.1109/JMEMS.2005.844746.

[59] B. Jiang *et al.*, "Noncovalent reversible binding-enabled facile fabrication of leak-free PDMS microfluidic devices without plasma treatment for convenient cell loading and retrieval," *Bioact Mater*, vol. 16, pp. 346–358, 2022, doi: 10.1016/j.bioactmat.2022.02.031.

[60] B. Jiang *et al.*, "Microscale investigation on the wettability and bonding mechanism of oxygen plasma-treated PDMS microfluidic chip," *ApSS*, vol. 574, p. 151704, Feb. 2022, doi: 10.1016/J.APSUSC.2021.151704.

[61] M. Manouchehri, "A comprehensive review on state-of-the-art antifouling super(wetting and anti-wetting) membranes for oily wastewater treatment," *Adv Colloid Interface Sci*, vol. 323, p. 103073, Jan. 2024, doi: 10.1016/J.CIS.2023.103073.

[62] R. A. Lawton, C. R. Price, A. F. Runge, W. J. Doherty, and S. S. Saavedra, "Air plasma treatment of submicron thick PDMS polymer films: effect of oxidation time and storage conditions," *Colloids Surf A Physicochem Eng Asp*, vol. 253, no. 1–3, pp. 213–215, Feb. 2005, doi: 10.1016/J.COLSURFA.2004.11.010.

[63] M. Morra, E. Occhiello, R. Marola, F. Garbassi, P. Humphrey, and D. Johnson, "On the aging of oxygen plasma-treated polydimethylsiloxane surfaces," *J Colloid Interface Sci*, vol. 137, no. 1, pp. 11–24, 1990, doi: 10.1016/0021-9797(90)90038-P.

[64] A. Tóth, I. Bertóti, M. Blazsó, G. Bánhegyi, A. Bognar, and P. Szaplonczay, "Oxidative damage and recovery of silicone rubber surfaces. I. X-ray photoelectron spectroscopic study," *J Appl Polym Sci*, vol. 52, no. 9, pp. 1293–1307, 1994, doi: 10.1002/app.1994.070520914.

[65] I.-J. Chen and E. Lindner, "The Stability of Radio-Frequency Plasma-Treated Polydimethylsiloxane Surfaces," *Langmuir*, vol. 23, no. 6, pp. 3118–3122, 2007, doi: 10.1021/la0627720.

[66] M. Hashimoto, S. S. Shevkoplyas, B. Zasońska, T. Szymborski, P. Garstecki, and G. M. Whitesides, "Formation of Bubbles and Droplets in Parallel, Coupled Flow-Focusing Geometries," *Small*, vol. 4, no. 10, pp. 1795–1805, 2008, doi: 10.1002/smll.200800591.

[67] S. H. Tan, N. T. Nguyen, Y. C. Chua, and T. G. Kang, "Oxygen plasma treatment for reducing hydrophobicity of a sealed polydimethylsiloxane microchannel," *Biomicrofluidics*, vol. 4, no. 3, 2010, doi: 10.1063/1.3466882.

[68] J. A. Juárez-Moreno, A. Ávila-Ortega, A. I. Oliva, F. Avilés, and J. V Cauich-Rodríguez, "Effect of wettability and surface roughness on the adhesion properties of collagen on PDMS films treated by capacitively coupled oxygen plasma," *Appl Surf Sci*, vol. 349, pp. 763–773, 2015, doi: 10.1016/j.apsusc.2015.05.063.

[69] S. Y. Yang, B. C. Bai, and Y. R. Kim, “Effective Surface Structure Changes and Characteristics of Activated Carbon with the Simple Introduction of Oxygen Functional Groups by Using Radiation Energy,” *Surfaces*, vol. 7, no. 1, pp. 12–25, 2024, doi: 10.3390/surfaces7010002.

[70] J. Kim, M. K. Chaudhury, M. J. Owen, and T. Orbeck, “The Mechanisms of Hydrophobic Recovery of Polydimethylsiloxane Elastomers Exposed to Partial Electrical Discharges,” *J Colloid Interface Sci*, vol. 244, no. 1, pp. 200–207, 2001, doi: 10.1006/jcis.2001.7909.

[71] D. Bodas and C. Khan-Malek, “Formation of more stable hydrophilic surfaces of PDMS by plasma and chemical treatments,” *Microelectron Eng*, vol. 83, no. 4–9, pp. 1277–1279, Apr. 2006, doi: 10.1016/J.MEE.2006.01.195.

[72] J. M. Grace and L. J. Gerenser, “Plasma Treatment of Polymers,” *J Dispers Sci Technol*, vol. 24, no. 3–4, pp. 305–341, 2003, doi: 10.1081/DIS-120021793.

[73] D. Hegemann, H. Brunner, and C. Oehr, “Plasma treatment of polymers for surface and adhesion improvement,” *Nucl Instrum Methods Phys Res B*, vol. 208, pp. 281–286, 2003, doi: 10.1016/S0168-583X(03)00644-X.

[74] M. J. Owen and P. J. Smith, “Plasma treatment of polydimethylsiloxane,” *J Adhes Sci Technol*, vol. 8, no. 10, pp. 1063–1075, 1994, doi: 10.1163/156856194X00942.

[75] E. A. Vogler, “Surface Modification for Biocompatibility,” in *Engineered Biomimicry*, Elsevier, 2013, pp. 189–220. [Online]. Available: https://linkinghub.elsevier.com/retrieve/pii/B9780124159952000088

[76] V. Bagiatis, G. W. Critchlow, D. Price, and S. Wang, “The effect of atmospheric pressure plasma treatment (APPT) on the adhesive bonding of poly(methyl methacrylate) (PMMA)-to-glass using a polydimethylsiloxane (PDMS)-based adhesive,” *Int J Adhes Adhes*, vol. 95, p. 102405, 2019, doi: 10.1016/j.ijadhadh.2019.102405.

[77] G. G. Morbioli, N. C. Speller, and A. M. Stockton, “A practical guide to rapid-prototyping of PDMS-based microfluidic devices: A tutorial,” *Anal Chim Acta*, vol. 1135, pp. 150–174, Oct. 2020, doi: 10.1016/J.ACA.2020.09.013.

[78] M. P. Wolf, G. B. Salieb-Beugelaar, and P. Hunziker, “PDMS with designer functionalities—Properties, modifications strategies, and applications,” *Prog Polym Sci*, vol. 83, pp. 97–134, 2018, doi: 10.1016/j.progpolymsci.2018.06.001.

[79] M. Ruzi, N. Celik, and M. S. Onses, “Superhydrophobic coatings for food packaging applications: A review,” *Food Packag Shelf Life*, vol. 32, p. 100823, Jun. 2022, doi: 10.1016/J.FPSL.2022.100823.

[80] S. Shen *et al.*, “Advances in wearable respiration sensors,” *Materials Today*, 2024, doi: 10.1016/j.mattod.2023.12.003.

[81] J. S. G. de Camargo, A. J. de Menezes, N. C. da Cruz, E. C. Rangel, and A. de O. Delgado-Silva, “Morphological and Chemical Effects of Plasma Treatment with Oxygen (O_2) and Sulfur Hexafluoride (SF_6) on Cellulose Surface,” *Materials Research*, vol. 20, pp. 842–850, 2018, doi: 10.1590/1980-5373-MR-2016-1111.

[82] P. K. Chu, J. Y. Chen, L. P. Wang, and N. Huang, “Plasma-surface modification of biomaterials,” *Materials Science and Engineering: R: Reports*, vol. 36, no. 5, pp. 143–206, 2002, doi: 10.1016/S0927-796X(02)00004-9.

[83] H. M. L. Tan, H. Fukuda, T. Akagi, and T. Ichiki, “Surface modification of poly(dimethylsiloxane) for controlling biological cells’ adhesion using a scanning radical microjet,” *Thin Solid Films*, vol. 515, no. 12, pp. 5172–5178, 2007, doi: 10.1016/j.tsf.2006.10.026.

[84] C. A. Pal *et al.*, “Fabrication of plasma-treated superhydrophobic polydimethylsiloxane (PDMS) – Coatėd melamine sponge for enhanced adhesion capability and sustainable oil/water separation,” *Sep Purif Technol*, vol. 330, p. 125483, 2024, doi: 10.1016/j.seppur.2023.125483.

[85] Z. Almutairi, C. L. Ren, and L. Simon, “Evaluation of polydimethylsiloxane (PDMS) surface modification approaches for microfluidic applications,” *Colloids Surf A Physicochem Eng Asp*, vol. 415, pp. 406–412, 2012, doi: 10.1016/j.colsurfa.2012.10.008.

[86] X. Zhu *et al.*, “Fabrication of reconfigurable protein matrices by cracking,” *Nat Mater*, vol. 4, no. 5, pp. 403–406, 2005, doi: 10.1038/nmat1365.

[87] F. Akther, S. B. Yakob, N.-T. Nguyen, and H. T. Ta, “Surface Modification Techniques for Endothelial Cell Seeding in PDMS Microfluidic Devices,” *Biosensors (Basel)*, vol. 10, no. 11, p. 182, 2020, doi: 10.3390/bios10110182.

[88] M. Ouyang, C. Yuan, R. J. Muisener, A. Boulares, and J. T. Koberstein, “Conversion of Some Siloxane Polymers to Silicon Oxide by UV/Ozone Photochemical Processes,” *Chemistry of Materials*, vol. 12, no. 6, pp. 1591–1596, 2000, doi: 10.1021/cm990770d.

[89] C. L. Mirley and J. T. Koberstein, “A Room Temperature Method for the Preparation of Ultrathin SiOx Films from Langmuir-Blodgett Layers,” *Langmuir*, vol. 11, no. 4, pp. 1049–1052, 1995, doi: 10.1021/la00004a001.

[90] H. Li *et al.*, “Extracellular Vesicular Analysis of Glypican 1 mRNA and Protein for Pancreatic Cancer Diagnosis and Prognosis,” *Advanced Science*, vol. 11, no. 11, p. 2306373, 2024, doi: 10.1002/advs.202306373.

[91] K. Efimenko, W. E. Wallace, and J. Genzer, “Surface Modification of Sylgard-184 Poly(dimethyl siloxane) Networks by Ultraviolet and Ultraviolet/Ozone Treatment,” *J Colloid Interface Sci*, vol. 254, no. 2, pp. 306–315, 2002, doi: 10.1006/jcis.2002.8594.

[92] K. Tsougeni, A. Tserepi, G. Boulousis, V. Constantoudis, and E. Gogolides, “Tunable poly(dimethylsiloxane) topography in O2 or Ar plasmas for controlling surface wetting properties and their ageing,” *Japanese Journal of Applied Physics, Part 1: Regular Papers and Short Notes and Review Papers*, vol. 46, no. 2, pp. 744–750, Feb. 2007, doi: 10.1143/JJAP.46.744/XML.

[93] Y. J. Fu *et al.*, “Effect of UV-Ozone treatment on poly(dimethylsiloxane) membranes: Surface characterization and gas separation performance,” *Langmuir*, vol. 26, no. 6, pp. 4392–4399, Mar. 2010, doi: 10.1021/LA903445X/ASSET/IMAGES/MEDIUM/LA-2009-03445X_0007.GIF.

[94] K. Ma, J. Rivera, G. J. Hirasaki, and S. L. Biswal, “Wettability control and patterning of PDMS using UV–ozone and water immersion,” *J Colloid Interface Sci*, vol. 363, no. 1, pp. 371–378, 2011, doi: 10.1016/j.jcis.2011.07.036.

[95] J. Song, D. Tranchida, and G. J. Vancso, “Contact mechanics of UV/ozone-treated PDMS by AFM and JKR testing: Mechanical performance from nano- to micrometer length scales,” *Macromolecules*, vol. 41, no. 18, pp. 6757–6762, Sep. 2008, doi: 10.1021/MA800536Y/SUPPL_FILE/MA800536Y_SI_001.PDF.

[96] C. Liu *et al.*, "Research progress of PVDF based piezoelectric polymer composites in water pollution remediation," *Journal of Water Process Engineering*, vol. 55, p. 104181, 2023, doi: 10.1016/j.jwpe.2023.104181.

[97] Y. Hashimoto, "Surface modification of polymers by vacuum ultraviolet Illumination containing low wavelength below 160 nm and microfluidic applications of irradiated polycarbonate," *Polymer (Guildf)*, vol. 287, p. 126439, 2023, doi: 10.1016/j.polymer.2023.126439.

[98] Y. Zhang and W. Jiang, "Effective strategies to enhance ultraviolet barrier ability in biodegradable polymer-based films/coatings for fruit and vegetable packaging," *Trends Food Sci Technol*, vol. 139, p. 104139, 2023, doi: 10.1016/j.tifs.2023.104139.

[99] A. Oláh, H. Hillborg, and G. J. Vancso, "Hydrophobic recovery of UV/ozone treated poly(dimethylsiloxane): adhesion studies by contact mechanics and mechanism of surface modification," *Appl Surf Sci*, vol. 239, no. 3–4, pp. 410–423, Jan. 2005, doi: 10.1016/J.APSUSC.2004.06.005.

[100] A. Fatona, Y. Chen, M. Reid, M. A. Brook, and J. M. Moran-Mirabal, "One-step in-mould modification of PDMS surfaces and its application in the fabrication of self-driven microfluidic channels," *Lab Chip*, vol. 15, no. 22, pp. 4322–4330, Oct. 2015, doi: 10.1039/C5LC00741K.

[101] S. Hu, X. Ren, M. Bachman, C. E. Sims, G. P. Li, and N. Allbritton, "Cross-linked coatings for electrophoretic separations in poly(dimethylsiloxane) microchannels," *Electrophoresis*, vol. 24, no. 21, pp. 3679–3688, 2003, doi: 10.1002/elps.200305592.

[102] J. Zhang, Y. Chen, and M. A. Brook, "Facile Functionalization of PDMS Elastomer Surfaces Using Thiol–Ene Click Chemistry," *Langmuir*, vol. 29, no. 40, pp. 12432–12442, 2013, doi: 10.1021/la403425d.

[103] J. Li, C. Zhou, and C. Chen, "PDMS-ZnO nano-composite enhanced the hydrophobicn, self-cleaning, and mechanical property of packaging corrugated paper," *Inorg Chem Commun*, vol. 158, p. 111508, 2023, doi: 10.1016/j.inoche.2023.111508.

[104] A. W. Adamson and A. P. Gast, *Physical chemistry of surfaces*, vol. 150. Interscience publishers New York, 1967.

[105] J. Seo and L. P. Lee, "Effects on wettability by surfactant accumulation/depletion in bulk polydimethylsiloxane (PDMS)," *Sens Actuators B Chem*, vol. 119, no. 1, pp. 192–198, Nov. 2006, doi: 10.1016/J.SNB.2005.12.019.

[106] G. Nam and S. H. Yoon, "Predicting the temporal wetting of porous, surfactant-added polydimethylsiloxane (PDMS)," *J Colloid Interface Sci*, vol. 556, pp. 503–513, Nov. 2019, doi: 10.1016/J.JCIS.2019.08.081.

[107] L. Montazeri, S. Bonakdar, M. Taghipour, P. Renaud, and H. Baharvand, "Modification of PDMS to fabricate PLGA microparticles by a double emulsion method in a single microfluidic device," *Lab Chip*, vol. 16, no. 14, pp. 2596–2600, 2016, doi: 10.1039/C6LC00437G.

[108] Y. Soriano-Jerez *et al.*, "Role of dynamic surface tension of silicone polyether surfactant-based silicone coatings on protein adsorption: An insight on the 'ambiguous' interfacial properties of Fouling Release Coatings," *Prog Org Coat*, vol. 186, p. 108079, Jan. 2024, doi: 10.1016/J.PORGCOAT.2023.108079.

[109] “Surfactants and Interfacial Phenomena, 4th Edition | Wiley.” Accessed: May 19, 2024. [Online]. Available: https://www.wiley.com/en-us/Surfactants+and+Interfacial+Phenomena%2C+4th+Edition-p-9780470541944

[110] A. Zdziennicka and B. Jańczuk, “Adsorption of cetyltrimethylammonium bromide and propanol mixtures with regard to wettability of polytetrafluoroethylene. I. Adsorption at aqueous solution–air interface,” *J Colloid Interface Sci*, vol. 317, no. 1, pp. 44–53, 2008, doi: 10.1016/j.jcis.2007.09.026.

[111] K. Boxshall, M.-H. Wu, Z. Cui, Z. Cui, J. F. Watts, and M. A. Baker, “Simple surface treatments to modify protein adsorption and cell attachment properties within a poly(dimethylsiloxane) micro-bioreactor,” *Surface and Interface Analysis*, vol. 38, no. 4, pp. 198–201, 2006, doi: 10.1002/sia.2274.

[112] “Entering a new era of surfactants - Evonik Industries.” Accessed: May 19, 2024. [Online]. Available: https://household-care.evonik.com/en/products/biosurfactants

[113] J. J. R. Stålgren, “Adsorption of Surfactants at the Solid-Liquid Interface: A Quartz Crystal Microbalance study,” 2002.

[114] S. Lee, R. Iten, M. Müller, and N. D. Spencer, “Influence of Molecular Architecture on the Adsorption of Poly(ethylene oxide)−Poly(propylene oxide)−Poly(ethylene oxide) on PDMS Surfaces and Implications for Aqueous Lubrication,” *Macromolecules*, vol. 37, no. 22, pp. 8349–8356, 2004, doi: 10.1021/ma049076w.

[115] A. Gökaltun, Y. B. (Abraham) Kang, M. L. Yarmush, O. B. Usta, and A. Asatekin, “Simple Surface Modification of Poly(dimethylsiloxane) via Surface Segregating Smart Polymers for Biomicrofluidics,” *Sci Rep*, vol. 9, no. 1, p. 7377, 2019, doi: 10.1038/s41598-019-43625-5.

[116] N. Kaushal and A. K. Singh, “Advancement in utilization of bio-based materials including cellulose, lignin, chitosan for bio-inspired surface coatings with special wetting behavior: A review on fabrication and applications,” *Int J Biol Macromol*, vol. 246, p. 125709, Aug. 2023, doi: 10.1016/J.IJBIOMAC.2023.125709.

[117] X. Song *et al.*, “Design, preparation, and characterization of lubricating polymer brushes for biomedical applications,” *Acta Biomater*, 2023, doi: 10.1016/j.actbio.2023.12.024.

[118] Y.-H. Dou, N. Bao, J.-J. Xu, and H.-Y. Chen, “A dynamically modified microfluidic poly(dimethylsiloxane) chip with electrochemical detection for biological analysis,” *Electrophoresis*, vol. 23, no. 20, pp. 3558–3566, 2002, doi: 10.1002/1522-2683(200210)23:20<3558::AID-ELPS3558>3.0.CO;2-#.

[119] G. Ocvirk, M. Munroe, T. Tang, R. Oleschuk, K. Westra, and D. J. Harrison, “Electrokinetic control of fluid flow in native poly(dimethylsiloxane) capillary electrophoresis devices,” *Electrophoresis*, vol. 21, no. 1, pp. 107–115, 2000, doi: 10.1002/(SICI)1522-2683(20000101)21:1<107::AID-ELPS107>3.0.CO;2-Y.

[120] C. S. Lim, E. Von Lau, K. E. Kee, and Y. M. Hung, “A comparative study of superhydrophobicity of 0D/1D/2D thermally functionalized carbon nanomaterials,” *Ceram Int*, vol. 47, no. 21, pp. 30331–30342, 2021, doi: 10.1016/j.ceramint.2021.07.213.

[121] P. N. Manoudis and I. Karapanagiotis, “Modification of the wettability of polymer surfaces using nanoparticles,” *Prog Org Coat*, vol. 77, no. 2, pp. 331–338, 2014, doi: 10.1016/j.porgcoat.2013.10.007.

[122] J. Li, M. Wang, and Y. Shen, “Chemical modification on top of nanotopography to enhance surface properties of PDMS,” *Surf Coat Technol*, vol. 206, no. 8, pp. 2161–2167, 2012, doi: 10.1016/j.surfcoat.2011.09.052.

[123] M. T. Alameda, M. R. Osorio, J. J. Hernández, and I. Rodríguez, “Multilevel Hierarchical Topographies by Combined Photolithography and Nanoimprinting Processes To Create Surfaces with Controlled Wetting,” *ACS Appl Nano Mater*, vol. 2, no. 8, pp. 4727–4733, 2019, doi: 10.1021/acsanm.9b00338.

[124] H. Wen *et al.*, “Robust super hydrophobic cotton fabrics functionalized with Ag and PDMS for effective antibacterial activity and efficient oil–water separation,” *J Environ Chem Eng*, vol. 9, no. 5, p. 106083, 2021, doi: 10.1016/j.jece.2021.106083.

[125] S. Barthwal, S. Barthwal, B. Singh, and N. Bahadur Singh, “Multifunctional and fluorine-free superhydrophobic composite coating based on PDMS modified MWCNTs/ZnO with self-cleaning, oil-water separation, and flame retardant properties,” *Colloids Surf A Physicochem Eng Asp*, vol. 597, p. 124776, 2020, doi: 10.1016/j.colsurfa.2020.124776.

[126] E. Sadler and C. R. Crick, “Suction or gravity-fed oil-water separation using PDMS-coated glass filters,” *Sustainable Materials and Technologies*, vol. 29, p. e00321, 2021, doi: 10.1016/j.susmat.2021.e00321.

[127] J. A. Vickers, M. M. Caulum, and C. S. Henry, “Generation of Hydrophilic Poly(dimethylsiloxane) for High-Performance Microchip Electrophoresis,” *Anal Chem*, vol. 78, no. 21, pp. 7446–7452, 2006, doi: 10.1021/ac0609632.

[128] S. L. Peterson, A. McDonald, P. L. Gourley, and D. Y. Sasaki, “Poly(dimethylsiloxane) thin films as biocompatible coatings for microfluidic devices: Cell culture and flow studies with glial cells,” *J Biomed Mater Res A*, vol. 72A, no. 1, pp. 10–18, Jan. 2005, doi: 10.1002/JBM.A.30166.

[129] H. P. Long, C. C. Lai, and C. K. Chung, “Polyethylene glycol coating for hydrophilicity enhancement of polydimethylsiloxane self-driven microfluidic chip,” *Surf Coat Technol*, vol. 320, pp. 315–319, 2017, doi: 10.1016/j.surfcoat.2016.12.059.

[130] T. Trantidou, Y. Elani, E. Parsons, and O. Ces, “Hydrophilic surface modification of PDMS for droplet microfluidics using a simple, quick, and robust method via PVA deposition,” *Microsyst Nanoeng*, vol. 3, no. 1, pp. 1–9, 2017, doi: 10.1038/micronano.2016.91.

[131] L. Lin and C. K. Chung, “PDMS Microfabrication and Design for Microfluidics and Sustainable Energy Application: Review,” *Micromachines 2021, Vol. 12, Page 1350*, vol. 12, no. 11, p. 1350, Oct. 2021, doi: 10.3390/MI12111350.

[132] E. Holczer and P. Fürjes, “Effects of embedded surfactants on the surface properties of PDMS; applicability for autonomous microfluidic systems,” *Microfluid Nanofluidics*, vol. 21, no. 5, p. 81, 2017, doi: 10.1007/s10404-017-1916-5.

[133] J. Vilčáková *et al.*, “Effect of Surfactants and Manufacturing Methods on the Electrical and Thermal Conductivity of Carbon Nanotube/Silicone Composites,” *Molecules*, vol. 17, no. 11, pp. 13157–13174, 2012, doi: 10.3390/molecules171113157.

[134] Z. Wu and K. Hjort, “Surface modification of PDMS by gradient-induced migration of embedded Pluronic,” *Lab Chip*, vol. 9, no. 11, pp. 1500–1503, 2009, doi: 10.1039/B901651A.

[135] M. Gonçalves *et al.*, “Polydimethylsiloxane Surface Modification of Microfluidic Devices for Blood Plasma Separation,” *Polymers 2024, Vol. 16, Page 1416*, vol. 16, no. 10, p. 1416, May 2024, doi: 10.3390/POLYM16101416.

[136] D. Baek, S. H. Lee, B. H. Jun, and S. H. Lee, “Lithography Technology for Micro- and Nanofabrication,” *Adv Exp Med Biol*, vol. 1309, pp. 217–233, 2021, doi: 10.1007/978-981-33-6158-4_9.

[137] D. J. O’Brien, A. J. H. Sedlack, P. Bhatia, C. J. Jensen, A. Quintana-Puebla, and M. Paranjape, “Systematic Characterization of Hydrophilized Polydimethylsiloxane,” *Journal of Microelectromechanical Systems*, vol. 29, no. 5, pp. 1216–1224, 2020, doi: 10.1109/JMEMS.2020.3010087.

[138] M. G. Krishna, M. Vinjanampati, and D. D. Purkayastha, “Metal oxide thin films and nanostructures for self-cleaning applications: current status and future prospects,” *The European Physical Journal Applied Physics*, vol. 62, no. 3, p. 30001, Jun. 2013, doi: 10.1051/EPJAP/2013130048.

[139] M. Wang, P. Kovacik, and K. K. Gleason, “Chemical Vapor Deposition of Thin, Conductive, and Fouling-Resistant Polymeric Films,” *Langmuir*, vol. 33, no. 40, pp. 10623–10631, 2017, doi: 10.1021/acs.langmuir.7b02646.

[140] T. Maturos, A. Wisitsora-at, T. Lomas, A. Sappat, and A. Tuantranont, “Oxygen plasma treatment of sputtered TiO2 thin film for surface modification of PDMS,” in *2007 7th IEEE Conference on Nanotechnology (IEEE NANO)*, 2007, pp. 911–913. doi: 10.1109/NANO.2007.4601331.

[141] N. Maheshwari, A. Kottantharayil, M. Kumar, and S. Mukherji, “Long term hydrophilic coating on poly(dimethylsiloxane) substrates for microfluidic applications,” *Appl Surf Sci*, vol. 257, no. 2, pp. 451–457, 2010, doi: 10.1016/j.apsusc.2010.07.010.

[142] S. Bhattacharya, A. Datta, J. M. Berg, and S. Gangopadhyay, “Studies on surface wettability of poly(dimethyl) siloxane (PDMS) and glass under oxygen-plasma treatment and correlation with bond strength,” *Journal of Microelectromechanical Systems*, vol. 14, no. 3, pp. 590–597, Jun. 2005, doi: 10.1109/JMEMS.2005.844746.

[143] L. B. Neves, I. S. Afonso, G. Nobrega, L. G. Barbosa, R. A. Lima, and J. E. Ribeiro, “A Review of Methods to Modify the PDMS Surface Wettability and Their Applications,” *Micromachines 2024, Vol. 15, Page 670*, vol. 15, no. 6, p. 670, May 2024, doi: 10.3390/MI15060670.

[144] K. Efimenko, W. E. Wallace, and J. Genzer, “Surface Modification of Sylgard-184 Poly(dimethyl siloxane) Networks by Ultraviolet and Ultraviolet/Ozone Treatment,” *J Colloid Interface Sci*, vol. 254, no. 2, pp. 306–315, Oct. 2002, doi: 10.1006/JCIS.2002.8594.

[145] K. Ma, J. Rivera, G. J. Hirasaki, and S. L. Biswal, “Wettability control and patterning of PDMS using UV–ozone and water immersion,” *J Colloid Interface Sci*, vol. 363, no. 1, pp. 371–378, Nov. 2011, doi: 10.1016/J.JCIS.2011.07.036.

[146] B. Schnyder, T. Lippert, R. Kötz, A. Wokaun, V. M. Graubner, and O. Nuyken, "UV-irradiation induced modification of PDMS films investigated by XPS and spectroscopic ellipsometry," *Surf Sci*, vol. 532–535, pp. 1067–1071, Jun. 2003, doi: 10.1016/S0039-6028(03)00148-1.

[147] J. Kim, M. K. Chaudhury, and M. J. Owen, "Hydrophobic Recovery of Polydimethylsiloxane Elastomer Exposed to Partial Electrical Discharge," *J Colloid Interface Sci*, vol. 226, no. 2, pp. 231–236, Jun. 2000, doi: 10.1006/JCIS.2000.6817.

[148] H. Makamba, J. H. Kim, K. Lim, N. Park, and J. H. Hahn, "Surface modification of poly(dimethylsiloxane) microchannels," *Electrophoresis*, vol. 24, no. 21, pp. 3607–3619, Nov. 2003, doi: 10.1002/ELPS.200305627.

[149] G. Sui *et al.*, "Solution-phase surface modification in intact poly(dimethylsiloxane) microfluidic channels," *Anal Chem*, vol. 78, no. 15, pp. 5543–5551, Aug. 2006, doi: 10.1021/AC060605Z/ASSET/IMAGES/LARGE/AC060605ZF00006.JPEG.

[150] A. R. Abate, D. Lee, T. Do, C. Holtze, and D. A. Weitz, "Glass coating for PDMS microfluidic channels by sol–gel methods," *Lab Chip*, vol. 8, no. 4, pp. 516–518, Mar. 2008, doi: 10.1039/B800001H.

[151] J. Xu and K. K. Gleason, "Conformal, amine-functionalized thin films by initiated chemical vapor deposition (iCVD) for hydrolytically stable microfluidic devices," *Chemistry of Materials*, vol. 22, no. 5, pp. 1732–1738, Mar. 2010, doi: 10.1021/CM903156A/ASSET/IMAGES/LARGE/CM-2009-03156A_0001.JPEG.

[152] H. Y. Chen, Y. Elkasabi, and J. Lahann, "Surface modification of confined microgeometries via vapor-deposited polymer coatings," *J Am Chem Soc*, vol. 128, no. 1, pp. 374–380, Jan. 2006, doi: 10.1021/JA057082H/SUPPL_FILE/JA057082HSI20051115_123913.PDF.

[153] Y. Soriano-Jerez *et al.*, "Role of dynamic surface tension of silicone polyether surfactant-based silicone coatings on protein adsorption: An insight on the 'ambiguous' interfacial properties of Fouling Release Coatings," *Prog Org Coat*, vol. 186, p. 108079, Jan. 2024, doi: 10.1016/J.PORGCOAT.2023.108079.

[154] P. Yi, R. A. Awang, W. S. T. Rowe, K. Kalantar-Zadeh, and K. Khoshmanesh, "PDMS nanocomposites for heat transfer enhancement in microfluidic platforms," *Lab Chip*, vol. 14, no. 17, pp. 3419–3426, Jul. 2014, doi: 10.1039/C4LC00615A.

[155] T. Fujii, "PDMS-based microfluidic devices for biomedical applications," *Microelectron Eng*, vol. 61–62, pp. 907–914, Jul. 2002, doi: 10.1016/S0167-9317(02)00494-X.

[156] A. Messier, G. Schorsch, J. Rouviere, and L. Tenebre, "On certain solved and unsolved problems with water/PDMS/surfactant systems," *Trends in Colloid and Interface Science III*, pp. 249–256, Dec. 1989, doi: 10.1007/BFB0116217.

[157] P. J. Ross, *Aplicações das técnicas Taguchi na engenharia da qualidade*. Makron Books, 1991.

[158] "Tabela Análise de Variância de Análise de variabilidade".

[159] A. G. Jerniti, A. El Ouafi, N. Barka, A. G. Jerniti, A. El Ouafi, and N. Barka, "A Predictive Modeling Based on Regression and Artificial Neural Network Analysis of Laser Transformation Hardening for Cylindrical Steel Workpieces," *J Surf Eng Mater Adv Technol*, vol. 6, no. 4, pp. 149–163, Oct. 2016, doi: 10.4236/JSEMAT.2016.64014.

[160] "(PDF) OTIMIZAÇÃO DE PARÂMETROS DE FRESAGEM USANDO O MÉTODO DE TAGUCHI COM A ANÁLISE RELACIONAL DE GREY." Accessed: May 16, 2024. [Online]. Available: https://www.researchgate.net/publication/334785056_OTIMIZACAO_DE_PARAMETROS_DE_FRESAGEM_USANDO_O_METODO_DE_TAGUCHI_COM_A_ANALISE_RELACIONAL_DE_GREY

[161] C. R. de Lacerda, "Otimização de parâmetros de soldadura GMAW utilizando o método Taguchi com a análise relacional de Grey," 2021. Accessed: May 16, 2024. [Online]. Available: https://bibliotecadigital.ipb.pt/handle/10198/23730

[162] S. K. Nayak, J. K. Patro, S. Dewangan, and S. Gangopadhyay, "Multi-objective Optimization of Machining Parameters During Dry Turning of AISI 304 Austenitic Stainless Steel Using Grey Relational Analysis," *Procedia Materials Science*, vol. 6, pp. 701–708, Jan. 2014, doi: 10.1016/J.MSPRO.2014.07.086.

[163] C. Lin and Z. Shan, "Use of the Taguchi Method and Grey Relational Analysis to Optimize Turning Operations with Multiple Performance Characteristics," *Materials and Manufacturing Processes*, pp. 209–212, Dec. 2004, doi: 10.1081/AMP-120029852.

[164] Sifeng Liu, Yingjie Yang, and Jeffrey Forrest, *Grey Data Analysis Methods, Models and Applications*, 8th edition. 2016.

[165] A. Panda, A. K. Sahoo, and A. K. Rout, "Multi-attribute decision making parametric optimization and modeling in hard turning using ceramic insert through grey relational analysis: A case study," *Decision Science Letters*, vol. 5, pp. 581–592, 2016, doi: 10.5267/j.dsl.2016.3.001.

[166] S. Pal, S. K. Malviya, S. K. Pal, and A. K. Samantaray, "Optimization of quality characteristics parameters in a pulsed metal inert gas welding process using grey-based Taguchi method," *International Journal of Advanced Manufacturing Technology*, vol. 44, no. 11–12, pp. 1250–1260, Oct. 2009, doi: 10.1007/S00170-009-1931-0/METRICS.

[167] Y. F. Hsiao, Y. S. Tarng, and W. J. Huang, "Optimization of Plasma Arc Welding Parameters by Using the Taguchi Method with the Grey Relational Analysis," *Materials and Manufacturing Processes*, vol. 23, no. 1, pp. 51–58, Dec. 2007, doi: 10.1080/10426910701524527.

[168] R. Ariati, F. Sales, V. Noronha, R. Lima, and J. Ribeiro, "Low-Cost Multifunctional Vacuum Chamber for Manufacturing PDMS Based Composites," *Machines 2022, Vol. 10, Page 92*, vol. 10, no. 2, p. 92, Jan. 2022, doi: 10.3390/MACHINES10020092.

[169] M. Gonçalves *et al.*, "Polydimethylsiloxane Surface Modification of Microfluidic Devices for Blood Plasma Separation," *Polymers 2024, Vol. 16, Page 1416*, vol. 16, no. 10, p. 1416, May 2024, doi: 10.3390/POLYM16101416.

[170] C. H. Wanke, J. L. Feijó, L. G. Barbosa, L. F. Campo, R. V. B. De Oliveira, and F. Horowitz, "Tuning of polypropylene wettability by plasma and polyhedral oligomeric silsesquioxane modifications," *Polymer (Guildf)*, vol. 52, no. 8, pp. 1797–1802, Apr. 2011, doi: 10.1016/J.POLYMER.2011.01.064.

[171] C. H. Wanke, L. G. Barbosa, J. V. M. Hübner, F. Horowitz, R. S. Mauler, and R. V. B. De Oliveira, "Recuperação hidrofóbica de polipropileno tratado por VUV ou plasma," *Polimeros*, vol. 22, no. 2, pp. 158–163, 2012, doi: 10.1590/S0104-14282012005000027.

[172] R. J. Good, "Contact angle, wetting, and adhesion: a critical review," *J Adhes Sci Technol*, vol. 6, no. 12, pp. 1269–1302, 1992, doi: 10.1163/156856192X00629.

[173] T. S. Chow, "Wetting of rough surfaces," *Journal of Physics: Condensed Matter*, vol. 10, no. 27, p. L445, 1998.

[174] A. Marmur, "Wetting on hydrophobic rough surfaces: To be heterogeneous or not to be?," *Langmuir*, vol. 19, no. 20, pp. 8343–8348, Sep. 2003, doi: 10.1021/LA0344682/ASSET/IMAGES/LARGE/LA0344682F00003.JPEG.

[175] A. Cassie, S. B.-T. of the F. society, and undefined 1944, "Wettability of porous surfaces," *pubs.rsc.orgABD Cassie, S BaxterTransactions of the Faraday society, 1944•pubs.rsc.org*, Accessed: Apr. 06, 2024. [Online]. Available: https://pubs.rsc.org/en/content/articlepdf/1944/tf/tf9444000546

[176] W. Sigmund, S. H.-E. of Membranes, and undefined 2016, "Cassie–Baxter Model," *cir.nii.ac.jp*, Accessed: Apr. 06, 2024. [Online]. Available: https://cir.nii.ac.jp/crid/1360574096353777280

[177] M. Miwa, A. Nakajima, A. Fujishima, K. Hashimoto, and T. Watanabe, "Effects of the surface roughness on sliding angles of water droplets on superhydrophobic surfaces," *ACS PublicationsM Miwa, A Nakajima, A Fujishima, K Hashimoto, T WatanabeLangmuir, 2000•ACS Publications*, vol. 15, no. 2, pp. 5754–5760, Jun. 1999, doi: 10.1021/la991660o.

[178] E. Bormashenko *et al.*, "Characterization of rough surfaces with vibrated drops," *Physical Chemistry Chemical Physics*, vol. 10, no. 27, pp. 4056–4061, Jul. 2008, doi: 10.1039/B800091C.

[179] K. S. Lee, N. Ivanova, V. M. Starov, N. Hilal, and V. Dutschk, "Kinetics of wetting and spreading by aqueous surfactant solutions," *Adv Colloid Interface Sci*, vol. 144, no. 1–2, pp. 54–65, Dec. 2008, doi: 10.1016/J.CIS.2008.08.005.

[180] H. Y. Erbil, G. McHale, and M. I. Newton, "Drop evaporation on solid surfaces: Constant contact angle mode," *Langmuir*, vol. 18, no. 7, pp. 2636–2641, Apr. 2002, doi: 10.1021/LA011470P/ASSET/IMAGES/LARGE/LA011470PF00004.JPEG.

[181] W. A. ZISMAN, "Relation of the Equilibrium Contact Angle to Liquid and Solid Constitution," vol. 14, pp. 1–51, Jan. 1964, doi: 10.1021/BA-1964-0043.CH001.

[182] "J.W. Gibbs, H.A. Bumstead, R.G. Van Name, W.R. Longley,... - Google Académico." Accessed: Apr. 06, 2024. [Online]. Available: https://scholar.google.com/scholar?q=J.W.%20Gibbs%2C%20H.A.%20Bumstead%2C%20R.G.%20Van%20Name%2C%20W.R.%20Longley%2C%20The%20Collected%20Works%20of%20J.%20Willard%20Gibbs%2C%20Longmans%2C%20Green%2C%201931.

[183] T. Hashimoto, Y. Matsui, A. Hagihara, and A. Miyamoto, "Thermal diffusivity measurement of polymer films by the temperature wave method using joule-heating," *Thermochim Acta*, vol. 163, no. C, pp. 317–324, Jun. 1990, doi: 10.1016/0040-6031(90)80413-S.

[184] T. M. Tritt, "Thermal Cndutivity Theoty, Properties and Application," *Kluwer Academic/Plenum Publication, New York*, vol. 111, no. 479, pp. 1009–1010, 1965, Accessed:

May 31, 2024. [Online]. Available: https://books.google.com/books/about/Thermal_Conductivity.html?hl=pt-BR&id=whJNfKmziiIC

[185] “Hot Disk Thermal Constants Analyser, Instruction... - Google Académico.” Accessed: Apr. 11, 2024. [Online]. Available: https://scholar.google.com/scholar?q=Hot%20Disk%20Thermal%20Constants%20Analyser%2C%20Instruction%20Manual%2C%20Revision%20date%202019-10-08.%2C%202019.

[186] R. R. Souza *et al.*, “An innovative PDMS cell to improve the thermal conductivity measurements of nanofluids,” *Thermal Science and Engineering Progress*, vol. 42, p. 101926, Jul. 2023, doi: 10.1016/J.TSEP.2023.101926.

Appendix a

List Of Publications

The development of this dissertation resulted in publications in international journals and publications in indexed journals.

Publications

Neves, L. et al., 2024. A Review of Methods to Modify the PDMS Surface Wettability and their Applications. https://doi.org/10.3390/mi15060670

Neves, L. et al., 2024. Optimization of PDMS Hydrophobicity and Thermal Conductivity Analysis in Microfluidic Devices: Comparison of Non-Ionic Surfactants. Article in submission process in Journal Polymers, MDPI.